EFFECT OF CLOSELY SPACED FOOTING SHAPE ON BEARING CAPACITY AND SETTLEMENT IN THE CASE OF ADAMA NATURAL SOIL DEPOSIT

Derara Guluma Hurisa

A Thesis Submitted to the Department of Civil Engineering
School of Civil Engineering and Architecture

Presented In Partial Fulfillment of the Requirement for the Degree of Masters of Science in Civil Engineering (Geotechnical Engineering)

Office of Graduate Studies
Adama Science and Technology University

October, 2023

Adama, Ethiopia

EFFECT OF CLOSELY SPACED FOOTING SHAPE ON BEARING CAPACITY AND SETTLEMENT
IN THE CASE OF ADAMA NATURAL SOIL DEPOSIT

Derara Guluma Hurisa

Advisor: Dr. Argaw Asha (PHD)

A Thesis Submitted to the Department of Civil Engineering
School of Civil Engineering and Architecture

Presented In Partial Fulfillment of the Requirement for the Degree of Masters of Science in Civil Engineering (Geotechnical Engineering)

Office of Graduate Studies
Adama Science and Technology University

October, 2023

Adama, Ethiopia

Declaration

I hereby declare that this thesis entitled **"Effect of closely spaced footing shape on bearing capacity and settlement in the case of Adama natural soil deposit"** is my original work. That is, it has not been submitted for the award of any academic degree, diploma or certificate in any other university. All sources of materials that are used for this thesis have been duly acknowledged through citation.

Derara Guluma

Name of the student	Signature	Date

Recommendation of advisor

I/we the advisors of this thesis, hereby certify that I/we have read the revised version of the thesis entitled **"Effect of closely spaced footing shape on bearing capacity and settlement in the case of Adama natural soil deposit"** prepared under my/our guidance by **Derara Guluma Hurisa** submitted in partial fulfillment of requirements for the degree of Masters of Science In Civil Engineering (Geotechnical Engineering). Therefore, I/we recommend the submission of revised version of the thesis to the department following the applicable procedures.

Major advisor	Signature	Date
Co-advisor	Signature	Date

Approval

I/we, the advisors of the thesis entitled **"Effect of closely spaced footing shape on bearing capacity and settlement in the case of Adama natural soil deposit"** and developed by Derara Guluma, hereby certify that the recommendation and suggestion made by the board of examiners are appropriately incorporated into the final version of the thesis.

______________________	______________	______________
Major advisor	Signature	Date
______________________	______________	______________
Co-advisor	Signature	Date

Approval of Board of Reviewers

We, the undersigned, members of the Board of Examiners of the thesis by Derara Guluma have read and evaluated the thesis entitled **"Effect of closely spaced footing shape on bearing capacity and settlement in the case of Adama natural soil deposit"** and examined the candidate during open defense. This is, therefore, to certify that the thesis is accepted for partial fulfillment of the requirement of the degree of Masters of Science in Civil Engineering (Geotechnical Engineering).

______________________	____________	____________
Chairperson	Signature	Date
______________________	____________	____________
Internal Examiner	Signature	Date
______________________	____________	____________
External Examiner	Signature	Date

Final approval and acceptance of the thesis is contingent upon submission of its final copy to the Office of Postgraduate studies (OPGS) through the Department Graduate Council (DGC) and School Graduate Committee (SGC).

______________________	____________	____________
Department Head	Signature	Date
______________________	____________	____________
School Dean	Signature	Date
______________________	____________	____________
Office of Postgraduate Studies, Dean	Signature	Date

ACKNOWLEDGEMENT

I would like to thank Dire Dawa University for its willingness to allow me to attend my M.Sc. Study. I also forward my gratitude and appreciation to my advisor Dr. Argaw Asha (Phd).

I would also like to extend my acknowledgment to my colleagues for their support. I forward my special tanks to Mr Zerihun Lamesa who gave me valuable comments on introduction part of this thesis. Deriba- Defersa general Contractor and Adama Construction Office has made the geotechnical soil investigation reports available and allow me to select the paper. The Organization's staff was very cooperative and welcoming.

Finally, I would like to express my deepest gratitude to my family for the fulfillment of all my interest.

ABSTRACT

Foundations are the most important components of any structure and any damage to the foundation results in catastrophic failure of superstructures. The estimation of the bearing capacity and settlement of the soil under foundations depends on shape, dimension, depth of footing and strength of the top soil. In this research, the effect of the shape of closely spaced footing subjected to vertical load were investigated. The objective of this research was to numerically investigate the effect of closely spaced footing shape on bearing capacity and settlement by PLAXIS 3D Connect Edition V20 in the case of the Adama natural soil deposit. The method that used for this research includes a review of related literature, Numerical analysis of bearing capacity and settlement by Mohr-Coulomb model using finite element software.

A total of 72 models were investigated on four different soils. A load settlement graph from PLAXIS 3D were used to obtain bearing capacity comparisons for interfered footings with isolated foundations. The result show that circular footing has lower bearing capacity as compared to square, strip and rectangular footing when acted as an isolated in all cases in this study. Isolated rectangular footing rest on soil with medium dense to dense consistency has maximum bearing capacity; However; strip soil rests on loose consistency soil has maximum bearing capacity. Interfered strip footing on medium dense to dense consistency has low bearing capacity. It was concluded that circular footing bearing capacity was lower than square, rectangular and strip when act as an isolated and strip footing has low bearing capacity in adjacent foundation. On average rectangular footing have higher bearing capacity in different soil layer and square footing show intermediate values. It was observed from the results that footing shapes, dimension, spacing ratio S/B and strength of top soil layer were the most parameter that effect bearing capacity and settlement of foundation.

Keywords: - Bearing capacity, load–settlement, Finite element analysis, Numerical

TABLE OF CONTENT

Acknowledgement vi

Abstract ..... *vii*

List of acronyms abbreviations xv

Chapter one introduction 1

1.1 Background of the research 1

1.3 Objective of the research 2

1.3.1 General objective 2

1.3.2 Specific objectives 3

1.4 Significance of the research: 3

1.6 Limitation of the research 4

1.7 Organization of the research. 4

2.7 Methodology 12

2.7.1 Introduction 12

2.7.2 Experimental method 13

2.7.3 Numerical methods 13

2.8 Related work 14

Chapter three methodolgy 22

3.1 Description of the research area 22

3.2 Research design 22

3.3 Materials 23

3.3.1 Geological condition and soil layer 23

3.4 Correlation of basic soil parameters 25

3.4.1 Modulus of elasticity (es) 26

3.4.2 Poisson's ratio 27

3.4.3 Cohesion 28

3.4.4 Angle of internal friction 28

3.4.5 Dilatancy 28
3.4.6 Tension cut-off and tensile strength 28
3.4.7 Saturated and unsaturated unit weight 28
3.5 Numerical model setup and method of numerical analysis 29
3.5.1 Numerical model setup........ 29
3.5.2 Interference........ 31
3.5.2 The analysis process 33
3.6 Comparison of plaxis 3d load-settlement output result 34
Chapter four result, discusion and parametric study. 36
4.1 Results and discussion 36
4.1.1 Introduction 36
4.2 Bearing capacity and settlements of shallow footing........ 38
4.2.1 Bearing capacity and settlement of square, circular, rectangular and strip isolated footings on different soil types........ 38
4.2.2. Bearing capacity and settlement of adjecent foundation........ 41
4.3 Comparision between numerical model results and analytical results 51
4.3 Parametric study 53
Chapter five conclision and recommendation 56
5.1Conclusion 56
5.2 Recommendation 57
Reference 58
Appendix 61
Appendix A results from software and analytical calculation 61
Appendix – B borehole log sheets 69
Appendix- C load settlement curves and tables for footing on different soil 74
Appendix – D some informative table from reference 86

LIST OF FIGURES

Figure 2.1 Failure surface in the soil at ultimate load for a continuous rough rigid foundation as assumed by Terzaghi 8

Figure 2.2 Failure mechanism of isolated foundation and closely spaced multiple footings (Lee & Eun, 2009). 9

Figure 2.3 Geometry, meshing and loading of the (a) Circular, (b) Square, (c) Strip, and (d) Ring foundation model 10

Figure 2.4 Experimental setup 13

Figure 2.6 Ultimate Pressure v/s L/B ratio 15

Figure 2.7Efficiency Factor v/s L/B ratio 15

Figure 2.8 2 D Load settlement curve. 16

Figure 2.9 3D Load settlement curve 16

Figure 2.10 Pressure settlement ratio plot for the rectangular footing on layered sand at ϕ1 (41°) and ϕ2 (31°) corresponding to different H/W ratio. 17

Figure 2.11 Dimensionless ultimate bearing capacity versus H/W curves for upper dense sand layer friction angle (ϕ1) (a) 41°, (b) 42° 17

Figure 2.12 vectorial displacement of layered sand at different H/W ratio 18

Figure 2.13 Load-Settlement curve for different shapes of footing in case of medium sand (Dr=60%) 18

Figure 2.14 Comparison of present BCR with BCR from literature: strip footing and circular footing 19

Figure 2.15 Plot for rectangular footing (length to width ratio=2) 21

Figure 3.1 Map of Adama town source https://images.app.goo.gl/P7psMNVJgWppoTL9 22

Figure 3.2 Research design flow chart. 23

Figure 3.3 dimension of soil cluster 30

Figure 3.5 3D soil element (10-node tetrahedrons) 33

Figure 4.1 A section veiw of plastic point distribution of isolated footing based on Mohr-Coulumb 36

Figure 4.2 A section veiw of plastic point distribution of footing based on Mohr-Coulumb square, circular, rectangular and strip as isolated and S/B ratio 1 to 7. 37

Figure 4.3 Load settlement curve of isolated footing on compact silt underlain by medium dense silty sands 38

Fugere 4.4 Load settlement curve of isolated footing on loose sandy silt underlain by a layer of medium dense sandy silt and dense fructured rock. 39

Figure 4.5 Load settlement curve of isolated footing on medium dense to dense silt with same sand overlain by very dense sandy silt with trace of gravel. 39

Figure 4.6 Load settlement curve of isolated footing on layers of dense, medium dense and dense clayey silt. 40

Figure 4.7 Load settlement curve of square footing with variying S/B ratio on soil 1 41

Figure 4.8 Load settlement curve of circular footing with variying S/B ratio on soil 1.. 41

Figure 4.9 Load settlement curve of circular footing with variying S/B ratio on soil 1.. 42

Figure 4.10 Load settlement curve of circular footing with variying S/B ratio on soil 42

Figure 4.11 a-h load- settlement curve footing with variying S/B ratio on soil 1..... 45

Figure 4.12 Variation of BCR (interferance coefficient) with S/B ratio for square, circular, rectangular and strip on soil 1.. 46

Figure 4.13 Variation of BCR (interferance coefficient) with S/B ratio for square, circular, rectangular and strip on soil 2.. 47

Figure 4.14 Variation of BCR (interferance coefficient) with S/B ratio for square, circular, rectangular and strip on soil 3.. 47

Figure 4.15 Variation of BCR (interferance coefficient) with S/B ratio for square, circular, rectangular and strip on soil 4.. 48

Figure 4.16 Ultimate bearing capacity) versus S/B ratio for square, circular, rectangular and strip on different soil 49

Figure 4.17 Variation of BCR (interferance coefficient) with S/B ratio for square, circular, rectangular and strip on different soil.. 50

Figure 4.18 qult versus S/B 51

Figure 4.19 Distribution of Settlement ratio by Schmertmann et al. 52

Figure 4.20 Accuracy and Reliability in settlement prediction 53

Figure 4.21 Ultimate bearing capacity versus S/B ratio.. 55

Figure 4.22 Ultimate bearing capacity versus S/B ratio on different soil 55

Figure B-1 a bore hole data for ODA mixed used building....................................... 69

Figure B-1 b bore hole data for ODA mixed used building....................................... 70

Figure B-2 bore hole data for Adama City Woreda Court Office building 71

Figure B-3 a bore hole data for ODA mixed used building....................................... 72

Figure B-3 b bore hole data for ODA mixed used building....................................... 73

Figure B-1 a-1 settlement curve of footing with variiying S/B ratio on soil 2........... 77

Figure B-2 a-n settlement curve of footing with variiying S/B ratio on soil 3........... 81

Figure B-3 a-l settlement curve of footing with variiying S/B ratio on soil 4........... 85

LIST OF TABLES

Table 2.1correlation equation of hear strength parameter. 12

Table 3.1 Layer thickness and soil type... 25

Table 3.2 correct SPT-N values... 27

Table 3.3 Properties of soils used in numerical modeling. 31

Table 3.4 Properties of footing material 32

Figure 3.4 3D soil block and foundation structures... 32

Table 4.1 effect of adjecent square, circular, rectangular and strip footings on ultimate bearing capacity 45

Table 4.2 Comparison of numerical model results with analytical method 52

Table A - 1 load settlement relation of soil 1 61

Table A - 2 load settlement relation of soil 2 61

Table A - 3 load settlement relation of soil 3 62

Table A - 4 load settlement relation of soil 1 63

Table A - 5 allowable and ultimate bearing capacity of soil 64

Table A - 6 Ultimate bearing capacity of square, circular, rectangular and strip footing with S/B=0 - 7 65

Table A - 7 BRC of square, circular, rectangular and strip footing with S/B=0-766

Table A - 8 Elastic settlement and rigid settlement of isolated square footing considering depth of influence H =2B and 5B 66

Table A - 9 Elastic settlement and rigid settlement of isolated circular footing considering depth of influence H =2B and 5B 67

Table A - 10 Elastic settlement and rigid settlement of isolated rectangular footing considering depth of influence H =2B and 5B 67

Table A - 11 Elastic settlement and rigid settlement of isolated strip footing considering depth of influence H =2B and 5B 67

Table A-12 Summary of effect of adjecent square, circular, rectangular and strip footings on ultimate bearing capacity 68

Table D.1 Correction factor for SPT N values 86

Table D.2 cohesion and friction angles of various soil type................................ 86

Table D.3 Poisons ratio of soil and concrete 87

Table D -4 Penetration resistance and properties of soil on the basis of SPT N value 87

Various soil cohesion and SPT N values for intermediate soils 87

Table D – 5 Correlation between cohesion and SPT-V values (Karol, 1960)...... 87

Table D – 5 Values of range of static stress-strain modulus Es for selected soil(Bowles, 1976). 88

Table D – 6 Presumptive values of bearing capacity for light loaded structures . 88

Table D – 7 Unit weight of different soil... 88

LIST OF ACRONYMS ABBREVIATIONS

$q_{u\ int}$ = ultimate bearing capacity of the interfering footings

$q_{u\ single}$ = ultimate bearing capacity of an identical isolated footing

$\delta_{v\ (int)}$ is the total displacement of the interfering footings

$\delta_{v\ (single)}$ is the total displacement of an identical isolated footing

ϕ = angle of internal friction of the soil

ASTM = American Society for Testing And Material

B= Width of footing

BCR = bearing capacity ratio

c = cohesion

Df = Depth of foundation

L = length of the footing

Nc, Nq, Nɣ = bearing capacity coefficients

q_u = ultimate bearing capacity of soil

S= Center to center spacing between two adjacent footing.

γ = Unit weight of soil

ξ_{cs} = Empirical shape factor

CHAPTER ONE INTRODUCTION

1.1 Background of The Research

Foundation construction is one of the basic activities in the field of geotechnical engineering. This issue has provided engineers with efficient analytical and numerical methods for designing various types of foundations over the years(Shafaghat et al., 2018). The load of the superstructure is transferred to the soil beneath it with the help of the footing. Depending upon the depth to width ratio a footing can be shallow or deep. The transmission of load beneath the footing must be such that it is safe against settlement and shear failure (A. Gupta et al., 2017). Design of foundations on a horizontal ground surface depends on the mechanical characteristics of the soil (unit weight and shear strength parameters) and the physical properties of the foundation (depth, width, and shape of the footing). There are two primary considerations to decide the allowable bearing pressures of shallow foundations (a) the safety factor against ultimate shear failure must be adequate, and (b) the settlements should not exceed the tolerable limits (Acharyya & Dey, 2017).

The estimation of the bearing capacity and settlement of the soil under foundations depends on parameters of load, shape, width, and depth of footing (Saravanan et al., 2020). The result obtained from the model test performed on a different footing to study the effect of the shape of the footing on the bearing pressure and settlement was quite acceptable (Saravanan et al., 2020; Shafaghat et al., 2018). Generally, shallow foundations with different shapes are commonly used on the construction site, such that rectangular, square, strip, and circular shape. The shape of the footing and size of the footing has to be selected based on the structural load, bearing capacity of the soil, and site condition by the horizontal cross-section.

1.2 Statement of Problem

Many pieces of research have been made in understanding the effect of the shape of shallow footings such as square, strip, circular, and ring subjected to vertical concentrated and distributed load on bearing capacity and settlement.

(Patel & Bhoi, 2019) carried out an experimental investigation to study footing, when rested on granular soil under centric loading conditions and observed that the shape of the footing has a significant effect on its bearing pressure and the settlement characteristics.

(Radwan, 2021) Numerically investigate the effect of footing shape (rectangular, circular, and square) of the same width and rectangular footing of L/B ratio 1.5 and 2 times the width of square footing on bearing capacity and settlement and conclude that shape of the foundation has a significant effect on its bearing capacity and settlement.

(Shafaghat et al., 2018) Numerically investigated the bearing capacity and settlement of two adjacent (square, circular, ring, and strip) footing of width 2m constructed on a sand layer and concluded that the presence of an adjacent foundation leads to the reduction in bearing capacity for round shape footings while it can increase the bearing capacity of rectangular shape i.e., square and strip in some specific distances.

Many research investigated on bearing capacity of shallow foundation were focused on width of the foundation as primary parameters to fix dimension of shallow foundation and the equal confining area of the footing were not considered. In this research, the effect of the shape of closely spaced (circular, rectangular, square, and strip) footing of equal area and proportional load per unit area subjected to vertical load on bearing capacity and settlement was investigated by varying spacing between footing. Four types of footing were considered and analyzed by various spacing ratios defined by S/B on four different layered soil. The goal of this research was achieved by conducting investigation using PLAXIS 3D Connect Edition V20 finite element software and analytically employed by available conventional equations and methods.

1.3 Objective of The Research

1.3.1 General Objective

The general objective of this research was to numerically investigate the effect of closely spaced footing shape on bearing capacity and settlement in the case of the Adama natural soil deposit.

1.3.2 Specific Objectives

- To analyze bearing capacity and settlement of the circular, rectangular square and strip footings numerically by PLAXIS 3D.
- To evaluate the change in bearing capacity and settlement for adjacent footings of same shape and size by varying spacing ratio.
- To compare and discuss the effect of footing shape on bearing capacity and settlement.

1.4 Significance of The Research:

This study conducts to numerically investigate the effect of the shape of closely spaced square, circular, rectangular and strip footing on bearing capacity and settlement using Mohr-Coulomb failure criteria in the case of Adama natural soil deposit and provide useful information to select proper footing at various spacing.

1.5 Scope of The Research

The scope of this research is to investigate the effect of closely spaced footing shape on bearing capacity and settlement by 3D PLAXIS finite element software and comparing the results to analytical elastic settlement computed depend on load obtained from PLAXIS output of allowable settlement values to determine the validity of the finite element model used to predict bearing capacity and settlement of various footing. The required soil investigation and design reports of separate project was obtained from various construction office. For the intended purpose unit weight, density, cohesion, modulus of elasticity, poison ratio and angle of internal friction (ϕ) data were correlated from available source obtained from soil investigation report. The analysis was performed using PLAXIS 3D software. Validation of the result were checked with analytical elastic settlement calculated from bearing capacity and settlement report.

1.6 Limitation of The Research

The research has the following limitation

Only finite element analysis is performed on two vertically loaded closely spaced footing without conducting the model test in the laboratory and field bearing capacity.

In literature few correlations of shear strength parameter are available in terms of SPT N value.

1.7 Organization of The Research.

The content of this research is organized to five chapters. The first chapter provides introduction with research objective, scope, significance and scope of the research. The second chapter contain major work done and methodology related to this research and review result done by PLAXIS from journals and theses. Chapter thee presents methodology, material properties and method of modeling by PLAXIS 3D. Further this chapter focus on numerical modeling of shallow footing by PLAXIS finite element software. This are material modeling, geometry, boundary condition, loading, mesh generation, calculation and output following PLAXIS model analysis steps. The fourth chapter analysis the result and parametric study. In this chapter result of various footings are discussed and compared. The fifth chapter provide conclusion derived from the research and limitation in the analysis and recommendation of future work.

CHAPTER 2 LITERATURE REVIEW

2.1 Introduction

Shallow foundations spread the load to the ground at shallow depth (BNBC, 2020). The bearing capacity of the foundations is a primary concern in the field of foundation engineering. The self-weight of the structure and the applied loading such as dead load, live load, wind load, and others are to be transferred to the soil safely and economically. The load at which the shear failure of the soil beneath the foundation occurs is called the ultimate bearing capacity of the foundation (Budhu, 2011; Das, 2011).

The magnitude of the ultimate bearing capacity depends on the mechanical characteristics of the soil and the physical characteristics of the footing. In the literature, several studies have been reported to estimate the bearing capacity of footings such as circular, square, strip rectangular (Patel & Bhoi, 2019)over single and double-layered soil. Footings shall generally be proportioned from the allowable bearing pressure and stress limitations imposed by limiting settlement(BNBC, 2020).

There are numerous methods for increasing the ultimate bearing capacity of the footing and decreasing the soil settlement reduction of the footing. However, a large no. of observations has been carried out for the development of the footing behavior. The behavior of square and rectangular footings resting on cohesive soils was also studied by some researchers (Patel & Bhoi, 2019). Taiebat and Carter performed numerical studies on the bearing capacity of shallow foundations on cohesive soil subjected to combine loading (Shafaghat et al., 2018).

2.2 General Bearing Capacity and Settlement Theory

The design of shallow foundations typically involves two steps: (1) the calculation of ultimate bearing capacity based on general bearing capacity theories and (2) the calculation of maximum contact pressure to produce an allowable total settlement. The allowable bearing capacity for the shallow foundation system is the lesser of the ultimate bearing capacity, divided by a factor of safety, and the computed maximum allowable contact pressure. Based on an allowable magnitude of the total settlement, the pressure–settlement curves are analyzed to compute the pertinent statistics for an allowable bearing resistance that are then utilized to develop the resistance factors.

The computed resistance factors are observed to be highly variable and are dependent on design uncertainty and shallow foundation size (Budhu, 2011; Das, 2011)

2.2.1 Bearing Capacity Equation.

A shallow foundation is one in which the ratio of the embedment depth to the minimum plan dimension (the width) is less than 2.5. A geotechnical engineer must ensure that the foundation satisfies the following two stability conditions: 1. the foundation must not collapse or become unstable under any conceivable loading. This is called the ultimate limit state. 2. Settlement of the structure must be within tolerable limits so as not to impair the design function of the structure. This is called the serviceability limit state. Both requirements must be satisfied. Often, it is the settlement that governs the design of shallow foundations (Altaweel & Shakir, 2021b; Budhu, 2011; Das, 2011).

Equations used for computing the theoretical value of bearing capacity for footing subjected to a vertical load expressed by Terzaghi: assume soil supporting a foundation is homogenous and extends to a considerable depth (Budhu, 2011; Das, 2011; Vanapalli & Oh, 2021).The minimum depth of foundation shall be 1.5 m for exterior footing of permanent structures in cohesive soils and 2 m in cohesionless soils(BNBC, 2020).

Strip footing $q_u = \boldsymbol{cN_c} + \boldsymbol{qN_q} + 0.5\boldsymbol{\gamma BN}$ (1)

Circular Footing $q_u = 1.3cN_c + \gamma DN_q + 0.3\gamma BN_\gamma$ (2)

Square Footing $q_u. = 1.3cN_c + \gamma DN_q + 0.4\gamma BN_\gamma$ (3)

Rectangle Footing $Q_{ult} = 1.3c\left(1 + \frac{0.3B}{L}\right) + \gamma DN_q + 0.5\gamma B(1 - \frac{0.3B}{L})N_\gamma$ (4)

Meyerhof 1963 bearing capacity equation

$$Q_{ult} = cN_c s_c d_{c+} \gamma DN_q s_q d_q + 0.5N_\gamma s_\gamma d_\gamma \quad (5)$$

The procedure for estimating bearing capacity for layered soil proposed by Meyerhof and Hanna 1978 and Meyerhof 1974

Where: c = cohesion., q = surcharge, γ = unit weight of soil, and Nc, Nq and Nγ= bearing capacity coefficients

For the simplest case of a strip footing on homogeneous clay (undrained conditions) without surface surcharge, equation (1) reduces to

$$q_u = C_u N_C \tag{6}$$

Where N_c is the dimensionless bearing-capacity factor ($2 + \pi$), an exact solution, first found by (Prandtl, 1920), and cu is undrained soil shear strength.

Equation (2) can be rewritten to include the effect of footing shape as follows:

$$q_u = C_u N_C \zeta_{cs} \tag{7}$$

The empirical shape factor ζ_{cs} is given by

$$\zeta_{cs} = 1 + \left(\frac{B}{L}\right) + \left(\frac{N_q}{N_c}\right) \tag{8}$$

(Salgado et al.; 2004) investigated the bearing capacities of strip, square, circular, and rectangular foundations in clay using a rigorous finite-element limit analysis. The results of the analyses proposed rigorous, definitive values of the shape and depth factors for foundations in clays. They proposed that for 1≤L/B≤5 and 0≤Df≤B≤1.

$$\zeta_{cs} = 1 + 0.12\left(\frac{B}{L}\right) + 0.7\sqrt{\frac{D_f}{B}} \quad square, circular\ and\ rectangular\ footings \tag{9}$$

To understand the variation of bearing capacity and total settlements of interfering footings, two dimensionless terms are used. These are the Bearing Capacity Ratio, BCR, and the settlement ratio, ξ_δ, defined in Equations (10) and (11), respectively.

$$BCR = If = \frac{q_{u(int)},}{q_{u\,(single)}} \tag{10}$$

Where $q_{u\,int}$ is the ultimate bearing capacity of the interfering footings, and $q_{u\,single}$ is the ultimate bearing capacity of an identical isolated footing.

$$\xi_\delta = \frac{\delta_{v\,(int)}}{\delta_{v\,(single)}} \tag{11}$$

Where $\delta_{v\,(int)}$ is the total displacement of the interfering footings corresponding to $q_{u(int)}$, and $\delta_{v\,(single)}$ is the total displacement of an identical isolated footing corresponding to $q_{u\,(single)}$

2.3 Ultimate Bearing Capacity Failure Mode

In this analysis, extraction for efficiency factor is done to find the effect of the interference of foundations on the soil's bearing capacity for the individual foundation, considering the soil failure theory under a rough-based strip foundation adopted by (Terzaghi, 1943) (Altaweel & Shakir, 2021; Das, 2011; *BUDHU, 2011*) as shown in the figure. 2.1.

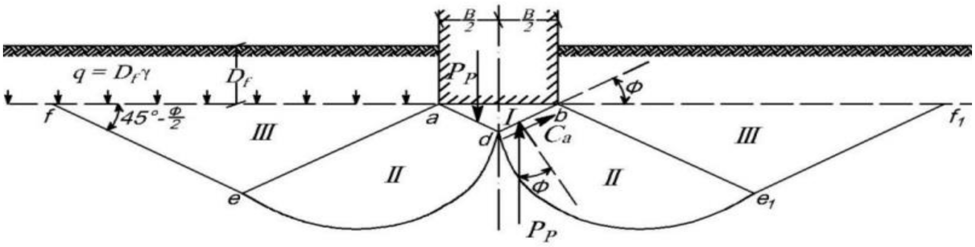

Figure 2.1 Failure surface in the soil at ultimate load for a continuous rough rigid foundation as assumed by Terzaghi

It illustrates the division of the failure envelope into three zones: (I) a wedge-shaped zone located beneath the loaded strip, in which the major principal stresses are vertical, (II) two zones of radial shear, ade, and bde_1, emanating from the outer edges of the loaded strip, whose boundaries intersect the horizontal at angles of ϕ and 45^o-$\phi/2$. (III) Two passive Rankine zones (Altaweel & Shakir, 2021).

The effect of closely continuously spaced foundations was theoretically examined by (Stuart, 1962) in cohesionless soil on the base of the limit equilibrium method. He assumed that the medium is homogeneous soil extending to great depth and that the failure mechanism will have a similar geometry to that rupture assumed by Terzaghi. The rupture surface developed beneath the shallow foundation comprises three zones; Rankine passive zone, radial zone, and triangular wedges (Figure. 2). Based on the center-to-center distance between the shallow foundations, (Stuart, 1962) concludes that as long as the rupture surfaces are only overlapping in Rankine passive zone, then there is no need to modified Terzaghi formula and should be applied directly (Alwalan, 2018).

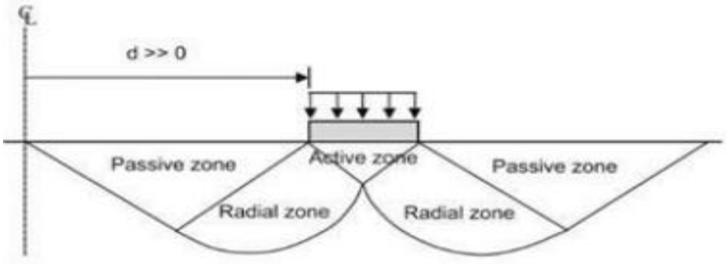

(a) The failure mechanism of isolated foundation.

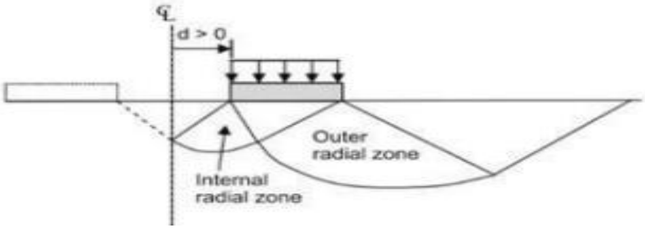

(b) The failure mechanism of closely spaced footings.

Figure 2.2 Failure mechanism of isolated foundation and closely spaced multiple footings (Lee & Eun, 2009).

2.4 Basic Finite Element Analysis

PLAXIS 3D is a finite element program that has been developed specifically to analyze the transformation and sustainability of geotechnical engineering projects. The process of graphically importing data makes the possibility that the complex samples of finite elements can be produced and analyzed easily in the minimum time. Conducting the calculation is automatic and based on the powerful finite element method. Actually, in PLAXIS, it is possible to model complex geotechnical problems such as soil and structure interaction. In the software, the Mohr-Coulomb behavior model, the hyperbolic model, the hardening soil model, softening model and Cam-Clay can be applicable. PLAXIS 3D is a finite element package considered for analysis of soil and foundation deformations and sustainability in geotechnical engineering and it possesses some features to calculate and deal with various aspects of complex geotechnical structures and construction procedures. In the finite element method, the Earth is essentially a continuous model and discontinuities can be modeled separately. The program environment is divided into a limited number of elements connected at node points. Each element is finite, i.e. It has specific geometry and a limited size (Shafaghat et al., 2018).

An equation system that relates unknown values to known ones is expressed in terms of a stiffness matrix. In addition, the basic components of the structural objects can be assigned to the geometric model for simulating the tunnel cover and the walls. After the components of the geometric model are created, some data sets should be imported for modeling the materials depending on the behavioral model chosen for the analysis of the finite element in the software (Shafaghat et al., 2018).

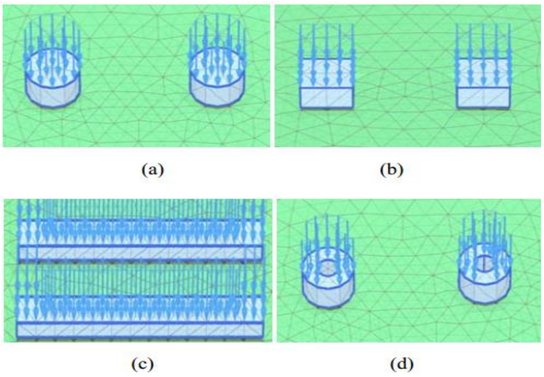

Figure 2.3 Geometry, meshing and loading of the (a) Circular, (b) Square, (c) Strip, and (d) Ring foundation model

2.5 Some Soil Test Methods

Index properties tests: - Moisture Content, Unit Weight, Specific Gravity. Index properties tests are used to compute soil volume and weight components. Ordinarily, determine moisture content for all the representative samples (disturbed or undisturbed) for classification and grouping of materials in principal strata.

Grain Size Analysis: - Sieve analysis test is performed to determine the percentage of different grain sizes contained within a soil. The mechanical or sieve analysis is performed to determine the distribution of the course, larger-sized particles, and the hydrometer method is used to determine the distribution of the finer particles.

Triaxial Shear Test: The tri-axial shear test is the most versatile of all the shear test testing methods for getting the shear strength of soil i.e. Cohesion (c) and Angle of Internal Friction (ϕ), though it is a bit complicated. This test can measure the total as well as effective stress parameters both. These two parameters are required for the design of slopes, calculation of bearing capacity of any strata, calculation of consolidation parameters, and many other analyses.

This test can be conducted on any type of soil, drainage conditions can be controlled, pore water pressure measurements can be made accurately and volume changes can be measured. In this test, the failure plane is not forced, the stress distribution of the failure plane is fairly uniform and the specimen can fail on any weak plane or can simply bulge.

2.6 Correlations Between Standard Penetrations Test (SPT) And Shear Strength Parameters

Estimating geotechnical parameters using in-situ tests such as the standard penetration test (SPT) is widely performed in civil engineering projects due to the lack of required types of equipment, time constraints, financial issues, and disturbed samples (Sivrikaya & Tougrol, 2006; Yagiz et al. 2008). Besides, geotechnical properties of various soils are widely studied to analyze their parameters and obtain the possible relations among them (Boadu 2018; Foroutan et al (Kumar et al., 2016a). The Standard Penetration Test (SPT) is widely used to determine the in-situ properties of soil. The test is especially suited for cohesionless soils as the correlation between the SPT value and φ is now well established. In Bangladesh this test is widely used for all types of soil(BNBC, 2020; Rahman, 2019).

When performing SPT, a standard sampler attached to a 63.5 kg hammer falls from 760 mm. A split spoon sampler placed in the bottom of the borehole is pushed 450 mm in the soil through this test(Md et al., 1902). However, the SPT-N number is the number of hammer's impact for the ultimate 300 mm running of the split spoon sampler in the soil(Chu et al., 2021). Based on Eq. (12) proposed by (Robertson and Fear, 1996), the SPT number based on 60% energy (N_{60}) can be corrected using the coefficients such as borehole diameter correction (C_B), sampler conditions (C_S), drilling rod length (C_R), and energy ratio of the hammer (C_E)(Ghoreishi et al., 2021).

$$N_{60} = N_{measured} * C_E * C_B * C_S * C_R \quad 12$$

$$N_{55} = CN * N_{measured} * C_E * C_B * C_S * C_R \quad 13$$

$$N_{70} = CN * N_{measured} * C_E * C_B * C_S * C_R \quad 14$$

$$(N_1)_{60} = CN * N_{60} \quad 15$$

(Bowles, 1976) $CN = \left(\frac{95.76}{\sigma'_0}\right)^{1/2}$

widely used relationships for CN (Data, 2015; Peck et al., 1974) $CN = 0.77 \log(\frac{2000}{\sigma'_0})$

Liao and Whitman"s relationship (1986) $CN = \sqrt{\frac{100}{\sigma'_0}}$

Where CN = Overburden pressure correction factor σ'_0 is in kN/m2 or kPa.

The derived empirical relationships to estimate the shear strength parameters based on SPT-N_{60}.

Where C is the cohesion in Kg/cm^2 and ϕ is the internal friction angle in degree.

Some relationships proposed by previous researchers (Kumar et al., 2016b)

Table 2.1correlation equation of hear strength parameter.

Relationships	References	Soil type
$\emptyset = 27.1 + 0.3N_{60} - 0.00054N_{60}^2$	Wolff (1989)	Sandy soils
$\emptyset = 0.7N_{60} + 18$	(Mujtaba et al., 2018)	Sandy soils
$\emptyset = \sqrt{0.3{N_{60}}^2 + 27}$	(Peck et al. 1953)	Sandy soils
$C = 0.014N_{60} - 0.18$ $\emptyset = 0.209N_{60} + 19.68$	(Mahmoud, 2013)	Silty clay with sand
$C = 0.0101N_{60} - 0.004$ $\emptyset = 0.83N_{60} + 1.24$	(Ghoreishi et al., 2021)	Clay soil
$E = 5(N + 15)$ $E = 3.33(N + 5)$ $E = 4(N + 12)$ Un corrected N values of SPT	Webb (1969)	Saturated silty sands Clayey sands Sands with intermediate fine contents

2.7 Methodology

2.7.1 Introduction

The methodology used to investigate effect of footing shape was a reviewed in different papers which are published in different year and countries that are related study on Effect of Footing Shape on Bearing Capacity and Settlement. The researchers were conducting analytical, experimental and numerical analysis to achieve the goal.

2.7.2 Experimental method

Besides these theoretical analyses a number of small-scale model test have been performed by different researchers (Alwalan, 2018). For the designing of any shallow foundation, it is obligatory to have experimental data related to finding bearing capacity of the soil at the suitable depth. For this plate load test is carried out on the site at desired depth. This test is performed on the field to examine ultimate bearing capacity of the soil at any suitable depth, the experimental details from the plate load test is helpful to confirm the design assumptions made from soil test(Patel & Bhoi, 2019).

For performing the experiment, the researchers used specially designed footings with different shapes; strip, circular, square, rectangular. All the tests were carried out on compacted layer. After placing the footings on sand layer load is applied through hydraulic jack gradually and the settlement for each increment of load is recorded through Dial gauges and LVDT (Linear Variable Deformation Transducer). The experiment program consists of the carrying out load bearing test on footing, solid circular footing, square and rectangular footings. The data obtained from the model tests were used to establish relationship between load, settlement and footing pressure (Patel & Bhoi, 2019).

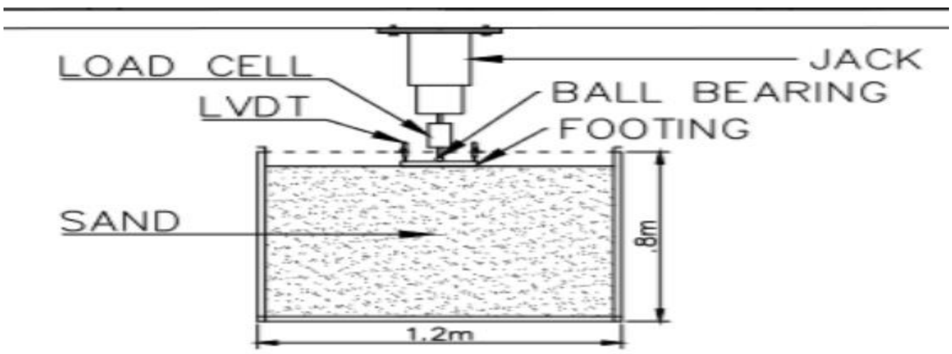

Figure 2.4 Experimental setup

2.7.3 Numerical methods

The ABAQUS, computer program (Optum G2) and advanced features of PLAXIS 2D/3D finite element program are applied to create the required load –displacement diagrams.

(S. Gupta & Mital, 2019)Finite element method (FEM) based software, used to accomplish the deformation and flow analysis of geotechnical engineering projects. 2D/3D analysis may be modeled by plain stain or axisymmetric model. Steps in PLAXIS analysis: -

- Geometry of soil model: - First, a geometric model was created with dimensions
- Material: - The Mohr-Coulomb model was adopted for dry sandy soil and the linear-elastic model was implemented for which contains five parameters, i.e., two elastic and three strength parameters. The values of elastic and strength parameter is (G/E kN/m3, μ=) and (C= kN/m3, ϕ= ^{0}, ψ =^{0}).
- Finite element meshing: - In this analysis, PLAXIS software generates automatically 2D/3D mesh.
- Calculations: - Calculating phase of the soil model
- Result analysis
- Failure mechanism

2.8 Related Work

(Altaweel & Shakir, 2021a), Conducts numerical analyses to determine the bearing capacity of soil under interference of two asymmetric strip foundations. The researchers were used limit equilibrium method considering the soil failure theory under a rough based strip foundation. For two adjacent foundations, the analysis presented in the study showed that the bearing capacity of soil for an individual foundation is affected by a quantity called the efficiency factor, when a neighboring foundation is at a distance located within the failure zone of the first foundation, and therefore the impact factor will be reflected on both foundations.

(Shafaghat et al., 2018) Investigating the effect of adjacent foundations' geometry on the bearing capacity and settlement on sandy soil and comparing with the similar state of an isolated foundation. The researchers compared data of bearing capacity and the settlement of each isolated and adjacent foundation and load-settlement diagrams of each model are no longer effect to each other after S/B=3.

(Patel & Bhoi, 2019) Experimentally investigate on the effect of shape of footing on its bearing pressure when rested on granular soil under centric loading. Plate load test were carried out on the dry river sand with two different relative densities (60% and 80%) to obtain the relation between load-settlement and L/B ratio. It has been observed that the bearing pressure varies in increasing order as Solid Circular, Square, and Rectangle.

It is found that the bearing pressure varies as the L/B ratio increases in the case of the square footing and square footing had higher bearing pressure than the circular footing. The failure of the footings occurred in order of circular, square, rectangular (case L/B = 2) and rectangular (case L/B =1.5). Performance of all the footings in 80% relative density is higher than that in 60% relative density.

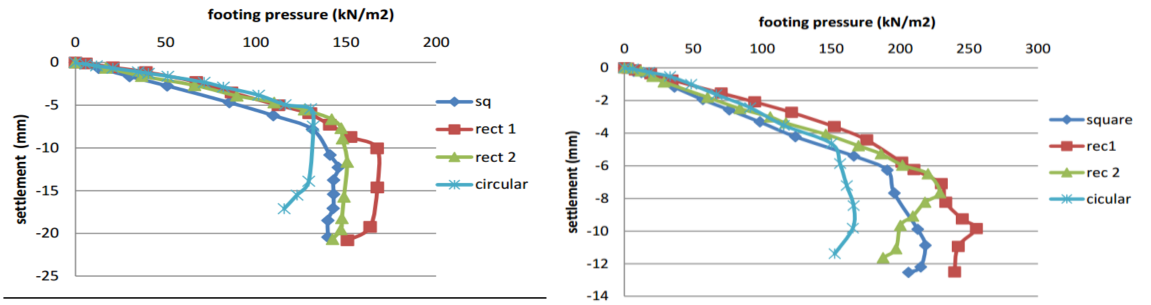

Figure 2.5 60% and 80% Relative Density

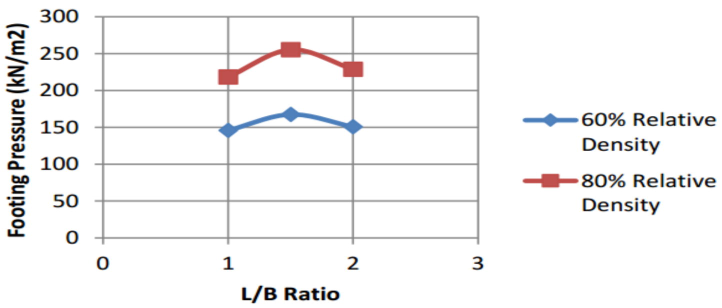

Figure 2.6 Ultimate Pressure v/s L/B ratio

It can be seen that for square footing at L/B ratio 1.5 the ultimate pressure is maximum after that it decreases

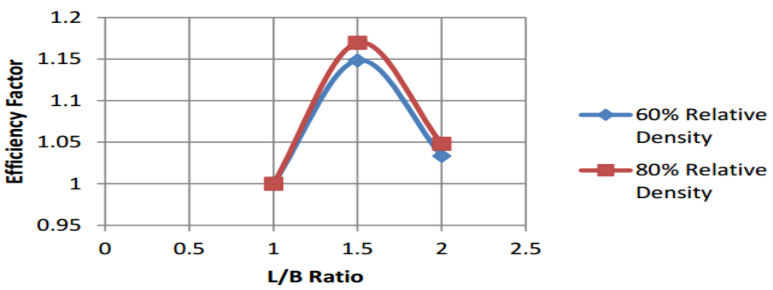

Figure 2.7Efficiency Factor v/s L/B ratio

The graph between the efficiency factor and L/B ratio is plotted for both the relative densities (60% and 80%) and shown in Fig 4.8 It is clearly observed that the Efficiency of the Square footing with L/B Ratio = 1.5 is maximum.

(S. Gupta & Mital, 2019) Conducted investigation on the effects of the soil bearing pressure values of the rectangular shape footing located on the horizontal ground surface using PLAXIS software. The values of elastic and strength parameter of the soil is (G=500kN/m3, μ= 0.33) and (C= 0 kN/m3, ϕ= 30^0, ψ =0).

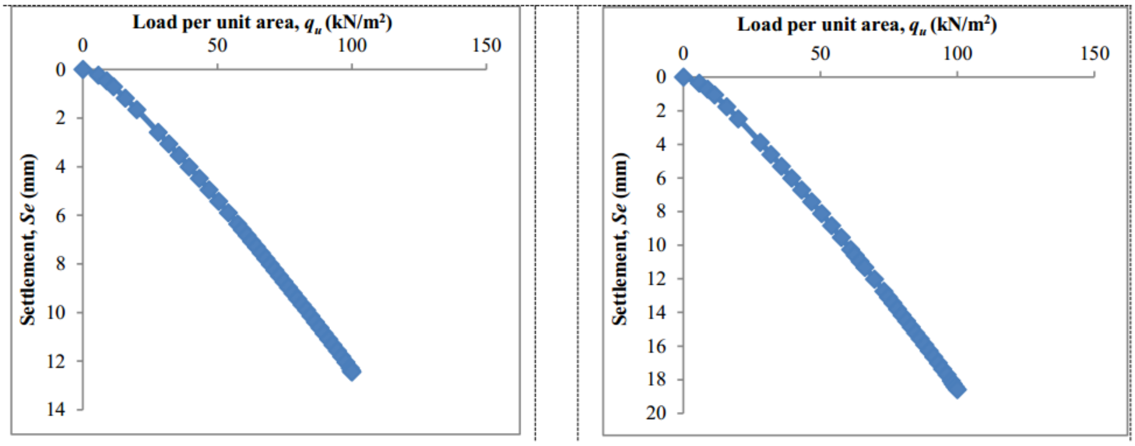

Figure 2.8 2 D Load settlement curve.

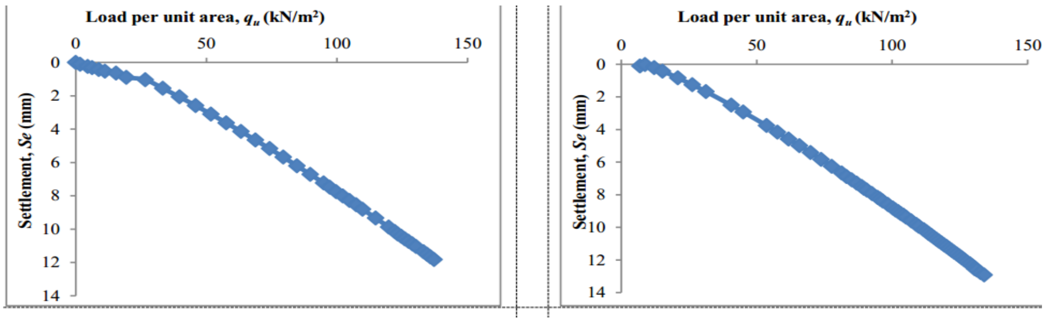

Figure 2.9 3D Load settlement curve

Failure mechanism: - The obtained failure mechanism in the 3D numerical analysis for corner and center located modeled. These figures are indicating that the total settlement and shear strain of the model foundation at peak load.

Allowable bearing pressure of the rectangular footing located at the left corner and center of the soil model was 112.3 KN/$m^2$and 111.8 KN/m^2 from 2D analysis and 132.3 kN/m^2 and 131.7 kN/m^2 from 3D analysis respectively. A comparison of 2D and 3D analysis gave a good estimation of the allowable bearing pressure of the soil. The 3D analysis gave a higher value of the ultimate bearing capacity as compared to 2D analysis.

(Panwar & Dutta, 2020)Investigated the ultimate bearing capacity of the rectangular footing with L/B ratio 1.5 and rested over layered sand using finite element method.

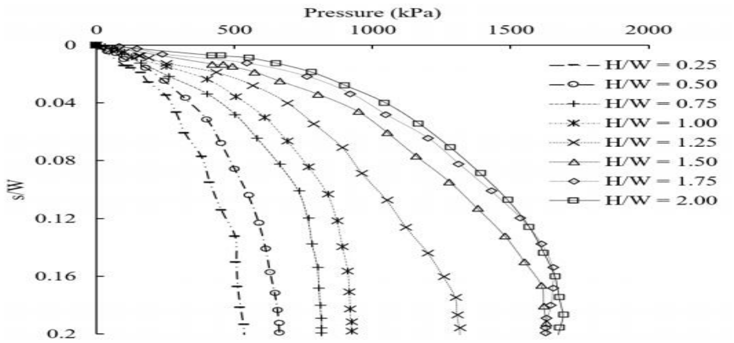

Figure 2.10 Pressure settlement ratio plot for the rectangular footing on layered sand at ϕ1 (41°) and ϕ2 (31°) corresponding to different H/W ratio.

The ultimate bearing capacity (qult) was taken as the minimum of peak pressure or pressure corresponding to normalized settlement (s/W) = 10%, whichever occurs earlier. In the this study the upper layer denser sand layer friction angle was varied from 41° to 46° and for the lower layer of loose sand, it was varied from 31° to 36° for the parametric study. The results reveal that the dimensionless ultimate bearing capacity was found to increase up to an H/W ratio of about 1.75 beyond which the increase was marginal. The results further reveal that the dimensionless ultimate bearing capacity was the maximum for the upper dense and lower loose sand friction angles of 46° and 36°, while it was the lowest for the upper dense and lower loose sands corresponding to the friction angle of 41° and 31°.

For H/W = 0.5 and 2, the dimensionless bearing capacity decreases with the increase in the L/W ratio from 0.5 to 6 beyond which the dimensionless ultimate bearing capacity remains constant for all combinations of parameters.

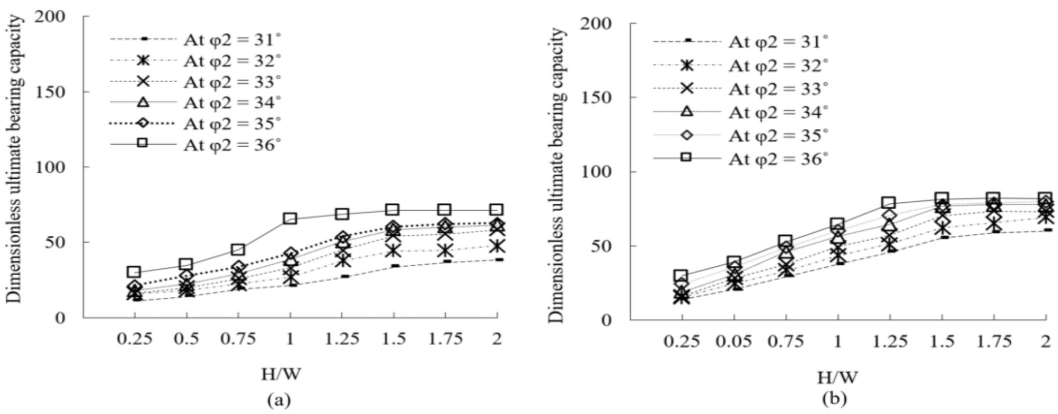

Figure 2.11 Dimensionless ultimate bearing capacity versus H/W curves for upper dense sand layer friction angle (ϕ1) (a) 41°, (b) 42°

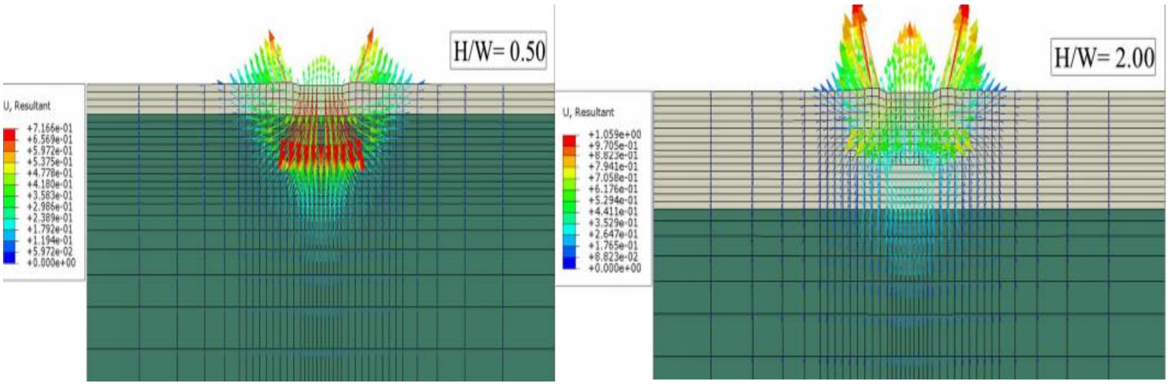

Figure 2.12 vectorial displacement of layered sand at different H/W ratio

Analysis of these the vectorial displacement vector shows a clear punching failure when the upper dense sand layer was having a very small thickness (H/W=0.5) as Vertical displacement vector reaching to the lower loose sand layer. Further, for H/W = 2, with the increase in the thickness of the upper dense sand layer, the vectorial displacement vector remains contained in the upper dense sand layer. This shows that, the dimensionless bearing capacity decreases with the increase in the L/W ratio from 0.5 to 6 beyond which the dimensionless ultimate bearing capacity remains constant for all parameters combinations.

This is attributed to the fact that under the constant load, the area of the rectangular footing increases with the increase in the L/W ratio resulting decrease in the dimensionless ultimate bearing capacity.

(Radwan, 2021) Investigated numerically the effect of foundations shape on bearing capacity The researchers used square, circular and rectangular footing of width to length ratios L/B=1.5 and 2 respectively on sand compacted to relative density 60% and 80%.

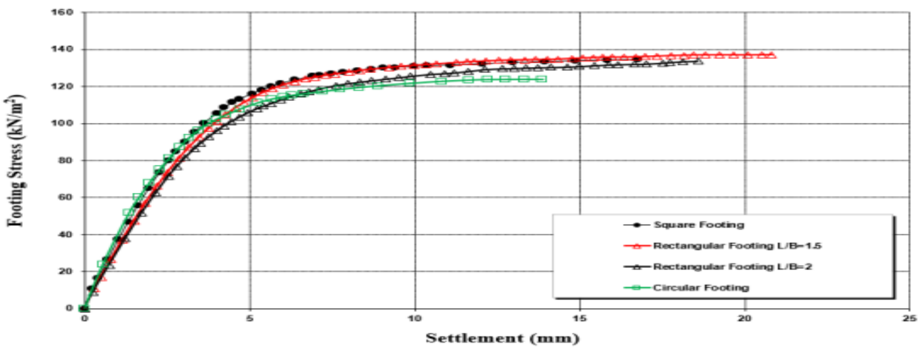

Figure 2.13 Load-Settlement curve for different shapes of footing in case of medium sand (Dr=60%)

It was observed that the ultimate bearing capacity of square footing has a higher value than rectangular and circular footings for both cases of medium and dense sand. Also, it was observed that the bearing capacity of rectangular footing with L/B ratio of 2 is less than the footing with L/B ratio of 1.5.

(Khatri et al., 2022) Conducted the bearing capacity of the strip and circular footings resting on layered sand was estimated using the computer Program (Optum G2 2019). Bearing capacity at failure and 10% settlement for the strip and the circular footings placed on layered sand with dense sand stratum lying over loose sand deposit was evaluated numerically following the finite element method.

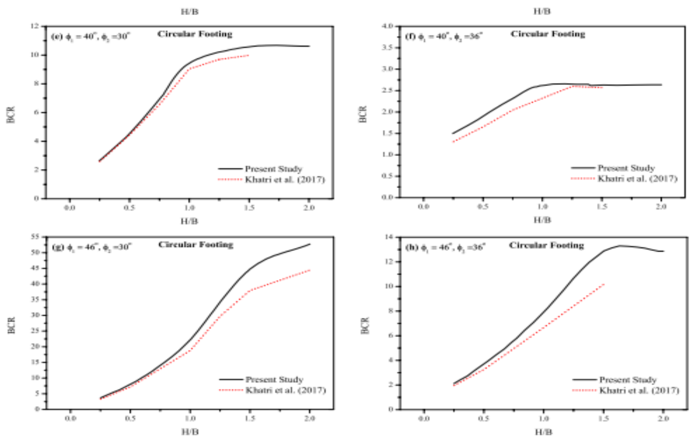

Figure 2.14 Comparison of present BCR with BCR from literature: strip footing and circular footing

$$SFR = \frac{\left(\frac{S}{B}\right) homogenous, peak - (\frac{S}{B}) layered}{(\frac{S}{B}) homogenous, peak} * 100,$$

$$BCR_U = \frac{q_u layered\ sand}{q_u\ homogenous\ sand}$$

Where SRF is defined as the ratio of the difference in the settlement

The bearing capacity was increased substantially by having a thin layer of dense sand just underneath the base of the footing. Both BCRu and BCR10 were increased with an improvement in the top-dense layer's friction angle; while the values for these two quantities decreased with a rise in the $\phi_2$of the loose-bottom sand layer for a fixed value of $\phi_1$for the dense top sand layer.

For foundation on layered sand, for a selected range of soil parameters, the improvement in ultimate bearing capacity was in the range of 104 to 146% and 125 to 252% for strip and circular footings, respectively. Whereas the bearing pressure corresponding to 10% settlement was found to lie between 572.4 to 5380.2kN/m^2 for strip footing and 891.6 to 6011.4 kN/m^{2}for circular footing.

- The BCRu and BCR10 values indicated the increase in the bearing capacity ratios; the increase was more significant for circular footing than strip footing. Furthermore, the bearing capacity became constant using a thin dense layer below a circular footing, whereas a thick, dense layer was required under the strip footing.
- The SRF value remained almost constant for all combinations of dense sand overlying loose sand. Furthermore, the SRF values were slightly higher for circular footing than strip footing, indicating that less settlement occurs using a circular footing than strip footing.

The normal stress for the case of layered sand was higher than its value on the homogeneous layer of sand. As H/B values increase further, the normal stress becomes significantly high.

(A. Gupta et al., 2017) Results are presented in the graphical form for the variation of normalized ultimate bearing capacity with normalized cohesive strength of clay $\frac{c}{\gamma_1 B}$ Thickness ratio $\frac{H}{B}$ dispersion angle of the load α and also with length to width ratio $\frac{L}{B}$ in case of rectangular footing.

Parameters were varied as follows. Normalized cohesive strength of clay=0.5 and 1.0. The soil friction angle ϕ =25^0, 30^0, 35^0 and 40^0. Mobilized angle of shearing resistance $\delta = \emptyset$ and $2\emptyset/3$.

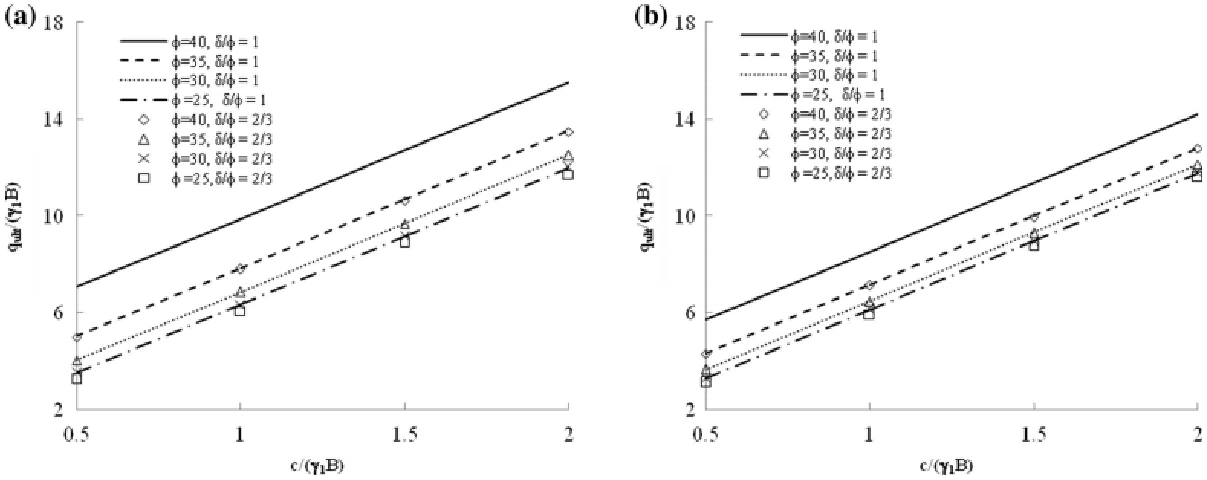

Figure 2.15 Plot for rectangular footing (length to width ratio=2)

Depicting the variation of normalized ultimate bearing capacity with normalized cohesive strength of clay when thickness ratio=0.5 and depth ratio=0, a $\alpha=0^0$and b $\alpha=30^0$

Fig. 4.18 a reveals that with the increase in normalized cohesive strength of clay from 0.5 to 2.0, the normalized ultimate bearing capacity increases as it is obvious from the proposed equations that there is a proportionate relation between normalized ultimate bearing capacity and normalized cohesive strength of clay. Moreover, with the increase in the undrained cohesive strength there is an increase in the overall bearing capacity of the layered soil. 4.18 b. Study of this figure reveals that the trend of variation of normalized ultimate bearing capacity with normalized cohesive strength of clay is similar to the case when dispersion angle of the load is 0^0, but the values of normalized ultimate bearing capacity are lower for soil friction angle of 25^0,30^0,35^0 and 40^0 in comparison to the case when dispersion angle of the load is 0^0. Normalized ultimate bearing capacity is inversely proportional to the dispersion angle of the load. With the increase in thickness ratio there is an increase in the normalized ultimate bearing capacity.

CHAPTER THREE METHODOLGY

3.1 Description of The Research Area

The soil data used in this research are secondary data collected from Adama town. Adama town, which is located in the main rift valley, East Showa zone of Oromia National Regional State in Ethiopia. Geographically the research area is located at 525,000m to 535,000m E Longitude and 935,000m to 950,000m N latitude. It is located at an average elevation of 1712m. The town is located 99 km southeast of the capital Addis Ababa. The climate condition of the town is whether: 21^0C, Wind NE at 16km/h and 42% humidity, and subtropical climate. It receives maximum rainfall during summer (July and August).

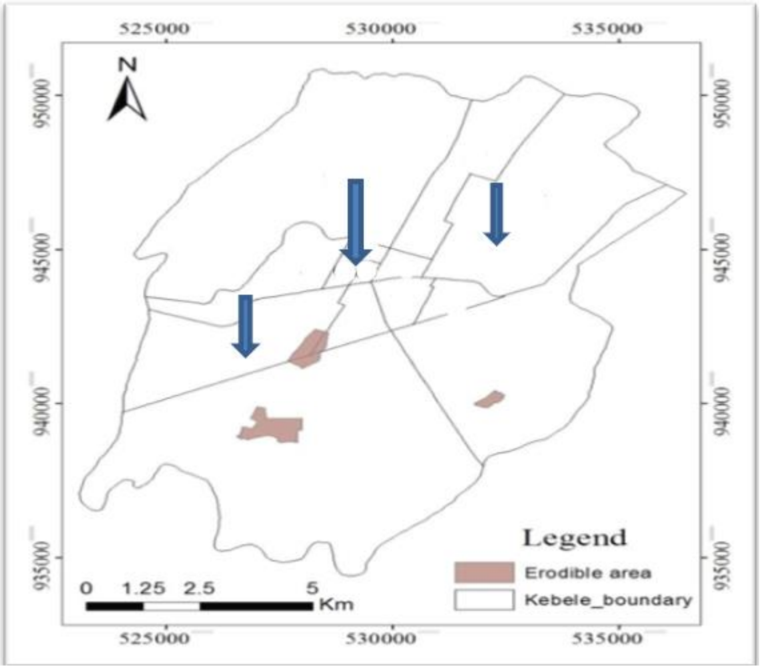

Figure 3.1 Map of Adama town source https://images.app.goo.gl/P7psMNVJgWppoTL9

3.2 Research Design

This chapter contains the methodology which were used to numerically investigate the effect of footing shape on bearing capacity and settlement. The research design was focus on a method to collect and analyze geotechnical data used by PLAXIS 3D to estimate bearing capacity and settlement of adjacent footing. The methods Starts from data collection and preparation. The next step is model setup and comparisons of the results.

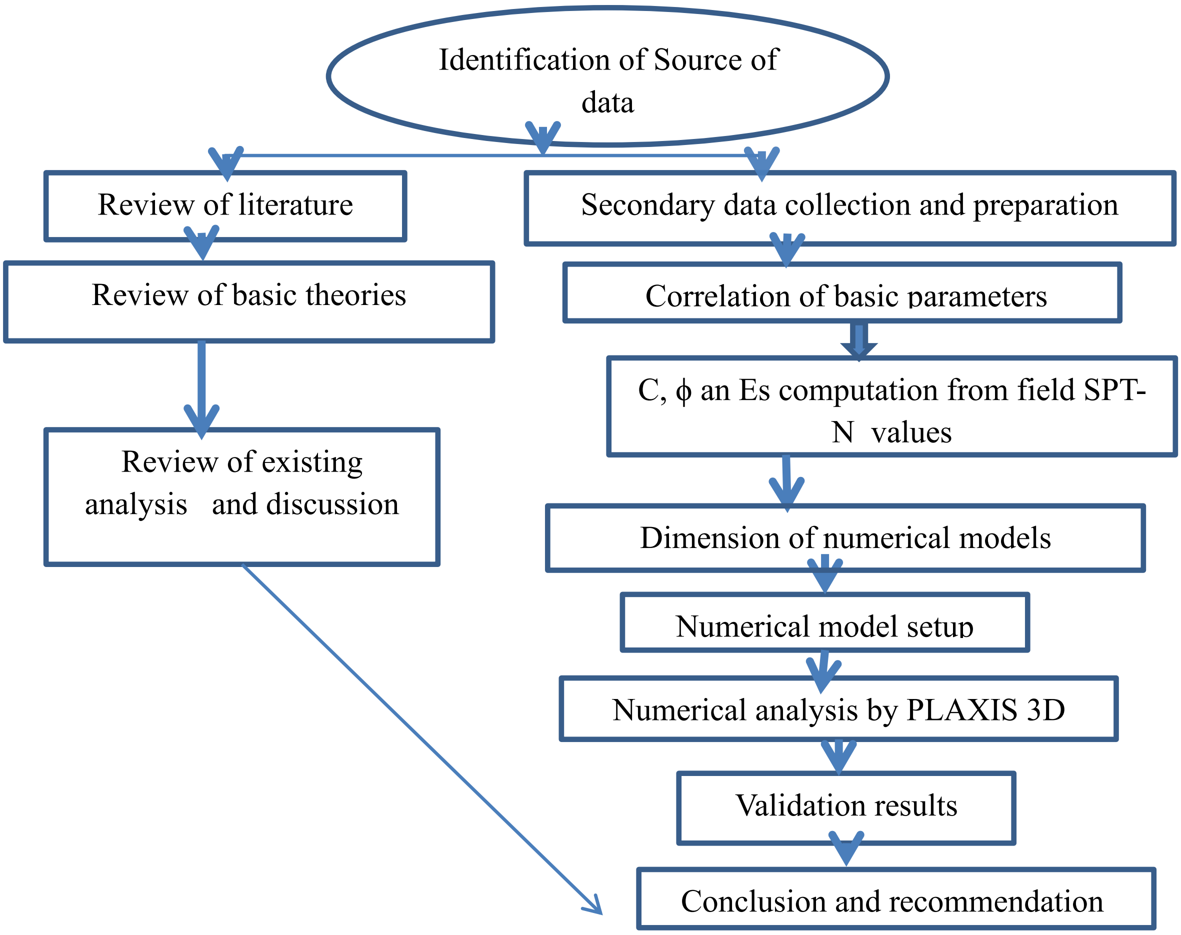

Figure 3.2 Research design flow chart.

3.3 Materials

The soil parameters considered for this study were obtained from four (4) soil investigation reports of separate projects in Adama city. The variables used for the design of this research: - unit weight, cohesion, modulus of elasticity, poison ratio and angle of internal friction (ϕ) were correlated from Standard Penetration Test (SPT) of soil investigation report. The analysis was performed using PLAXIS 3D Connect Edition V20.

3.3.1 Geological Condition and Soil Layer

Sub-surface geotechnical investigation was conducted for building which includes drilling borehole in-situ and laboratory test as reported by Jeroccia Geotechnical Service and PLC, Rak Engineering and Construction PLC, Dynamic Geotechnics PLC and ZTY Engineering PLC.

In the first soil location three soil layer was appeared made ground or fill material with maximum thickness of 2m, silt with same sand extends below the top soil layer with thickness of 15.2m and the third soil layer completely weathered rock into yellowish dense silty sand with same gravel and it appears with maximum layer thickness of 9m. From investigation of the second and third soil location two main geotechnical layers are identified. The layers are light reddish medium stiff low plastic silty sand with minor gravel extends to 4.5m and reddish stiff low plastic silty sand with minor gravel from 6m for second location and light brownish medium dense to dense, non-plastic Silt with some sand extend to thickness of 7.5 m from surface and brownish, very dense, non-plastic sandy silts with trace of gravel from 7.5 to 16m for third location. The fourth location have two layers, Dark brown, stiff medium to high plastic clayey silt with trace of sand and gravel maximum layer thickness of 2m from ground, light grey to yellowish, dense/stiff to very stiff, non to low plastic silty sand /clayey sand with trace of gravel is encountered from the upper layer to the end of drilling. Ground water was not encountered in borehole during investigation in all cases.

The data for this thesis study were soil investigation report of Dagaagaa kebele, Dembela Sub-city, Odaa kebele Abbaa Gadaa sub-city and Dhaddacha Araraa kebele Boolee sub-city.

Table 3.1 Layer thickness and soil type

Layer No	Layer thickness (m)		Location 1 Soil type	USCS designation
1	13	Soil 1	Dense High plasticity silt with same sand	ML
2	2.2		Medium plasticity silts with same sand	ML
3	2.8		Dense to Medium dense yellowish Silty sand	SM
4	7			SM
1	4.5	Soil 2	Loose low plasticity sandy silt with minor gravel.	ML /MH
2	1.5		Medium dense sandy silt with minor gravel	ML
3	14		Dense fractured rock	SG
1	6	Soil 3	Medium dense to dense, non-plastic SILT with some sand	ML
2	10		Very dense, non-plastic sandy SILT with trace of gravel	ML
1	2	Soil 4	Dark brown very dense medium to high plastic clayey silt with trace of sand and gravel	MH
2	6		Light grey to yellowish Non to low plastic Clayey Silt with same sand and trace of gravel	ML
3	4		Light grey to yellowish Medium plastic silt, or clayey silt with minor sand and trace of gravel	ML
4	4		Light grey to yellowish Non to low plastic silt or clayey silt with minor sand and trace of gravel	ML
5	9		Light grey to yellowish Medium plastic clayey silt with trace of gravel	ML

3.4 Correlation of Basic Soil Parameters

The soil type used in this study that have been collected from soil investigation report are shown in preceding section and Appendix-B. However, the data from soil investigation reports are not complete in terms of the requirements of soil parameters used for the numerical analysis. From geotechnical reports only basic soil parameter are obtained directly and the parameters used for numerical analysis in this research have been derived by empirical correlation based on literature, geotechnical codes and standards.

3.4.1 Modulus of Elasticity (Es)

Describe the load settlement behavior of soils and governs the results of settlement- related problems. It is the ratio of the stress along an axis over the strain along that axis in the range of elastic soil behavior. To obtain better simulation of actual soil condition, it is highly recommended to use reasonable practical values that represent the in-situ soil condition. Several empirical correlations were available to obtain modulus of elasticity values from SPT-N values corrected for overburden pressure.

Empirical correlation of Es in kN/m^2 for different type of soil (BNBC, 2020; Bowles, 1976; Transportation, 2017).

Soil type	Equivalent Elastic Modulus (kN/m^2)
Silts, sandy silts slightly cohesive mixture	$400(N_1)_{60}$
	$300(N_{55}+6)$
Clean fine to medium sands and slightly silty sands	$700(N_1)_{60}$
Coarse sands and sands with little gravel	$1{,}000(N_1)_{60}$
Sandy gravel	$1{,}200(N_1)_{60}$
Clayey sand	$320(N_{55}+15)$
Sand normally consolidated	E = 500(N_{55}+15)
	=$7000\sqrt{N_{55}}$
	=6000N_{55}
Gravely Sand	E= 1200(N_{55}+6)
	=600(N_{55}+6), N$\leq$ 15
	=600(N_{55}+6) +2000, N>15

The SPT-N values obtained from field test was adjusted for (energy, borehole, sampler and road length) factors reasonably to standardize (Skempton, 1986).

$N_{60} = N_{measured} * C_E * C_B * C_S * C_R$, and $(N_1)_{60} = CN * N_{60}$ 3.1

$N_{55} = CN * N_{Measured} * C_E * C_B * C_S * C_R$ 3.2

The overburden pressure $CN = (\frac{95.76}{\sigma'_0})^{1/2}$ (Bowles, 1976) 3.3

$CN = 0.77 \log(\frac{2000}{\sigma'_0})$ (Data, 2015; Peck et al., 1974) 3.4

Table 3.2 correct SPT-N values

Layer	Average corrected SPT-N value				
	N_{55}	N_{70}	N_{60}	$(N_1)_{60}$	
1	16.1	12.6	16.1	14.8	
2	15.6	12.3	16.1	14.3	
3	13.7	10.7	14.1	12.5	
4	13.4	10.5	13.8	12.2	Soil 1
1	6.3	7.4	4.3	6.3	
2	17.5	22.2	18.2	14.5	
3	32.0	39.7	37.5	29.0	Soil 2
1	19.0	15.0	15.0	18.0	
2	29.0	23.0	35.0	26.0	Soil 3
1	50.6	39.8	39.9	46.4	
2	46.0	36.2	39.1	42.2	
3	17.2	13.6	17.3	15.8	
4	22.2	17.4	22.8	20.3	
5	22.9	18.0	23.6	21.0	Soil 4

3.4.2 Poisson's Ratio

Poisson's ratio is a characteristic that represent a material volume change in direction perpendicular to the load application. For elastic material Poisson's ratio, the shear modulus G' cannot be (-) and $-1 \leq \mu \leq 0.5$. The range of Poisson's ratio for soil that are not elastic is from about $-1 \leq \mu \leq 1$ (Bowles, 1976). Standard drained triaxial testes may yield a significant rate of volume decrease at the very beginning of axial loading and, consequently, a low initial value of Poisson's ratio(μ_s). For same cases, such as particular unloading problems, it may be realistic to use such a low initial value, but in general when using Mohr-Coulomb model the use of higher value is recommended (PLAXIS, 2020).

(Bowles, 1976) recommends a Poisson's ratio of 0.3-0.4 for cohesionless medium and dense soil and 0.2- 0.35 for loose to medium soil. For numerical analysis of this study Poisson's ratio were used from table Appendix- C 3 (Bowles, 1976) as recommended by PLAXIS manual.

Poisson's ratio may be taken equal to 0.2 for uncracked concrete and 0 for cracked concrete(CEN (European Committee for Standardization), 2004; Development, 2013).

3.4.3 Cohesion

A correlation has been built between soil cohesion with their corresponding SPT-N values as follows:

$C = -2.2049 + 6.484N$ $(R^2 = 0.998)$ (Kumar et al., 2016) where, C cohesion, kPa; N SPT N value (range 2–30).

$C = -16.5 + 2.15N$ $(R^2 = 0.998$ (Kumar et al., 2016) where, C cohesion, kPa; N SPT N value (range 10–30).

For soil with SPT N values greater than 30 cohesions were used from table Appendix C 2.

3.4.4 Angle of Internal Friction

Angle of internal friction obtained by correlation methods provided in literature and geotechnical manual.

$\emptyset = 27.12 + 0.2857N$ (Kumar et al., 2016) for N ranges from (4 to 50) where ∅ = Angle of friction, (in degree); N is uncorrected SPT N values

Friction angle of granular soil has been correlated to SPT- N values by relation provided by (Hatanaka and Uchida, 1996)

$\emptyset = \sqrt{N_{1_{60}}} + 20$ where $N_{1_{60}}$ is SPT-N value normalized to 95.6kN/m^2

3.4.5 Dilatancy

Dilatancy angle, ψ is specified in degrees. Clay soils tend to show little dilatancy $\psi \approx 0$, dilatancy of sands depends on both density and friction angle(PLAXIS, 2020). The dilatancy of cohesionless soil was determined by $\psi = \emptyset - 30^0$

3.4.6 Tension Cut-Off and Tensile Strength

For Mohr-Coulomb model the tension cut-off is, by default selected with tensile strength of zero (PLAXIS, 2020).

3.4.7 Saturated and Unsaturated Unit Weight

The bulck unit weight used in this study was obtained from geotechnical soil investigation reports and Correlation method provided by (Peck et al., 1974). And the bulk unit weight is determined based on (Bowles, 1977; *Caltrans Geotechnical Manual*, 2021).

3.5 Numerical Model Setup and Method of Numerical Analysis

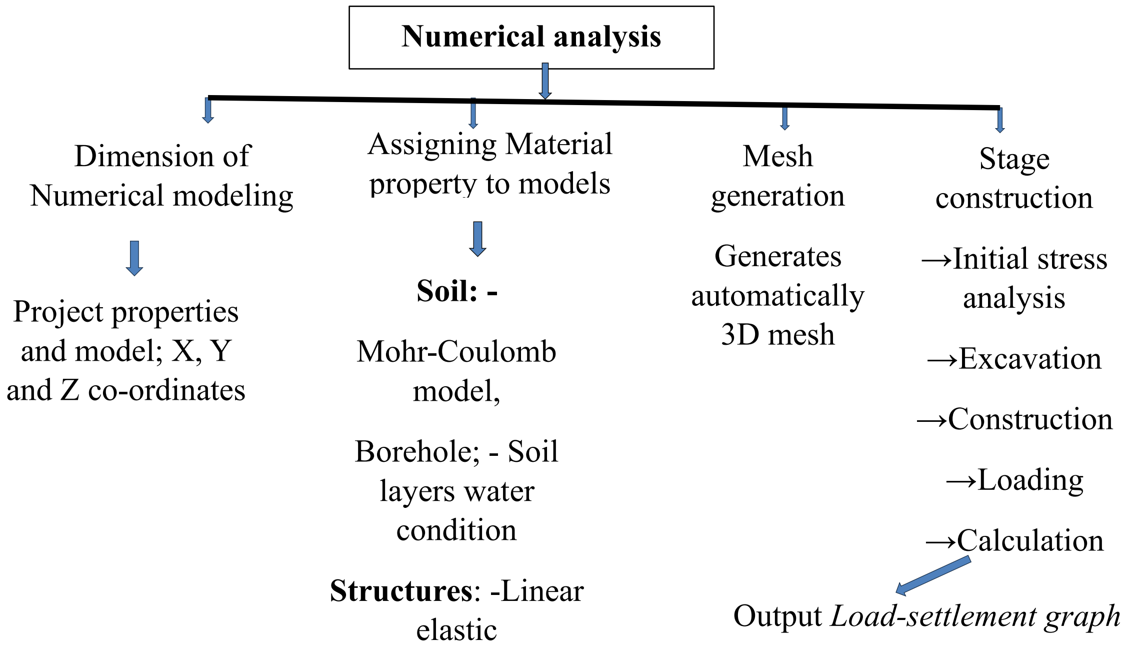

3.5.1 Numerical Model Setup

To achieve the objectives of this research review of related literature, basic facts, theories and correlation of soil parameter have been done before conducting numerical model setup. PLAXIS 3D Connect Edition V20 computer program was used to predict bearing capacity and settlement of isolated and adjacent shallow footing. Three-dimensional finite element analysis by PLAXIS 3D requires dimension, soil and interface properties material model types, basic soil parameter (young's modulus of elasticity, Poisson's ratio, unit weight, friction angle and dilatancy angle).

PLAXIS 3D is a finite element software that have been developed for the analysis of deformation, stability, and groundwater flow in geotechnical engineering. Conducting calculation is automatic and based on powerful finite element software(PLAXIS, 2019). In this research PLAXIS was used for simulating soil-structure interaction and analyzing settlement to develop load-settlement behavior of shallow foundation. Numerical model setup procedure used for different footing are presented. PLAXIS supports different models to simulate the behavior of soil and continua(PLAXIS, 2019). The models are linear elastic model, Mohr-Coulomb model, hardening soil model, soft soil model, and modified calm clay model.

For this study PLAXIS 3D was used. Linear elastic material model was used for plate and column and Mohr-Coulomb Model used for soil models. Mohr-Coulomb failure model is an elastic, perfectly plastic model based on soil parameter known in most practical situations used to compute realistic bearing capacity and collapse load of footings. It was selected for availability of basic parameter.

In addition to selecting appropriate material model the accuracy of finite element analysis depends on boundary condition, generation of mesh and stage construction for calculation. To compute bearing capacity and settlement of footing numerical modeling and analysis was done by PLAXIS 3D Connect Edition V20 finite element software. The geometrical modeling, mesh generation, stage construction and analysis used in this study are depicted below.

A. Dimension of Numerical Modeling

The dimension of the numerical model must represent a behavior when the foundations are on the ground. Minimum dimension should be considered to observe the stress development under and around the foundations. To avoid direct effect of boundaries on analysis appropriate dimension should be taken for model. Soil cluster should be included in height of 2.5L and width of 2.5L(1-μ) (Shafaghat et al., 2018; Vesic, 1973). In this study the ground level surface and bottom layer surface was modeled based on information obtained from borehole and the soil cluster dimension depths are 25m, 16m,16m, 25m for soil 1,2,3 and 4 respectively and width 50m*50m. In this study the dimension of square, circular, rectangular and strip footings are 2m*2m, 2.26m, 1.6*2.5m and 1m*10m respectively.

Minimum depth of foundation shall be 1.5m for exterior footing of permanent structure in cohesive soil and 2m in cohesionless soils(BNBC, 2020). For design of footing depth of 2m was used in this study.

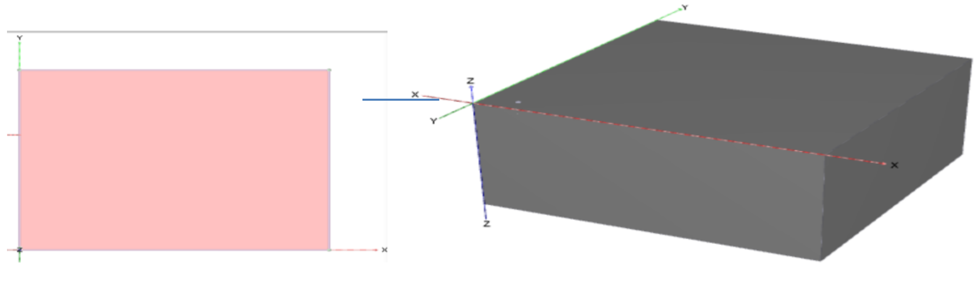

Figure 3.3 dimension of soil cluster

B. Set Material Properties to Material Models

In PLAXIS soil properties and material properties of structures are stored in material data sets. After all data sets are stored in the data base it can be assigned to the soil cluster or to the corresponding structural objects in geometry model.

Properties of Soil

For these studies four soil investigation data was collected from four different places in Adama town as mentioned in table 3.1. the Mohr- Coulomb soil model was used to represent the soil cluster.

Table 3.3 Properties of soils used in numerical modeling.

Layer thickness	Modulus of Elasticity	Unit weight (KN/m3)	Cohesion kPa	Angle of friction	dilatancy	Poisson's ratio	Soil type
	E (kPa)	γ	c	φ	ψ	μ	
13	6629	15.99	39	34.53	4.53	0.35	Soil 1
2.2	6480	15.66	46	35.39	5.39		
2.8	14087	16.53	44	35.10	5.10		
7	13753	16.48	46	35.39	5.39	0.4	
4.5	2,533	18	5	28.98	-	0.3	Soil 2
1.5	5,800	18	38	34.41	4.41	0.35	
14	34,800	19	0.3	44.08	14.08	0.4	
6	7,200	21.5 0	30	33.23	3.23	0.35	Soil 3
10	10,400	22.00	48	41.41	11.41	0.35	
2	16,607	19.11	10.00	41.52	11.52		Soil 4
6	15,613	19.44	7.00	41.39	11.39		
4	6,966	18.06	40.48	34.96	4.96	0.35	
4	8,443	19.19	7.00	39.24	9.24		
9	8,674	19.75	77.00	41.39	11.39		

3.5.2 Interference

The interference element is used to simulate the thin zone of intensively shearing at the contact between the plate and surrounding soil. The interface strength has been selected according to (PLAXIS, 2019, 2020) when the interface should not have a reduced strength with respect to the strength in surrounding soil the interface assigned as rigid Rint = 1 and if soil-structure interaction interface is weaker or more flexible than the surrounding soil Rint = {2/3, 1). In this research rigid interface strength Rint =1 was used.

Plate

The PLAXIS program allows elastic material behavior in plate or footing elements. In this study elastic plate elements were used for different size of footings. The plate material used in this project is concrete. The unit weight of normal concrete equals 24kNm2 and increased by 1kN/m2 for reinforced concrete(Development, 2013; Eurocode, 2006).

Table 3.4 Properties of footing material

Properties	Values
Material	Concrete
Unit weight (kN/m^2)	25
Material model	Linear Elastic
Drainage	Non-porous
E(MPa)	31*10^3
Poisson's ratio	0.15

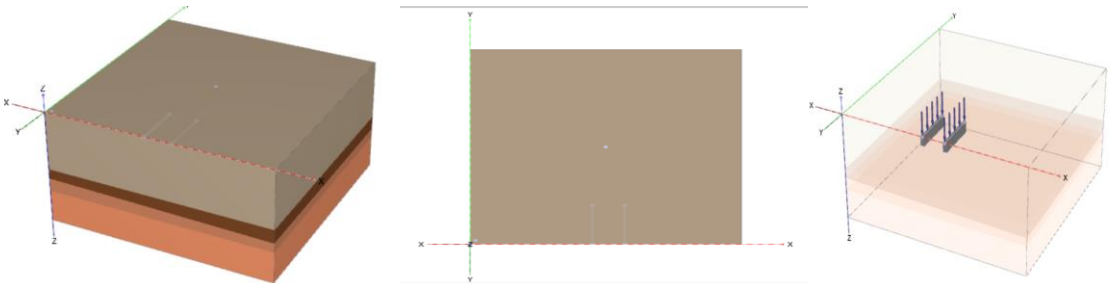

Figure 3.4 3D soil block and foundation structures

Mesh Generation

After geometry modeling was completed by mesh generation, stage construction and calculation were proceeded. Mesh used to divide geometry in to finite element in order to perform finite element calculation. Fine mesh was used to obtain accurate numerical results. The basic soil elements of the 3D finite element mesh are 10-nodede tetrahedral elements. For soil-structure interaction,12-node interface elements are used to simulate the behavior.

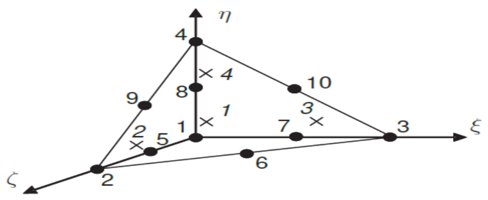

Figure 3.5 3D soil element (10-node tetrahedrons)

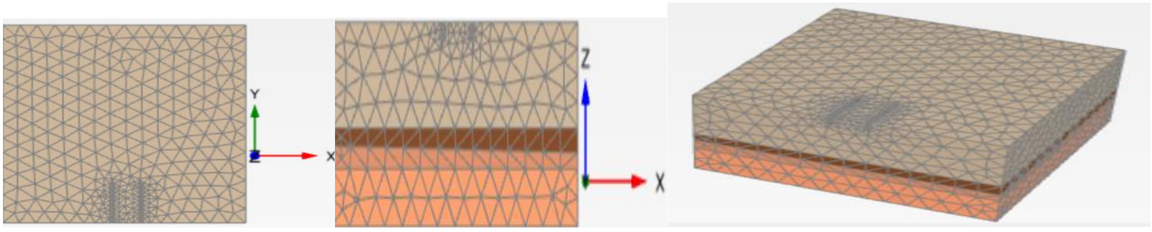

Figure 3.5 PLAXIS 3D finite element mesh

3.5.2 The Analysis Process

In PLAXIS analysis first calculation type was defined.

Initial stress analysis: - the initial phase K0 procedure generate initial stress state of soil.

Excavation: - Soil excavation for installation of plate was defined by deactivating the corresponding volume in the model. The excavation soil above the foundation was removed during this stage.

Construction: -this stage is the installation of plate and other structural objects by heading the corresponding soil volume above foundation level to check the construction level is installed correctly.

Loading

The point load was applied vertically at the center of footing column for square, circular and rectangular footings and line load applied at the center of footing wall on strip footing to estimate bearing capacity and settlement of shallow foundation. In this stage the loads are applied and geometry is checked for calculation.

OUT PUT

Bearing capacity and settlement of isolated and adjacent foundation was obtained from load settlement curves. The bearing capacity of interfering foundation was estimated based on interference (bearing capacity ratio) BCR.

$$BCR = \frac{q_{ult(int)}}{q_{ult(isolate)}} \quad 3.5$$

Where $q_{ult(int)}$ =the ultimate bearing capacity of interfered foundation

$q_{ult(isolate)}$ = the ultimate bearing capacity of isolated foundation

3.6 Comparison of PLAXIS 3D Load-Settlement Output Result

Bearing capacity and settlement output obtained from numerical analysis of isolated shallow foundation using PLAXIS 3D was compared with analytical settlement calculated for allowable load obtained from Load settlement curves. The elastic settlement of shallow foundation has been estimated using theory of elasticity.

$$S_e = q_o(\alpha B')\frac{1-\mu_s^2}{E_s} I_s I_f \quad 3.6$$

Where: - q_o = net applied pressure on foundation

μ_s = Poisson's ratio of soil

α=a factor that depends on the location on the foundation where settlement is being calculated.

Es =Average modulus of elasticity of soil under the foundation, measured from z=0 to about z=5B

B' = B/2 for the center of foundation

Is = shape factor (Steinbrenner, 1934) and

$$I_s = F_1 + \frac{1-2\mu_s}{1-\mu_s} F_2, \qquad F_1 = \frac{1}{\pi}(A_0 + A_1), \qquad F_2 = \frac{n'}{2\pi}\tan^{-1} A_2 \quad 3.7$$

$$A_o = m' \ln \frac{(1+\sqrt{m'^2+1})\sqrt{m'^2+n'^2}}{m'(1+\sqrt{m'^2+n'^2+1})}, \quad A_1 = \ln \frac{(m'+\sqrt{m'^2+1})\sqrt{1+n'^2}}{m'+\sqrt{m'^2+n'^2+1}}, \quad A_2 = \frac{m'}{n'\sqrt{m'^2+n'^2+1}} \quad 3.8$$

To calculate settlement at the center of the foundation α=4, m' =L/B and n'=H/(B/2)

If= depth factor (Fox, 1948) =f(D_f/B, μ_s, and L/B)

Settlement of rigid foundation estimated as

$$S_{e(rigid)} = 0.93 S_{e(flexible,center)} \quad 3.9$$

The probabilistic design charts provide a baseline from which all settlement prediction methods can be compared against each other. The most popular settlement prediction methods are: -

Burland and Burbidge

$$f(x) = 0.0142(x - 0.16)^{-0.21}(4.33 - x)^{1.65} \quad for \;\; 0.16 \leq x \leq 6 \qquad 3.10$$

Terzagh and peck

$$f(x) = 0.025(x - 0.55)^{-0.51}(14.29 - x)^{0.77} \quad for \;\; 0.55 \leq x \leq 14.29 \qquad 3.11$$

Schmertmann et al.:

$$f(x) = 0.0046(x - 0.39)^{-0.29}(11.3 - x)^{1.72} \quad for \;\; 0.39 \leq x \leq 11.3 \qquad 3.12$$

Statistical probability distribution function of standard deviation σ and average mean μ

$$f(x) = \frac{1}{\sigma\sqrt{2\pi}} e^{\frac{-(x-\mu)^2}{2\sigma^2}} \qquad 3.13$$

The equation 3.10 -3.12 were used to compare settlement computed by different method to limiting value 25mm. A good estimation has accuracy closer to one and reliability closer to 100%.

The probability of failure, p_f, can be defined as the probability that the actual settlement will exceed the specified limiting value. When the calculated settlement is S, and the settlement determined by PLAXIS is Y, the settlement ratio X= (S/Y) is a random variable modelled by the probability distributions given in equations (3.10) – (3.12). If the limiting value is 25 mm, the probability of failure, pf, is given by

Pf p[Y≥25} =p([S/X≥ 25] =P[X≤ $S/25$] 3.14

CHAPTER FOUR RESULT, DISCUSION AND PARAMETRIC STUDY.

4.1 Results and discussion

4.1.1 Introduction

This chapter includes the investigation of the effect of shape footing and adjacent footing geometry on bearing capacity and settlement. The effect of adjacent footing was expressed in terms of similar isolated footing. To establish the comparison 72 finite element modeling has been carried out by PLAXIS 3D Connect Edition V20. The influence of footing shape on different soil layer was also correlated by changing S/B ratio for adjacent footing.

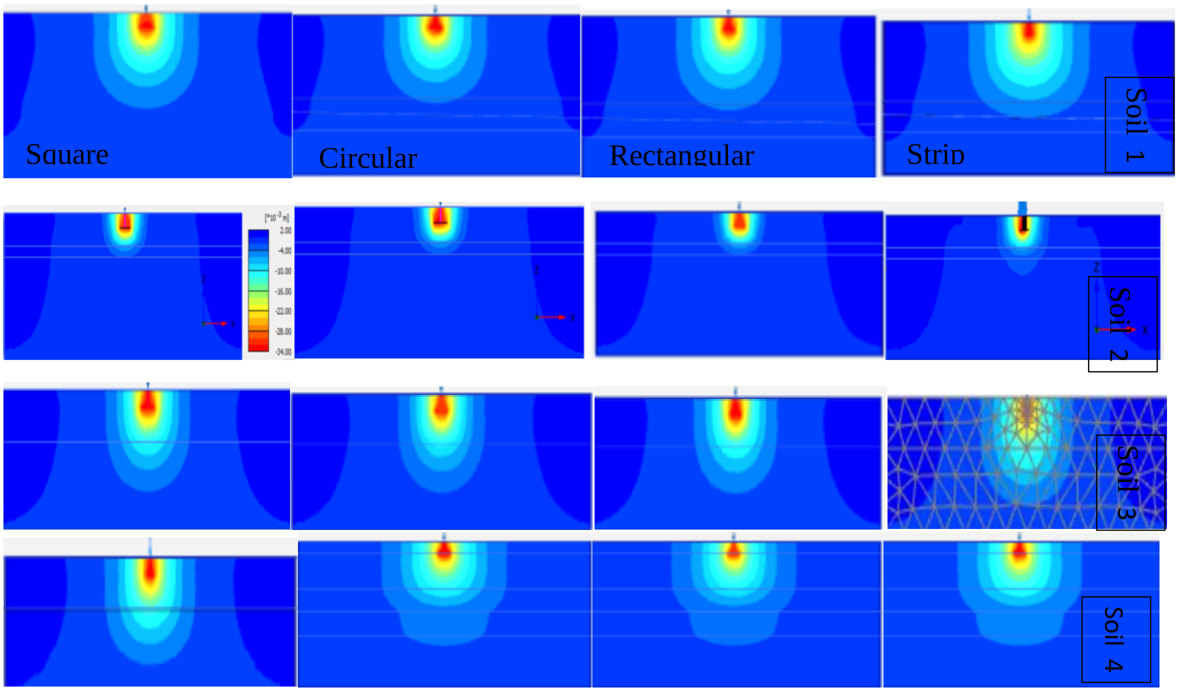

Figure 4.1 A section veiw of plastic point distribution of isolated footing based on Mohr-Coulumb

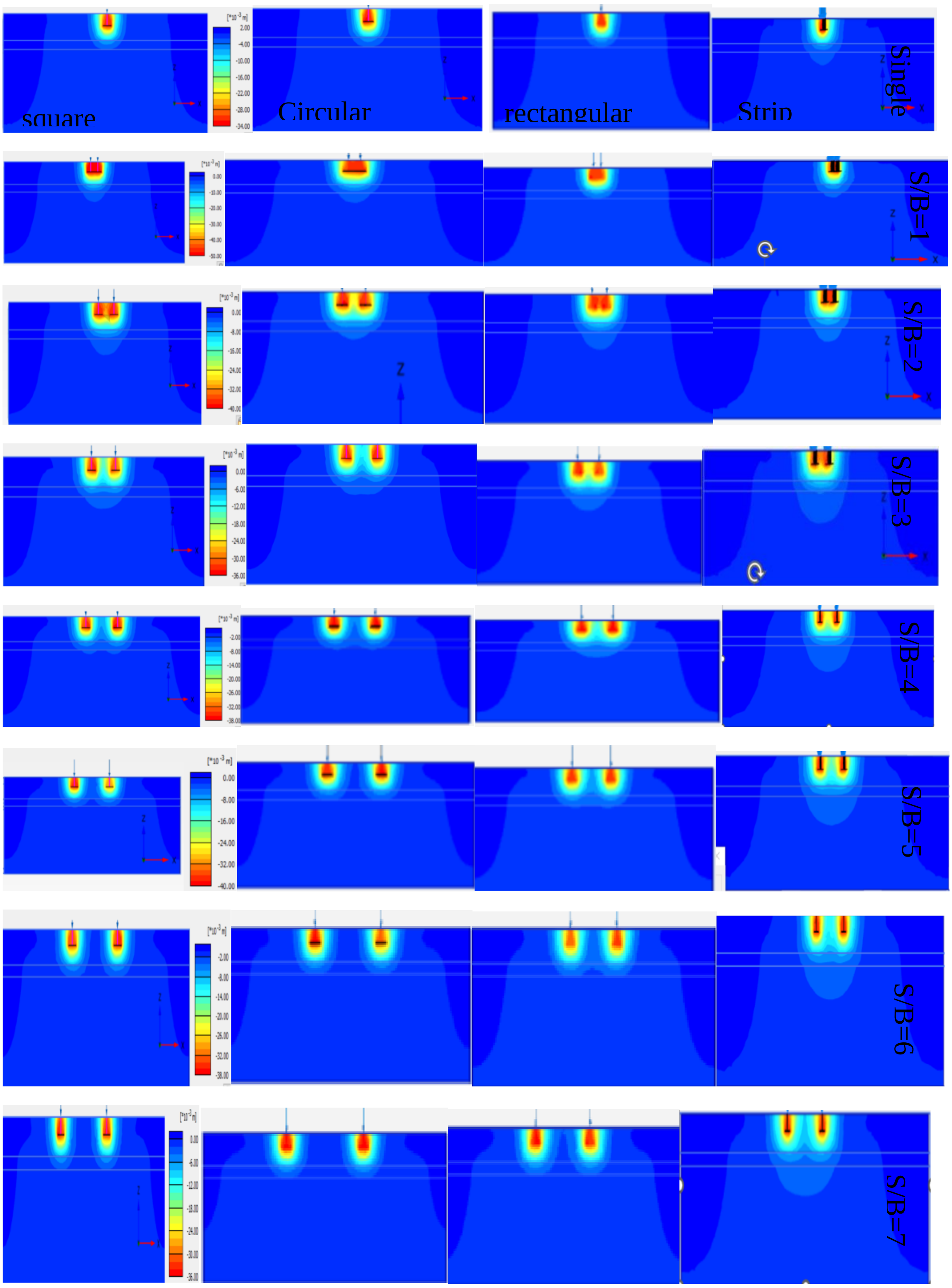

Figure 4.2 A section veiw of plastic point distribution of footing based on Mohr-Coulumb square, circular, rectangular and strip as isolated and S/B ratio 1 to 7.

Figure 4.2 represent stress distribution and plastic points under the footing and surrounding soil. The figure suggest that strip and rectangular shapes affect the surrounding soil more wider and make more plastic points adjecent to them. However circular and square footings has closer plastic distribution compared to strip and rectangular footing. Read and yellow coulor show points of high plastic distribution.

4.2 Bearing capacity and settlements of shallow footing

4.2.1 Bearing Capacity And Settlement of square, circular, rectangular and strip Isolated Footings On Different Soil Types

The load settlement curve results of isolated footing on different soil layer were depicted below. The soil in this study area continouly deformed under loading

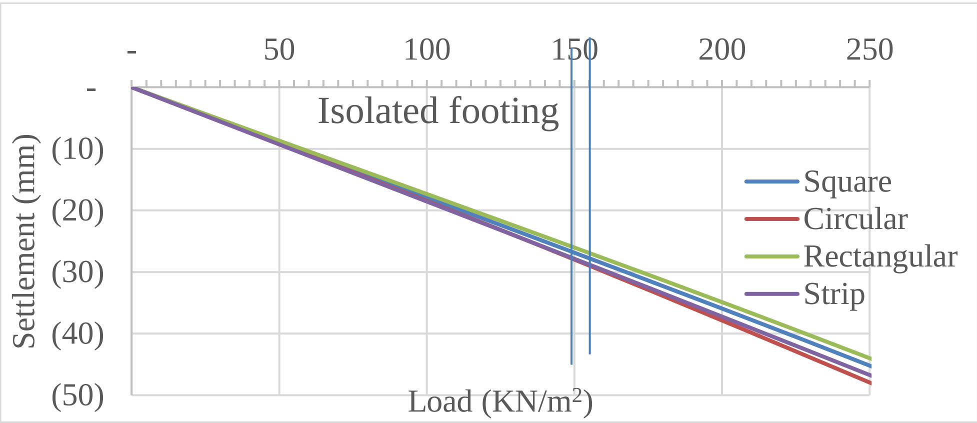

Figure 4.3 Load settlement curve of isolated footing on compact silt underlain by medium dense silty sands

Figure 4.3 shows the load-settlement curves of isolated square, circular, rectangular and strip footing on compact silt underlain by medium dense silty sands. It can bee seen that the load settlement graph is linear and the soil is continueily deformed under loading. Bearing capacity increase in order of circular → strip → square → rectangular. It was observed from the results circular footings has low bearing capacity and rectangular have maximum bearing capacity when acted as an isolated. The allowable bearing capacity of square, circular, rectangular and strip isolated footing correponding to limit settlement 25mm are (140, 135, 145 and 135) KN/m^2 respectively.

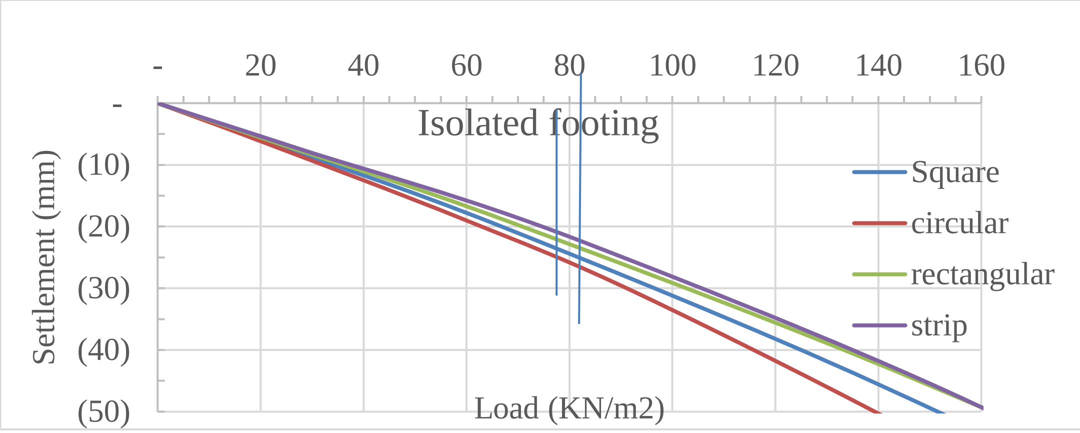

Fugere 4.4 Load settlement curve of isolated footing on loose sandy silt underlain by a layer of medium dense sandy silt and dense fructured rock.

Figure 4.4 suggested the load-settlement curves of isolated square, circular, rectangular and strip footing on loose sandy silt underlain by a layer of medium dense sandy silt and dense fructured rock. Bearing capacity increase in order of circular → square → rectangular → strip. It was observed from the results circular footings has low bearing capacity and strip have maximum bearing capacity when acted as an isolated. The allowable bearing capacity of square, circular, rectangular and strip isolated footing correponding to limit settlement 25mm are (82, 79, 87.5 and 92) KN/m^2 respectively.

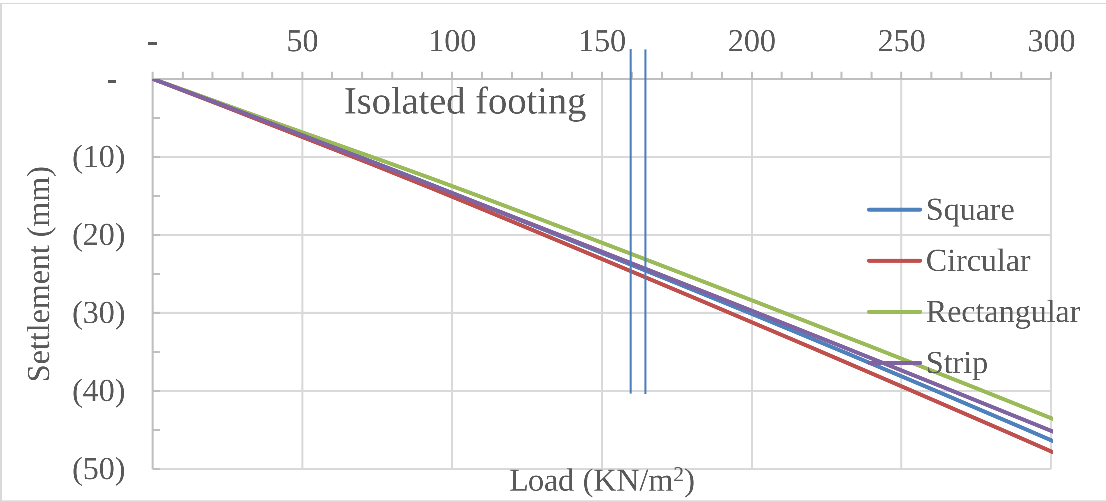

Figure 4.5 Load settlement curve of isolated footing on medium dense to dense silt with same sand overlain by very dense sandy silt with trace of gravel.

Figure 4.5 represents the load-settlement relationship for different shapes of footing resting on medium dense to dense silt with same sand overlain by very dense sandy silt with trace of gravel to investigate the effect of footing shape. Bearing capacity increase in order of circular → square → Strip → rectangular.

From the curve it was observed that the allawble bearing capacity of rectangular footing has higher values than strip,, square and circular and footing has lower value of bearing capacity. The allowable bearing capacity of square, circular, rectangular and strip isolated footing correponding to limit settlement 25mm are (169, 161, 178 and 170) KN/m^2 respectively.

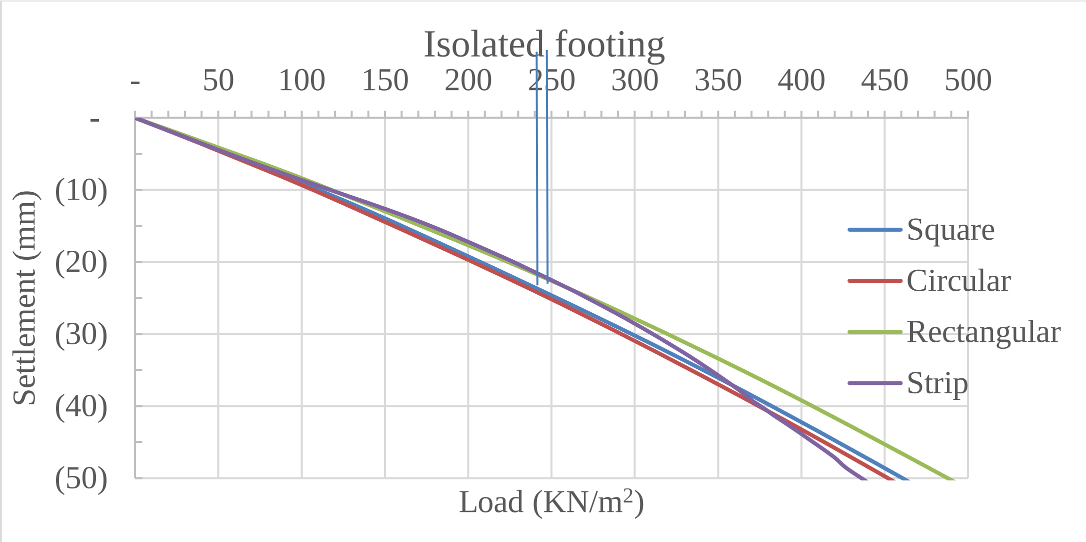

Figure 4.6 Load settlement curve of isolated footing on layers of dense, medium dense and dense clayey silt.

Figure 4.6 represents the load-settlement relationship for different shapes of footing resting on layers of dense, medium dense and dense clayey silt to investigate the effect of footing shape. Bearing capacity increase in order of circular →square → strip →rectangular. From the curve it was observed that the allawble bearing capacity of rectangular footing has higher values than strip,, square and circular and footing has lower value of bearing capacity. The allowable bearing capacity of square, circular, rectangular and strip isolated footing correponding to limit settlement 25mm are (251, 247, 274 and 272) KN/m^2 respectively.

In moderately compresible soils, and soils of medium relative density/consistency significant vertical displacement may take place due to local shear failure. Local shear failure retains some characteristics of both general and punching mode of failure soil compres beneath the footing as shown in figure 4.1 and 4.2 (Das, 2011; Foundations-general, 2015; Vesic, 1973).The load settlement curve was characterized by relatively large settlement and ultimate bearing capacity is not clearly defined. In cases where a peak load cannot be estabilished with certainity, it is expedient for the practice to adopt a limit of critical settlement(Vesic, 1973).

In this research the allowable capacity was defined based on allowable total settlement and ultimate bearing capacity calculated using facter of safty 3. For normal structure with isolated foundation the differential settlements and maximum total settlelement are 20mm and 25mm respectevely (EN, 2004; Transportation, 2017). The results obtained satisfied the safe bearing capacity requarements set by (Republic, 2013; Transportation, 2017) Appendix C – table C- 6.

4.2.2. Bearing capacity and settlement of adjecent foundation

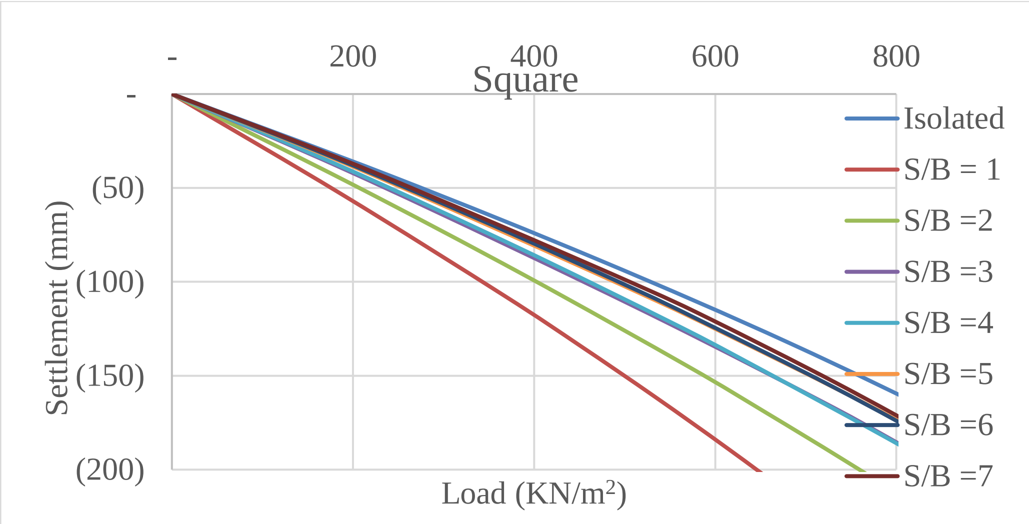

Figure 4.7 Load settlement curve of square footing with variying S/B ratio on soil 1

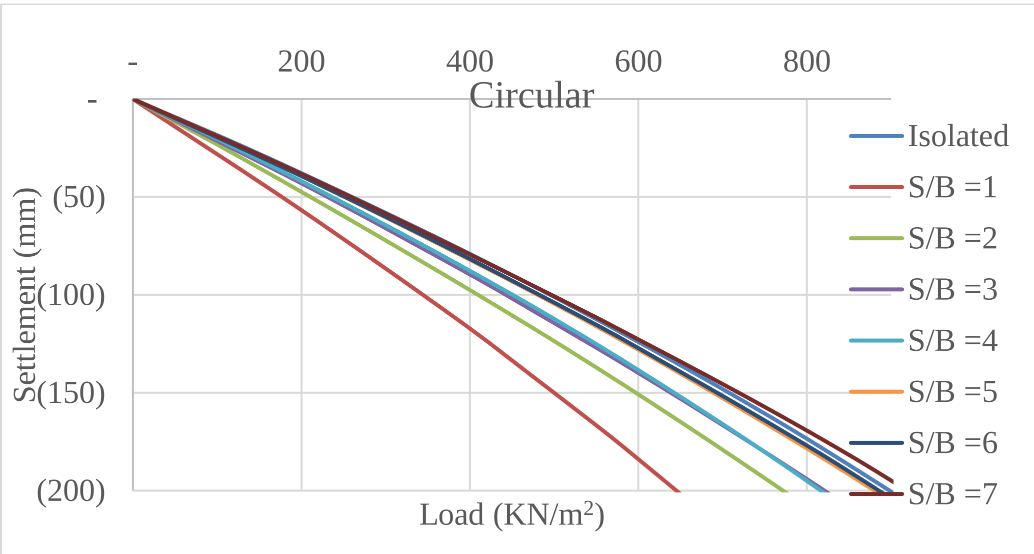

Figure 4.8 Load settlement curve of circular footing with variying S/B ratio on soil 1

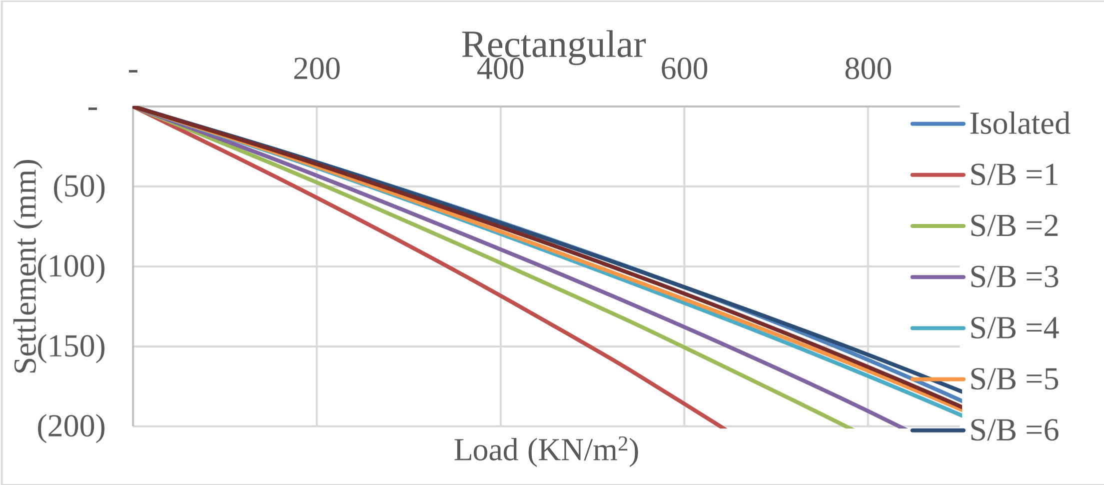

Figure 4.9 Load settlement curve of circular footing with variying S/B ratio on soil 1

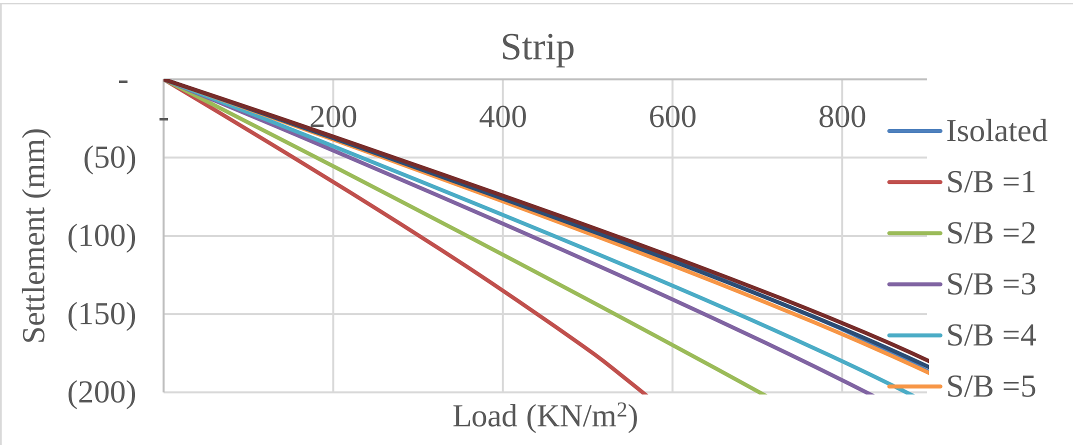

Figure 4.10 Load settlement curve of circular footing with variying S/B ratio on soil

Figure 4.7 – 4.10 show that bearing capacity increase with increasing S/B ratio of interfered footing until it act as an isolated.

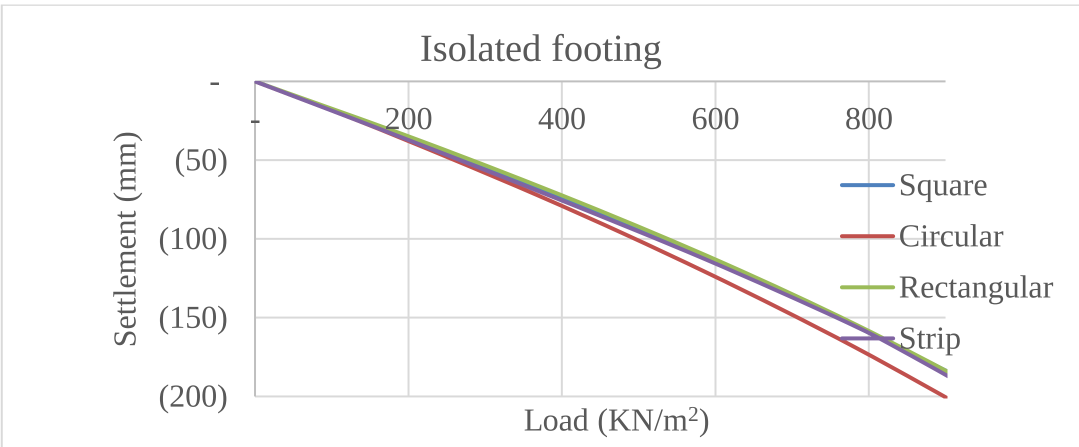

(a)

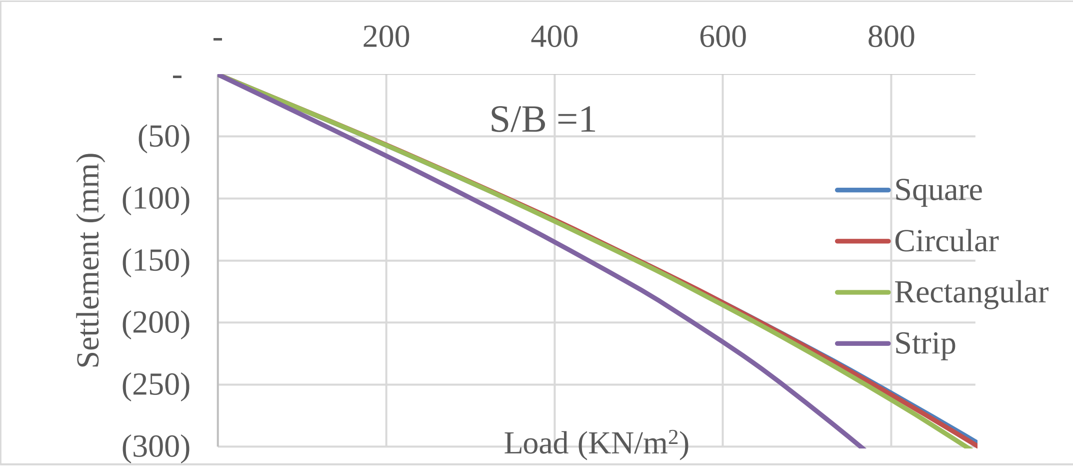

S/B =1
Settlement (mm)
Load (KN/m2)
-
200
400
600
800
-
(50)
(100)
(150)
(200)
(250)
(300)
Square
Circular
Rectangular
Strip

(b)

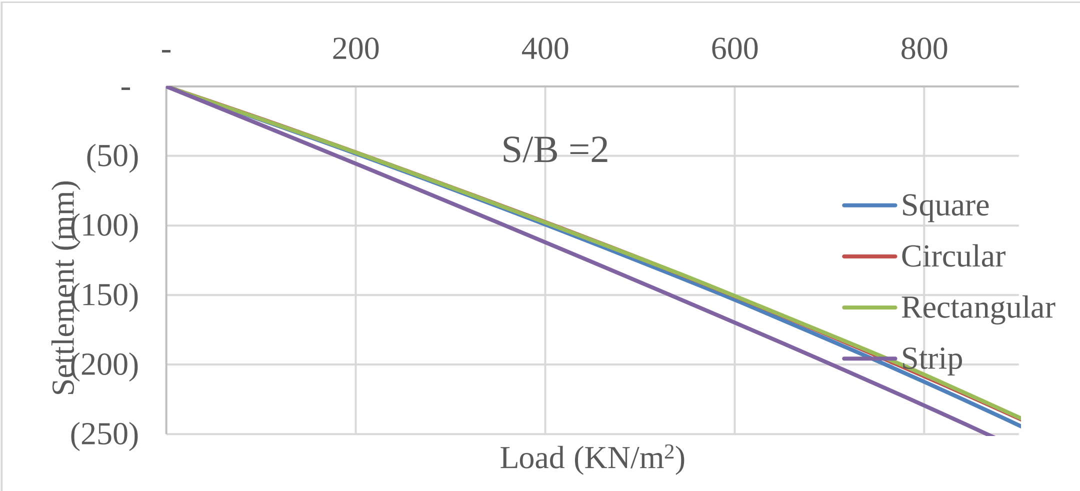

S/B =2
Settlement (mm)
Load (KN/m2)
-
200
400
600
800
-
(50)
(100)
(150)
(200)
(250)
Square
Circular
Rectangular
Strip

(c)

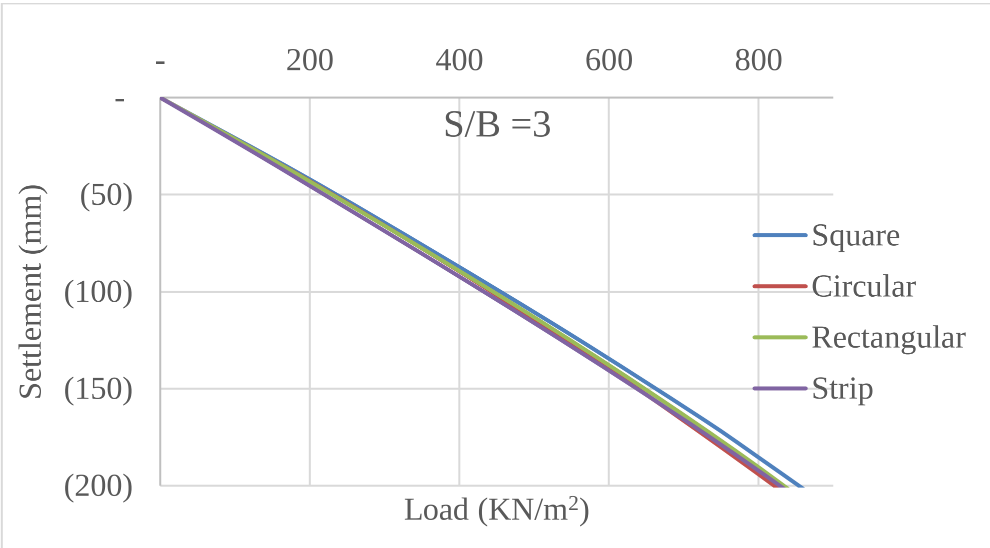

S/B =3
Settlement (mm)
Load (KN/m2)
-
200
400
600
800
-
(50)
(100)
(150)
(200)
Square
Circular
Rectangular
Strip

(d)

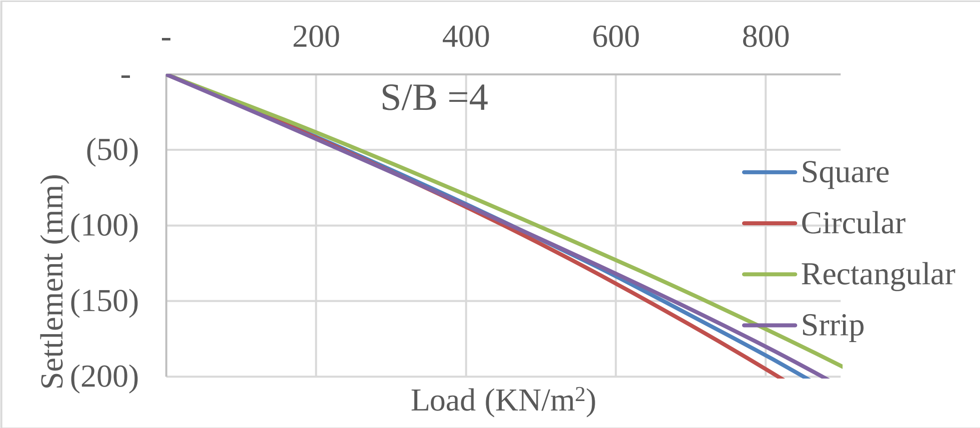

S/B =4
-
200
400
600
800
-
(50)
(100)
(150)
(200)
Settlement (mm)
Load (KN/m²)
Square
Circular
Rectangular
Srrip

(e)

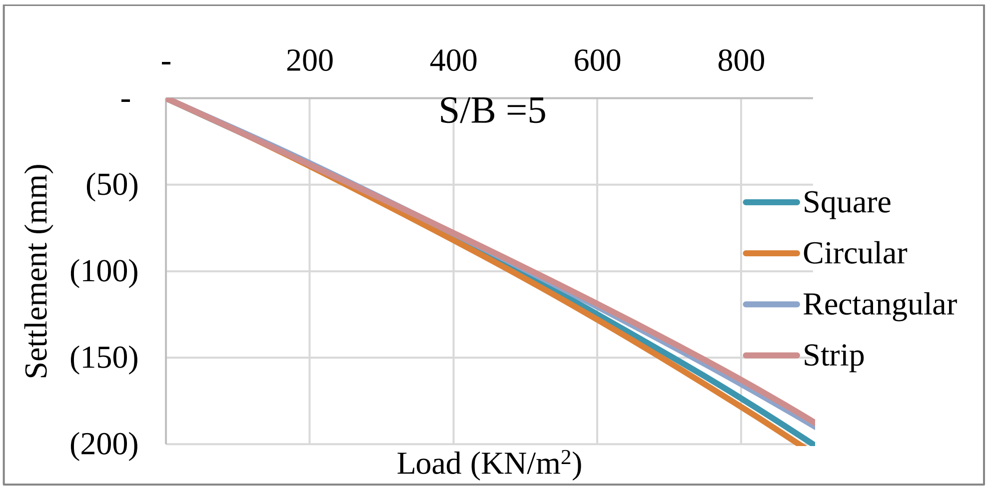

S/B =5
-
200
400
600
800
-
(50)
(100)
(150)
(200)
Settlement (mm)
Load (KN/m²)
Square
Circular
Rectangular
Strip

(f)

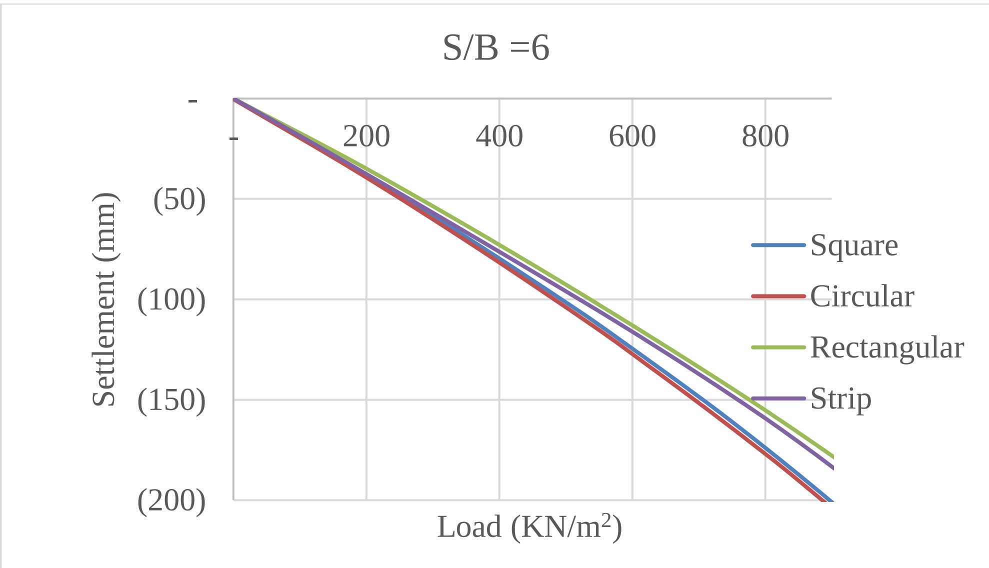

S/B =6
-
200
400
600
800
-
(50)
(100)
(150)
(200)
Settlement (mm)
Load (KN/m²)
Square
Circular
Rectangular
Strip

(g)

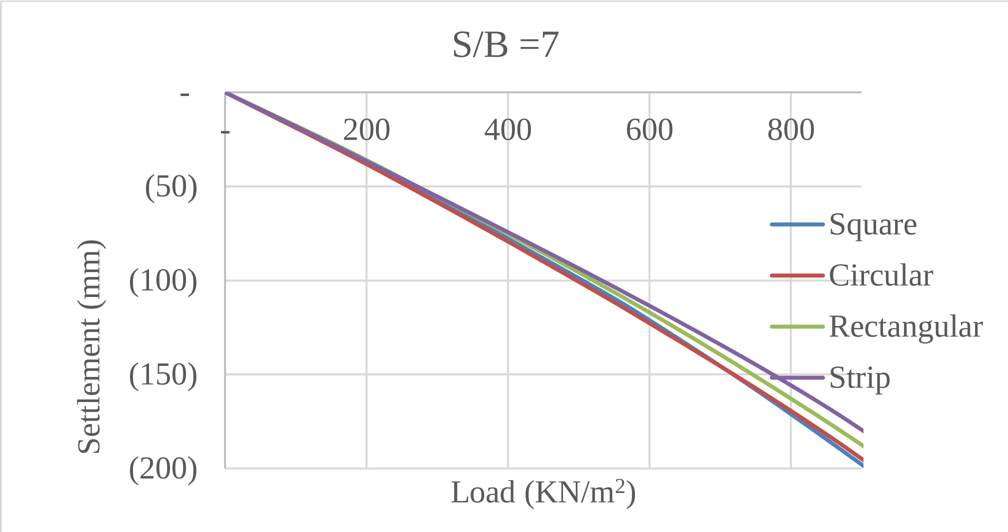

(h)

Figure 4.11 a-h load- settlement curve footing with variiying S/B ratio on soil 1

Figure 4.11 a-h Show the load-settlement behavior of square, circular, rectangular and strip footing on compact silt underlain by medium dense silty sands. The graphs shows footing shape which have low bearing capacity and maximum bearing capacity as compared to each other and the relation was summerized in table 4.1. the bearing capacity was compared for S/B ratio 0 -7 where 0 represent isolated footing and S/B ratio 1-7 for interfered footing spacing computed in terms of width B.

Table 4.1 effect of adjecent square, circular, rectangular and strip footings on ultimate bearing capacity

S/B	Ultimate bearing capacity increase from left to right	
0	Circular → strip → square → rectangular	Soil 1 figure 4.7 to 4.10 and Figure 4.11, a-h
1	Strip → *square* → *rectangular* → circular	
2	Strip → square → rectangular → circular	
3	Strip →*rectangular* → *circular* → square	
4	Strip → circular → square → rectangular	
5,6 &7	Circular → square → Strip → rectangular	

Table 4.1 represents the summary of load-displacement curve in order of increasing allowable and ultimate bearing capacity from left to right as shown by direction of arrow in the table. The summary of load-settlement curve of two interfered footing of the same size and shape at various S/B ratio rest on soil 2, soil 3 and soil 4 were depicted in Appendix B. And the effect of square, circular, rectangular and strip footing on bearing capacty and settlement was summerized in Appendix -A table A-12.

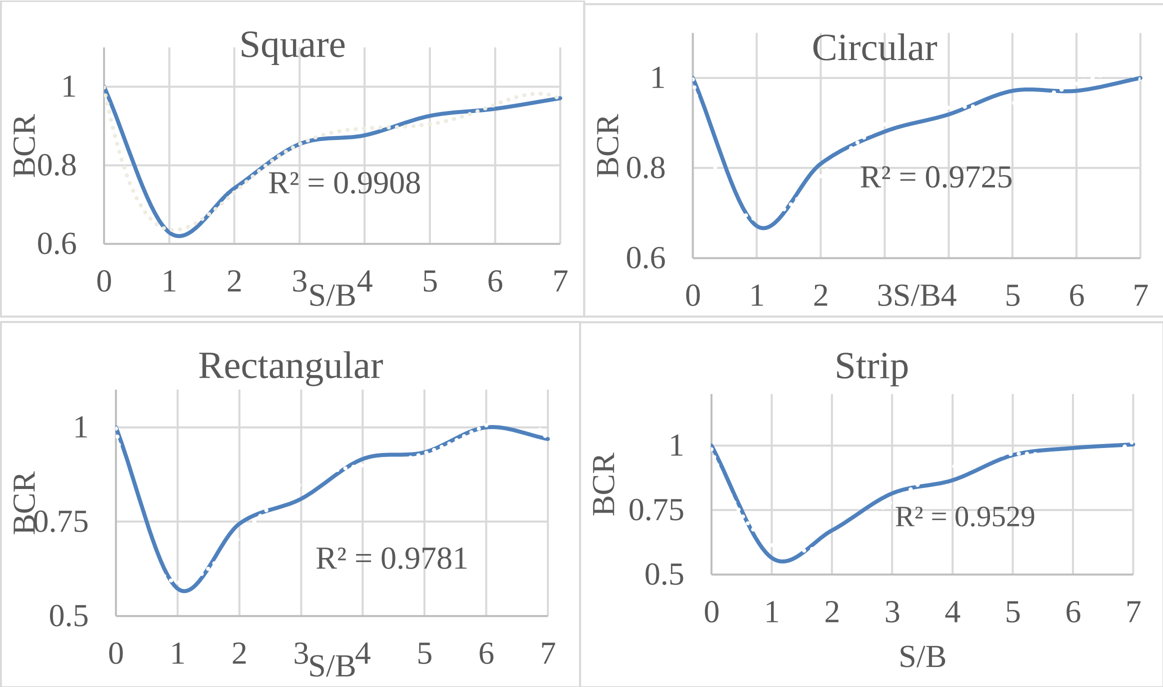

Figure 4.12 Variation of BCR (interferance coefficient) with S/B ratio for square, circular, rectangular and strip on soil 1

In this study the results of effect of foundation geometry are compared in four different soils. Figure 4.12 show the relationship between interference coefficient (BCR) and spacing ratio S/B.The result of interferance cofficient to S/B relation show that increasing spacing on compact silt underlian by medium dense silty sands, the bearing capacity of of square, circular, rectangular and strip decreace upto S/B ratio 1.2 and increase with increasing rate untlil S/B ratio reaches 4 and increase with decreasing rate for S/B ratio greater than 4. Circular footing acts as isolated after S/B =7, rectangular and strip footing act as an isolated foundation at S/B = 6.

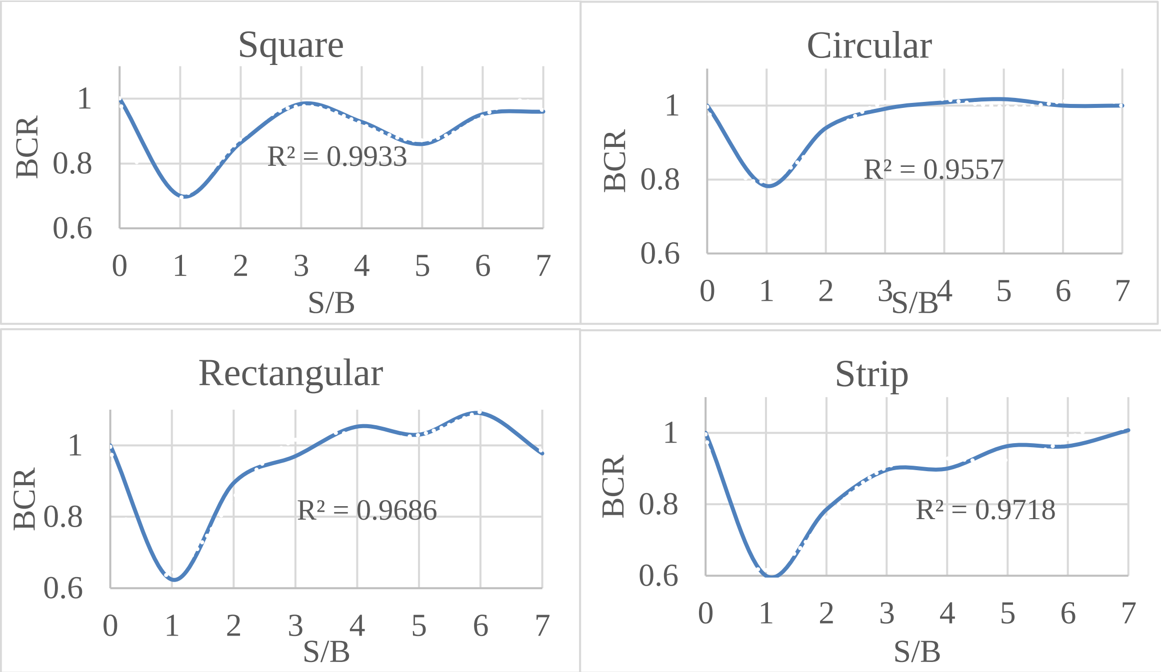

Figure 4.13 Variation of BCR (interferance coefficient) with S/B ratio for square, circular, rectangular and strip on soil 2

It can be observed that by increseang the spacing bearing capacity of square, circular, rectangular and strip decrease (S/B=1.2) and increace with increasing trend upto (S/B=2), with decreacing trend until S/B reaches 3in soil 2. Bearing capacity of square footing decrease for S/B= 3-5. Square, circular and rectngular footing acts as an isolated after S/B= 3 and strip footing act as an isolated after S/B =7.

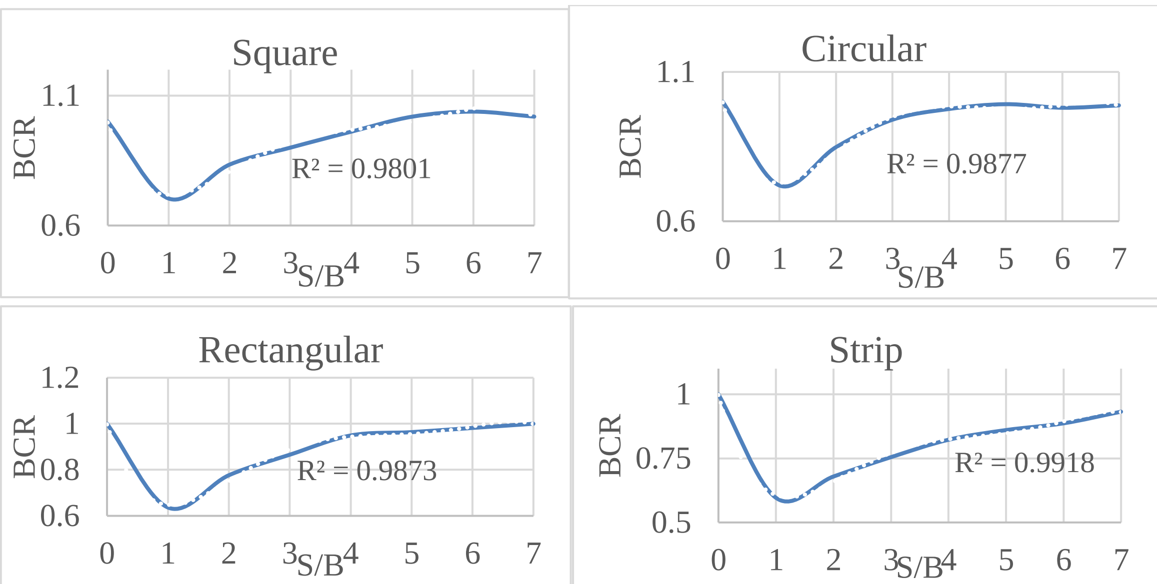

Figure 4.14 Variation of BCR (interferance coefficient) with S/B ratio for square, circular, rectangular and strip on soil 3

Figure 4.14 represents the influence factor versus S/B ratio of different footing on isolated foundation on medium dense to dense silt with same sand overlain by very dense sandy silt with trace of gravel. The bearing capacitiy decreace and, increase with increacing rate (S/B=1.2-4) and increase with decreacing trend upto S/B =5 for square and circular and S/B=7 for rectangular and strip. Square and circular footing act as single footing at S/B= 5. Similarly rectangular footing act as an isolated at S/B=7.

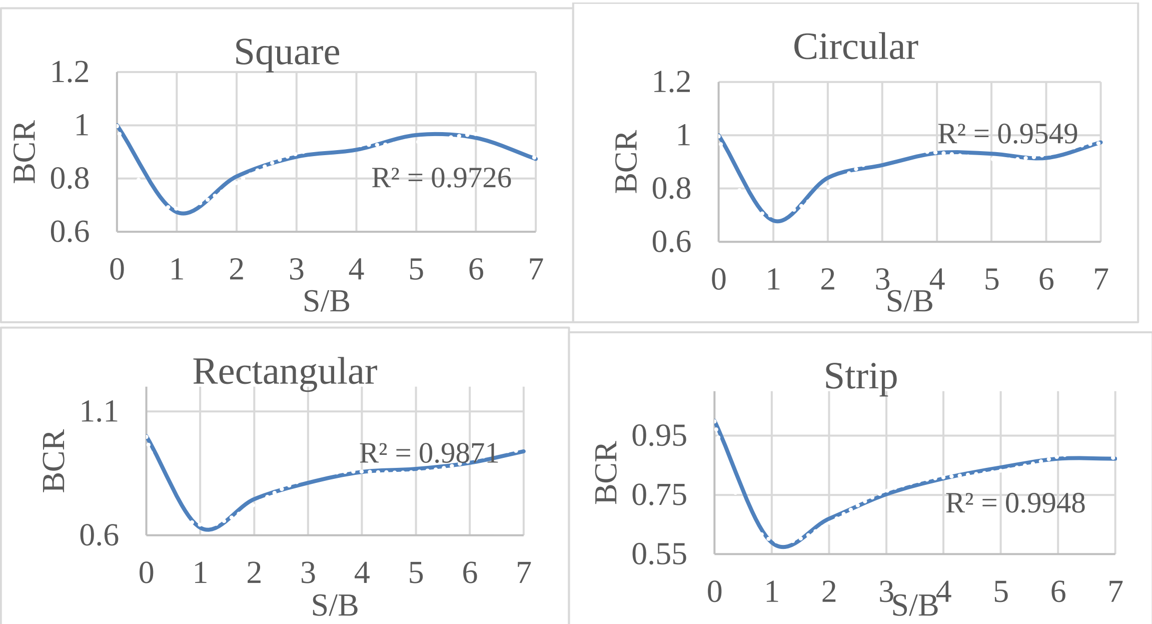

Figure 4.15 Variation of BCR (interferance coefficient) with S/B ratio for square, circular, rectangular and strip on soil 4

Figure 4.15 show the relation between interference factor versus S/B ratio of footing rested on layers of dense, medium dense and dense clayey silt. Figure show that bearing capacity increase with increaceng trend until it reaches S/B =1.2 - 5 for square and circular and S/B =1.2 -7 for rectangular and strip.

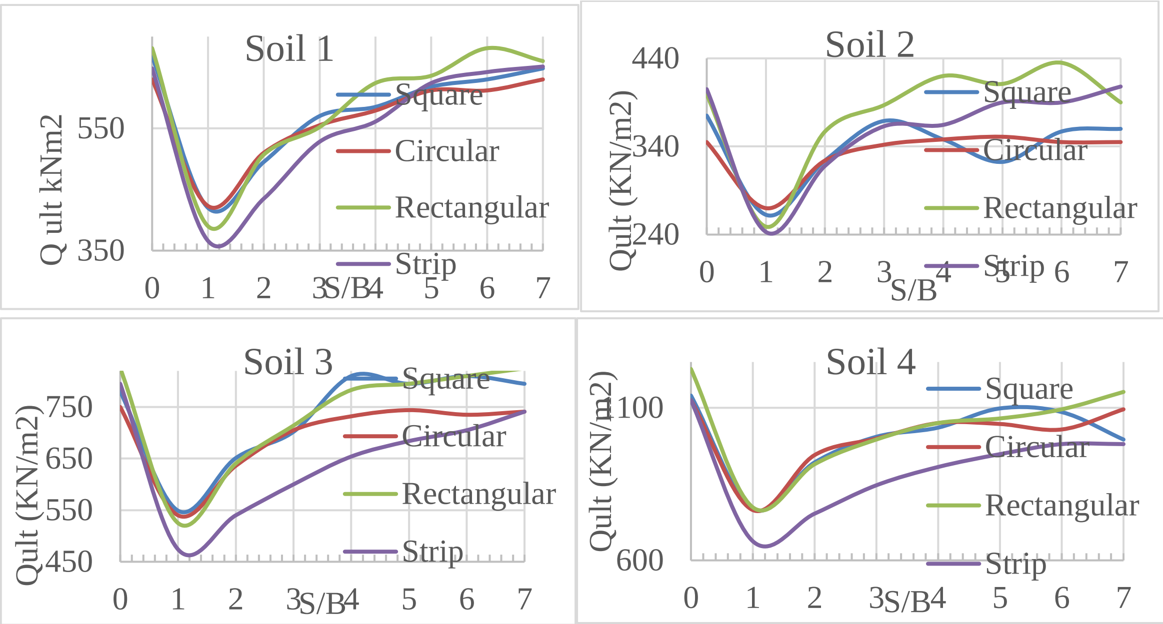

Figure 4.16 Ultimate bearing capacity) versus S/B ratio for square, circular, rectangular and strip on different soil

A graph of ultimate bearing capacity versus S/B ratio of square, circular, rectangular and strip footing on four different soil were shown in figure 4.16. It clearly shows that for S/B ratio 1.2 the ultimate bearing capacity is low as seen from the graph for all soils and incease similarly after that. Strip footing show low ultimate bearing capacity as compared to square , rectangle and circular footing on layer of dense to very dense soil and rectangular and square have maximum ultimate bearing capacity. However the ultimate bearing capacity of strip footing exceds that of square and circular after S/B ratio 3 for foundation rest in loose top soil.

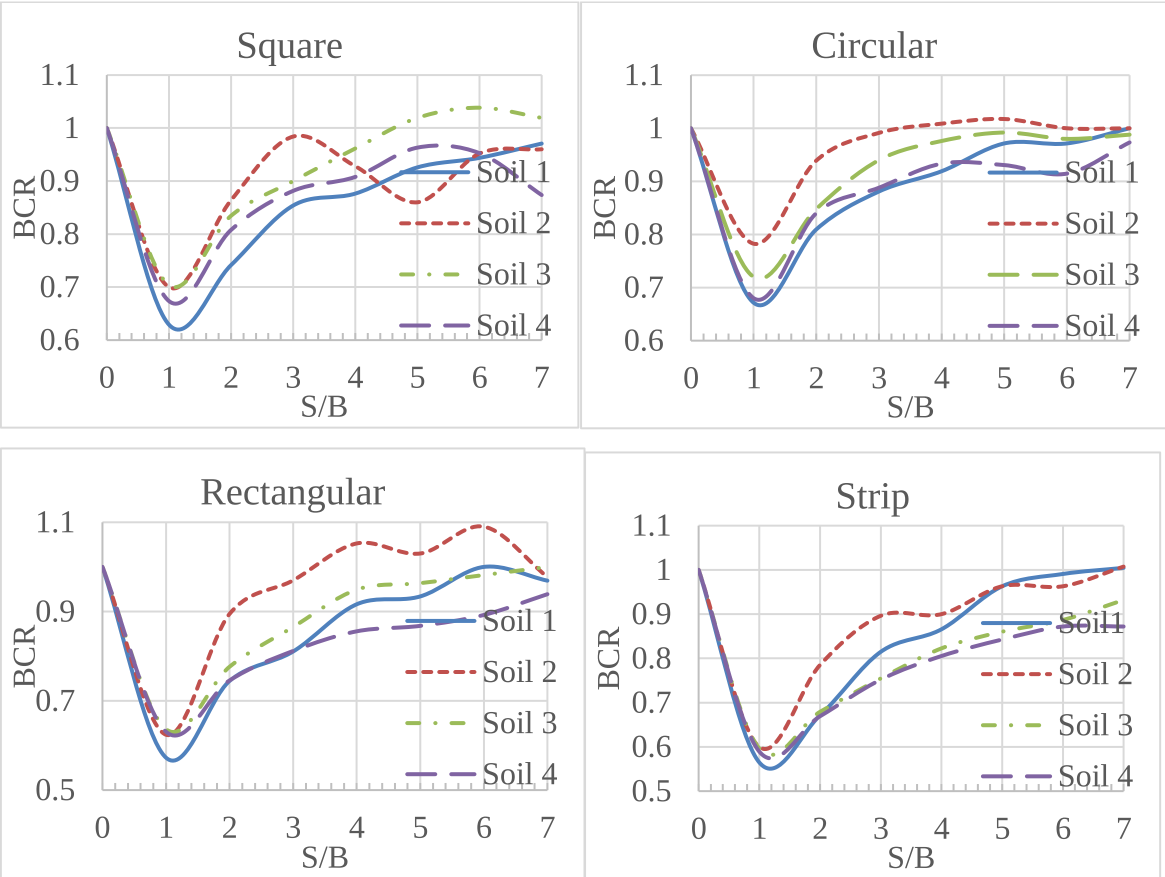

Figure 4.17 Variation of BCR (interferance coefficient) with S/B ratio for square, circular, rectangular and strip on different soil

A coefficient is factor described as a ratio of ultimate bearing capacity of adjecent foundation to altimate bearing capacity of islolated foundation with the same dimension. Density of the top soil layer bellow the footing level were loose, medium dense, medium dense to dense and dense for soil 1, 2, 3 and 4 respectevely depend on SPT-N values. The result from SPT-N values and the graph of BCR versus S/B ratio show that soil with low density/ consistency have maximum BRC factors. This indicate that such soil has low bearing capacity; However, the bearing capacity of adjacent foundation increase with increasing S/B ratio as compared to medium dense and dense soil in contact with the base of foundation.

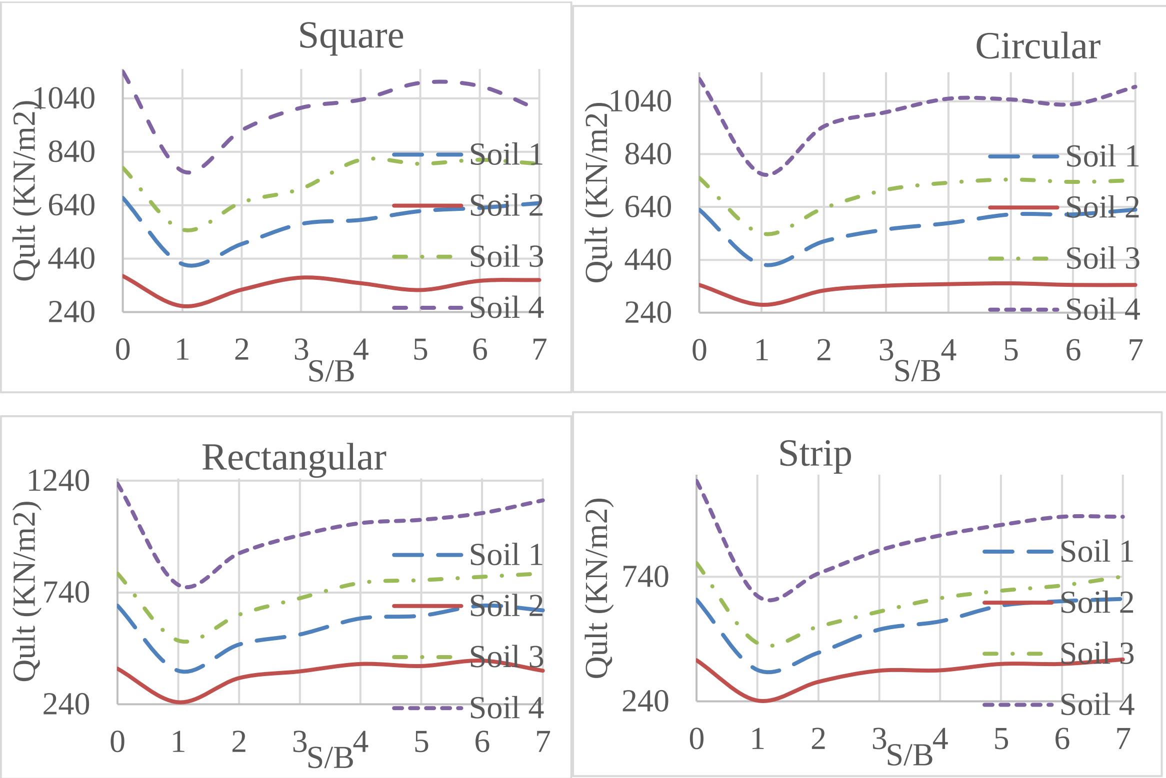

Figure 4.18 qult versus S/B

Figure 4.18 show that the comparison of ultimate bearing capacity of different soil with different consistency by varying S/B ratio. It was clearly indicated that bearing capacity of soil with different consistency have parallel relationships.

4.3 Comparision between Numerical model results and Analytical results

A total of 32 analyitical calculation has been done for comparion of PLAXIS results. Result obtained from numerical model conducted using PLAXIS 3D Connect Edition V20 were compared with analytical approach of elastic settlement by (Bowles, 1987). The allowable bearing capacity values are obtained by reading the load corresponding to allowable settlement 25mm from load-settlement curves. Analytical settlement was calculated for allowable load obtained from Load settlement curves using equation 3.6 to 3.9 in section 3.8.

The table shows the comparisons of PLAXIS results with analytical results. The comparisons were done based on Load at total allowable settlement 25mm from PLAXIS and settlement were calculated based on theory of elasticity.

Table 4.2 Comparison of numerical model results with analytical method

Isolated Footing shape	Soil type	Load (kN/m^2)	Settlement (mm)			Difference of PLAXIS and analytical for rigid foundation
			PLAXIS (FEM)	Analytical		
				$S_{e(flexible)}$	$S_{e(rigid)}$	
Square	1	140	25	25.85	24.04	0.96
	2	82	25	26.91	25.02	-0.02
	3	169	25	22.82	21.23	3.77
	4	251	25	22.49	20.92	4.08
Circular	1	135	25	29.43	27.37	-2.37
	2	79	25	30.60	28.46	-3.46
	3	161	25	25.67	23.87	1.13
	4	247	25	26.13	24.30	0.7
Rectangular	1	145	25	26.73	24.86	0.14
	2	87.5	25	28.66	26.65	-1.65
	3	178	25	24.00	22.32	2.68
	4	274	25	24.51	22.79	2.21
Strip	1	135	25	30.3	28.18	-3.18
	2	92	25	35.1	32.65	-7.65
	3	170	25	27.91	25.95	-0.95
	4	272	25	29.63	27.55	-2.55

Table 4.2 show the load at total settlement 25mm obtained from load-displacement curve and elastic settlement calculated for each load.

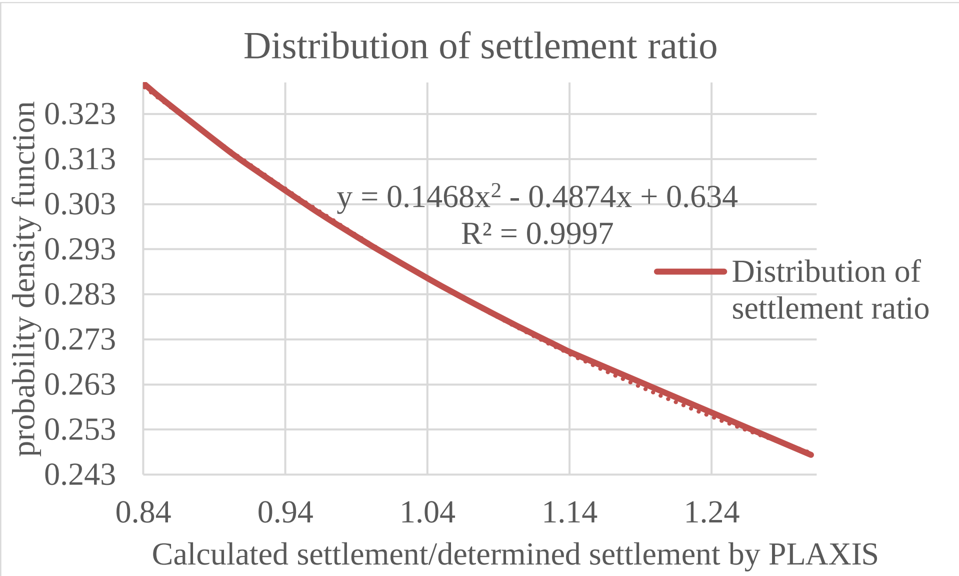

Figure 4.19 Distribution of Settlement ratio by Schmertmann et al.

The probability design charts provided a base line from which all settlement prediction methods compared against each other. The probability that the calculated settlement exceeds the predicted settlement from PLAXIS was 0.5 (50%).

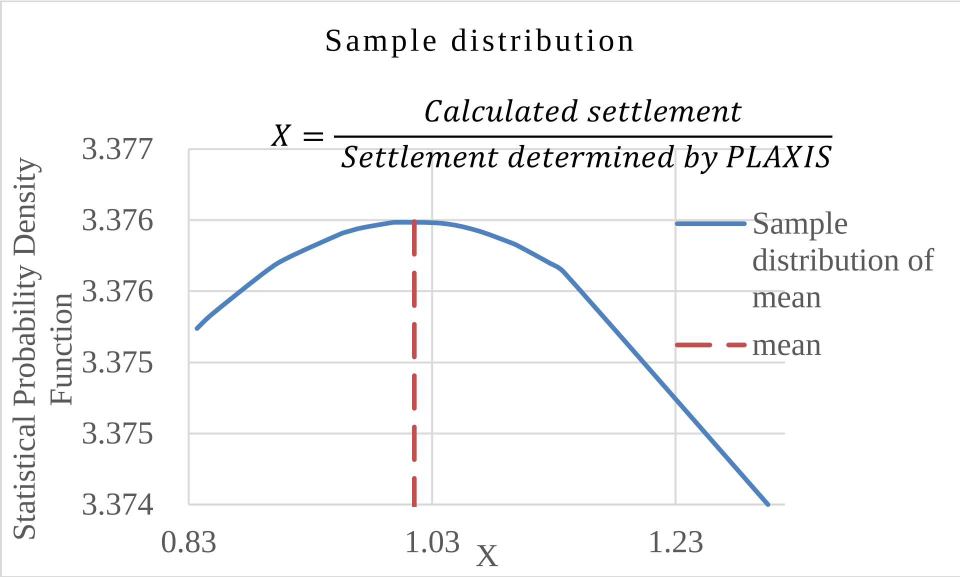

Figure 4.20 Accuracy and Reliability in settlement prediction

The comparison analysis was carried out taking as standard limit values of settlement obtained from PLAXIS, with the settlement calculated by analytical method. The results show that the ΔX between the settlement obtained by PLAXIS and those obtained by calculation the upper confidence limit UCL maximum error of attenuation of 95% confidence level was 3.5mm. The higher values 3.77 and 4.08 which exceeds UCL matching with the square footing acting on soil 3 (Medium dense to dense silt with same sand overlain by very dense sandy silt with trace of gravel) and soil 4 (Dense, medium dense and dense clayey silt). The highest value of 7.65 was occurred when strip. Footing acted on Loose sandy silt underlain by a layer of medium dense sandy silt and dense fractured rock (Abis, 2021; Das & Sivakugan, 2007)which show the tendency of compression of top loose consistency soil under strip footing with minimum footing width as compared to square rectangular and circular. The result show that there is a good agreement between numerical and analytical results.

4.3 Parametric study

In the previous sections of this thesis, the bearing capacity and settlement of four different location were analyzed using PLAXIS 3D Connected Edition V20 finite element software and the result were presented. From the comparison made PLAXIS give reliable values. Thus, the parametric study in this section were based on results from software. The numerical analysis of bearing capacity and settlements of isolated and adjacent foundation used to obtain results in the above sections.

There are number of variables that have been considered for practical importance and reported to have significant influence in load-settlement calculation system. The main parameters are the shape, dimensions, density/ consistency of the top soil and spacing ratio S/B.

The shape and dimension of shallow foundation can be considered as variable in parametric study. Square, circular, rectangular and strip foundation considered in this thesis have equal area and have been tested for proportional load per unit area. The result has been suggested load settlement varies with shape. The dimension L/B ratio have also significant influence on bearing capacity and settlement. As discussed above in the above section and literature square and rectangular footing of the same area reported varied in bearing capacity and settlement.

Table 4.3 Footing pressure (kN/m2)

Settlement (mm)	Load in (kN/m^2) for isolated footing of following shape				Soil type
	Square	Circular	Rectangular	Strip	
25	140	135	145	135	Soil 1
25	82	79	87.5	92	Soil 2
25	169	161	178	170	Soil 3
25	251	247	274	272	Soil 4

Spacing ratio S/B of adjacent foundation can be considered as another variable for this study, in this study proportional vertical static load was applied on square, circular, rectangular and strip footings. Bearing capacity had been reported varying increasing S/B ratio. The result suggested that the increases and decreases patterns of bearing capacity of footing considered in study change differently with S/B ratio of footing on different soil consistency.

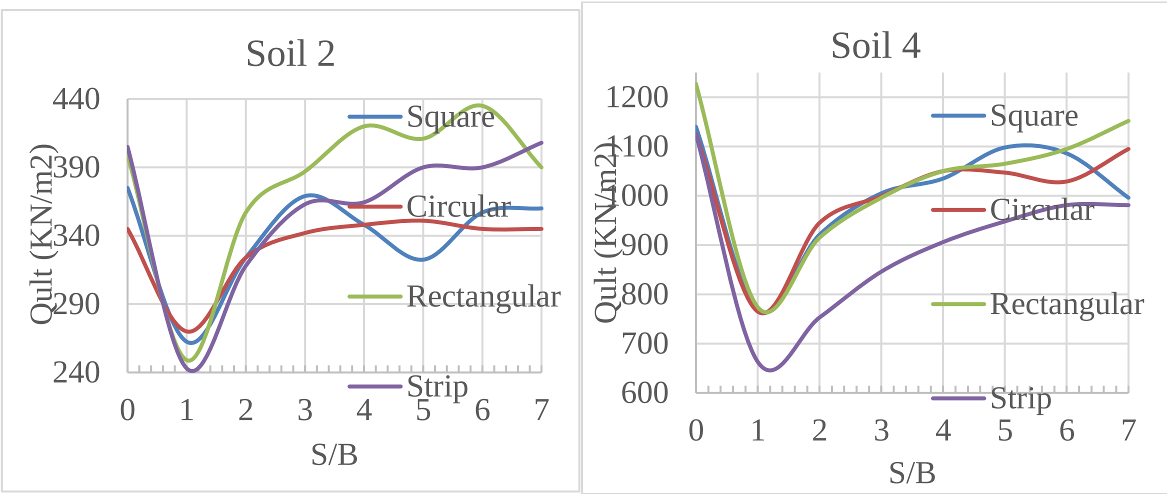

Figure 4.21 Ultimate bearing capacity versus S/B ratio

The parameters used for this study were combinations of different soil types from loose to very dense consistency. Consistency of top soil below footing level varies in consistency than the bottom layers.

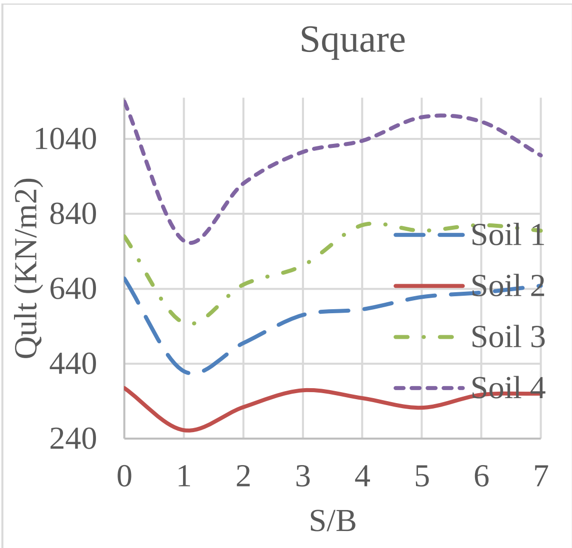

Figure 4.22 Ultimate bearing capacity versus S/B ratio on different soil

CHAPTER FIVE CONCLISION AND RECOMMENDATION

5.1Conclusion

The following conclusion can be drown based on the results obtained from PLAXIS 3D Connected Edition V20 finite element software. As observed from both numerical analyses, of bearing capacity and empirical elastic settlement drown for allowable load bearing capacity is influenced by the density/consistency of top soil layer.

- The result show that circular footing has lower bearing capacity as compared to square, strip and rectangular footing when acted as an isolated in all cases in this study.
- Isolated rectangular footing rest on soil with medium dense to dense consistency has maximum bearing capacity, however; strip soil rests on loose consistency soil has maximum bearing capacity.
- Interfered strip footing on medium dense to dense consistency has low bearing capacity. Closely spaced rectangular footing on loose consistency soil has maximum bearing capacity for S/B = 2-6.
- Strip footing bearing capacity was low for adjacent foundation off S/B=1-5. Strip footing rest on dense to very dense clayey silts have law bearing capacity when acted as an isolated.
- For the case of rectangular footing bearing capacity was higher when acted as an isolated and increase with increasing S/B ratio.
- Circular footing has higher bearing capacity at S/B=1 on soil 1, 2 and 3 in this study.
- On average rectangular footing have higher bearing capacity on soil 1. 2 and 3.
- It was concluded that circular footing bearing capacity was lower than square, rectangular and strip when act as an isolated.
- The relation between bearing capacity and settlement of foundation on soil of different consistency shown parallel to each other.

It was concluded that footing shape, dimension and strength of the top soil layer have significant effect on bearing capacity and settlements. For adjacent foundation S/B ratio were the most significant factor that affect bearing capacity and settlements.

5.2 Recommendation

Many researchers conducted investigation on bearing capacity and settlement of isolated and adjacent footing on homogenous and two layered soils. Extensive researches are required to investigate further relationship between analytical, experimental and numerical method for footing on layered soil.

Further studies required to wards the following points.

- Using other numerical modeling such as Hardening soil model and soft soil creep model to compare with Mohr-Coulomb
- Investigation of foundation subject to inclined load on layered soil
- Comparison of PLAXIS with another finite element software
- Dynamic investigation of isolated and adjacent foundation by numerical methods.
- It is recommended to increase selection of footing based on their effect on bearing capacity and settlement in both isolated and adjacent cases

Reference

Abis. (2021). Structural deformation - abis. Https://www.abis.com.au/structural-deformation/

Acharyya, r., & dey, a. (2017). Finite element investigation of the bearing capacity of square footings resting on sloping ground. *Inae letters*, *2*(3), 97–105.

Altaweel, a. A., & shakir, r. R. (2021a). Analytical model for bearing capacity of two closely spaced foundations. *Journal of physics: conference series*, *1973*(1).

Altaweel, a. A., & shakir, r. R. (2021b). The effect of interference of shallow foundation on settlement of clay soil. *Iop conference series: materials science and engineering*, *1094*(1), 012043. Https://doi.org/10.1088/1757-899x/1094/1/012043

Alwalan, m. F. (2018). Interaction of closely spaced shallow foundations on sands and clays: a review. *International journal of advanced engineering research and science*, *5*(9), 101–110.

Bnbc. (2020). Bangladesh national building code (bnbc) 2020. *Ministry of housing and public works*, *1*, 2583–5042.

Bowles, j. E. (1976). *Foundation analysis and design,1996*.

Budhu, m. (2011). *Soil mechanics aand foundation* (3rd editio). John wiley & sons, inc.

Caltrans geotechnical manual. (2021). *March*, 1–35.

Cen (european committee for standardization). (2004). Eurocode 2 : part 1-1: general rules and rules for buildings. In *eurocode 2: vol. Bs en 1992*. Http://www.python.org/doc/

Chu, y., liu, s., & cai, g. (2021). Characterization on the correlation between spt-n and small strain shear modulus gmax of jiangsu silts of china. *Earth sciences research journal*, *25*(2), 225–235.

Das, b. M. (2011). Principals of foundation engineering, seventh edition. In *successful project management*.

Das, b. M., & sivakugan, n. (2007). Settlements of shallow foundations on granular soil - an overview. *International journal of geotechnical engineering*, *1*(1), 19–29.

Data, m. (2015). *Bangladesh : bangladesh national building code (bnbc) 2015 (final draft) bangladesh national building code 2015* (vol. 1).

Development, u. (2013). *Ebcs-2 design of concrete structures final draft*.

En. (2004). European committee for standardization. Bs en 1992: design of concrete structures - part 1-2: general rules - structural fire design. *Eurocode 2*, *3*, 97.

Eurocode. (2006). Bsen 1992-3-e-2006. *Eurocode 2: design of concrete structures*, *3*(en 1992-3:2006).

Foundations-general, p. (2015). *Footing foundations 4-1* (pp. 1–25).

Ghoreishi, b., khaleghi esfahani, m., alizadeh lushabi, n., amini, o., aghamolaie, i., hashim, n. A. A. N., & alizadeh, s. M. S. (2021). Assessment of geotechnical properties and determination of shear strength parameters. *Geotechnical and geological engineering*, *39*(1), 461–478.

Gupta, a., dutta, r. K., shrivastava, r., & khatri, v. N. (2017). Ultimate bearing capacity of square/rectangular footing on layered soil. *Indian geotechnical journal*, *47*(3), 303–313.

Gupta, s., & mital, a. (2019). Numerical analysis of bearing capacity of rectangular footing. *Journal of physics: conference series*, *1240*(1).

Khatri, v. N., singh, n., dutta, r. K., & yadav, j. S. (2022). Numerical estimation of bearing capacity of shallow footings resting on layered sand. *Transportation infrastructure geotechnology*, *0123456789*.

Kumar, r., bhargava, k., & choudhury, d. (2016). Estimation of engineering properties of soils from field spt using random number generation. *Inae letters*, *1*(3–4), 77–84.

Mahmoud, m. A. A. N. (2013). Reliability of using standard penetration test (spt) in predicting properties of silty clay with sand soil. *International journal of civil and structural engineering*, *3*(3), 545–556.

Md, manzur, rahman, b., sc, m., & sc. (1902). *Standard penetration test: corrections and correlations 1.1 general 1.2 standard penetration test (spt). 01712833954*.

Mujtaba, h., farooq, k., sivakugan, n., & das, b. M. (2018). Evaluation of relative density and friction angle based on spt-n values. *Ksce journal of civil engineering*, *22*(2), 572–581.

Panwar, v., & dutta, r. K. (2020). Numerical study of ultimate bearing capacity of rectangular footing on layered sand. *Journal of achievements in materials and manufacturing engineering*, *101*(1), 15–26.

Patel, m., & bhoi, m. (2019). Effect of different shape of footing on its load-settlement behaviour (circular, square and rectangular). *World congress on civil, structural, and environmental engineering*, 1–7.

Peck, r. B., hanson, w. E., & thornburn, t. H. (1974). *Foundation engineering* (second edi).

Plaxis. (2019). *Plaxis connect edition v20*. 196.

Plaxis. (2020). Plaxis material models. *Plaxis handbook 2d*.

Radwan, n. A. A. (2021). Numerical study on the effect of footing shape on the bearing capacity. *International journal of scientific & engineering research*, *12*(4), 687–692.

Rahman, m. (2019). Foundation design using standard penetration test (spt) n-value.

Republic, c. (2013). *European standard ebcs en 1997-1 : 2013 ethiopian annex*.

Saravanan, r., murthi, p., poongodi, k., shyam sundar, g., & gobinath, r. (2020). Scale effect of rectangular and square footing of shallow foundation resting on cohesive soil. *Iop conference series: materials science and engineering*, *981*(3).

Shafaghat, a., khabbaz, h., & moravej, s. (2018). *Effect of footing shape on bearing capacity and settlement of closely spaced footings on sandy soil hybrid renewable energy system view project numerical modelling of static and dynamic pile load testing by advanced soil models view project*. *November*.

Transportation, u. S. . D. Of. (2017). *Geotechnical site characterization*. *5*(132031).

Vanapalli, s. K., & oh, w. (2021). *Analytical and numerical methods for prediction of the*. *44*(3), 1–18.

Vesic, a. S. (1973). Analysis of ultimate loads of shallow foundations. In *asce j soil mech found div* (vol. 99, issue sm1, pp. 45–73).

Appendix

Appendix A results from software and analytical calculation

Table A - 1 load settlement relation of soil 1

Square		Circular		Rectangular		Strip	
Load in (KN/m^2)	Settlement (mm)	Load in (KN/m^2)	Settlement (mm)	Load in (KN/m^2)	Settlement (mm)	Load in (KN/m^2)	Settlement (mm)
-	-	-	-	-	-	-	-
243.43	(43.97)	130.67	(24.25)	218.76	(38.28)	200.90	(37.41)
471.56	(88.33)	252.91	(48.53)	423.78	(77.02)	396.66	(74.97)
682.42	(132.69)	370.81	(72.84)	611.37	(115.50)	586.57	(112.84)
878.12	(178.14)	482.33	(97.07)	782.94	(154.34)	763.10	(151.08)
1,057.35	(223.95)	587.68	(121.14)	938.48	(193.65)	841.34	(170.40)
1,224.98	(269.97)	687.27	(145.00)	1,081.36	(233.20)	981.04	(209.23)
1,383.11	(315.82)	782.28	(168.86)	1,215.19	(272.86)	1,103.00	(248.40)
1,532.83	(361.66)	871.83	(192.78)	1,341.33	(312.76)	1,217.40	(287.82)
1,675.35	(407.53)	958.36	(216.89)	1,462.93	(352.84)	1,325.39	(327.48)
1,811.02	(453.38)	1,123.07	(265.20)	1,694.92	(433.25)	1,528.51	(407.21)
1,940.63	(499.20)	1,276.66	(313.60)	1,910.68	(513.86)	1,717.17	(487.31)
2,190.39	(590.88)	1,422.85	(362.08)	2,115.56	(594.81)	1,896.69	(567.58)
2,426.88	(682.87)	1,561.58	(410.51)	2,310.67	(675.95)	2,068.13	(648.03)

Table A - 2 load settlement relation of soil 2

Square		Circular		Rectangular		Strip	
Load in (KN/m^2)	Settlement (mm)	Load in (KN/m^2)	Settlement (mm)	Load in (KN/m^2)	Settlement (mm)	Load in (KN/m^2)	Settlement (mm)
-	-	-	-	-	-	-	-
22.48	(6.64)	20.40	(6.30)	22.95	(6.40)	27.68	(7.45)
66.33	(19.85)	59.36	(18.81)	68.12	(19.17)	82.36	(22.40)
139.33	(45.32)	94.10	(31.17)	147.04	(44.73)	168.56	(52.76)
199.96	(70.85)	151.48	(55.39)	213.33	(70.45)	227.42	(83.63)
303.01	(122.11)	200.00	(78.99)	320.89	(121.83)	281.20	(114.67)
483.70	(225.04)	287.42	(125.74)	512.80	(225.22)	331.44	(145.96)
648.34	(327.08)	443.23	(218.47)	689.60	(329.08)	380.25	(177.37)
802.70	(428.20)	586.33	(310.63)	855.14	(433.40)	427.65	(208.91)
949.36	(529.18)	721.22	(402.33)	1,014.44	(538.07)	518.50	(272.28)
1,090.25	(630.08)	849.71	(493.69)	1,168.13	(643.20)	604.78	(335.91)
1,226.33	(730.94)	972.81	(584.53)	1,316.20	(748.79)	687.50	(399.74)
1,357.89	(831.68)	1,092.14	(675.11)	1,458.95	(854.67)	767.32	(463.69)
1,484.31	(932.26)	1,207.50	(765.47)	1,596.12	(960.93)	844.67	(527.74)
1,606.14	(1,032.65)	1,318.45	(855.35)	1,728.49	(1,067.56)	919.83	(591.90)
1,724.35	(1,132.84)	1,425.66	(944.75)	1,856.38	(1,174.70)	992.94	(656.14)

1,839.13	(1,232.90)	1,529.29	(1,033.58)	1,979.81	(1,282.41)	1,064.34	(720.46)
1,949.49	(1,332.83)	1,629.14	(1,121.75)	2,098.93	(1,390.58)	1,133.95	(784.87)
2,056.11	(1,432.67)	1,725.78	(1,209.41)	2,213.72	(1,499.10)	1,201.58	(849.36)
2,158.83	(1,532.36)	1,819.11	(1,296.40)	2,324.35	(1,607.92)	1,267.82	(913.90)
2,257.55	(1,631.89)	1,909.63	(1,382.84)	2,430.84	(1,717.02)	1,332.30	(978.51)

Table A - 3 load settlement relation of soil 3

Square		Circular		Rectangular		Strip	
Load in (KN/m^2)	Settlement (mm)	Load in (KN/m^2)	Settlement (mm)	Load in (KN/m^2)	Settlement (mm)	Load in (KN/m^2)	Settlement (mm)
-	-	-	-	-	-	-	-
32.44	(4.71)	35.65	(5.31)	38.14	(5.25)	36.02	(5.20)
96.65	(14.13)	105.20	(15.94)	113.95	(15.75)	106.39	(15.60)
217.33	(32.87)	237.47	(37.33)	256.72	(36.88)	244.06	(36.45)
332.65	(51.79)	363.91	(58.72)	393.18	(58.13)	377.27	(57.39)
442.29	(70.71)	480.18	(79.94)	522.22	(79.49)	502.79	(78.44)
542.50	(89.80)	588.92	(101.34)	642.41	(100.97)	615.25	(99.60)
635.22	(108.80)	690.66	(123.00)	750.27	(122.59)	711.26	(120.88)
723.06	(127.95)	786.30	(144.71)	847.59	(144.59)	798.42	(142.30)
805.28	(147.26)	877.29	(166.58)	939.52	(166.64)	880.78	(163.80)
883.68	(166.64)	965.47	(188.59)	1,115.01	(210.94)	1,036.32	(206.96)
960.33	(186.12)	1,051.60	(210.71)	1,280.56	(255.20)	1,181.88	(250.36)
1,035.85	(205.66)	1,218.40	(255.04)	1,438.47	(299.51)	1,319.89	(293.95)
1,183.38	(244.91)	1,375.37	(299.37)	1,741.30	(388.19)	1,452.03	(337.67)
1,324.64	(284.30)	1,524.93	(343.67)	1,800.00	(405.72)	1,578.95	(381.50)
1,460.83	(323.92)	1,800.00	(427.98)			1,701.74	(425.40)
1,592.11	(363.64)					1,800.00	(461.55)
1,800.00	(429.20)						

Table A - 4 load settlement relation of soil 1

Square		Circular		Rectangular		Strip	
Load in (KN/m^2)	Settlement (mm)	Load in (KN/m^2)	Settlement (mm)	Load in (KN/m^2)	Settlement (mm)	Load in (KN/m^2)	Settlement (mm)
-	-	-	-	-	-	-	-
24.25	(2.13)	17.79	(1.60)	37.80	(3.12)	58.36	(5.17)
71.34	(6.41)	52.42	(4.80)	110.99	(9.37)	99.64	(8.61)
160.22	(15.01)	118.91	(11.24)	244.01	(22.01)	128.63	(10.92)
318.88	(32.39)	241.25	(24.20)	361.75	(34.73)	150.62	(12.68)
460.38	(49.96)	351.58	(37.18)	467.85	(47.51)	170.83	(14.41)
590.24	(67.67)	453.04	(50.15)	568.52	(60.37)	188.99	(16.11)
710.30	(85.52)	548.47	(63.23)	664.99	(73.40)	221.73	(19.43)
824.71	(103.42)	638.46	(76.46)	757.80	(86.58)	235.17	(20.88)
936.00	(121.36)	725.22	(89.77)	847.58	(99.85)	260.27	(23.68)
1,152.89	(157.30)	809.84	(103.12)	935.02	(113.14)	270.37	(24.87)
		974.59	(129.94)	1,104.65	(139.76)	289.56	(27.22)
		1,135.02	(156.99)	1,269.34	(166.45)	306.83	(29.47)
		1,292.53	(184.15)	1,430.60	(193.20)	320.98	(31.41)
		1,447.53	(211.40)	1,588.86	(220.06)	332.57	(33.05)
		1,599.30	(238.72)	1,897.62	(273.85)	341.05	(34.34)
		1,748.40	(266.08)	2,193.48	(327.79)	348.24	(35.46)
		1,894.13	(293.47)	2,400.00	(366.50)	354.30	(36.42)
		2,037.36	(320.87)			359.46	(37.27)
		2,315.57	(375.70)			363.63	(37.97)
		2,400.00	(392.71)			366.13	(38.43)
						367.88	(38.76)
						368.47	(38.87)
						369.81	(39.11)
						370.85	(39.33)
						371.92	(39.48)
						374.34	(39.83)
						378.76	(40.52)
						382.06	(41.08)

Table A - 5 allowable and ultimate bearing capacity of soil

S/B	Qall (KN/m^2) at allowable settlement 25mm				Sample
	squa.	Circ.	Rec.	Str.	
Isolated	140	135	145	135	Soil 1
1	88	89	87	77	
2	105	108	106	97	
3	121	119	118	112	
4	122.5	122.5	132.5	118	
5	129	129	135	130	
6	132.5	127	145	133	
7	136	133	141	136	
Isolated	82	79	87.5	92	Soil 2
1	56	62	84	53	
2	70	72	76	67	
3	79	75	82	76	
4	76	76	82	90	
5	73	79	89	85	
6	78.5	78	94	86	
7	80	78	86	90	
Isolated	169	161	178	170	Soil 3
1	118	116	112.5	102	
2	138	134	136	112	
3	151	151.5	152	129	
4	159	158	167	137	
5	169	159	169	145	
6	172	157	172	149	
7	169	160	178	158	
Isolated	251	247	274	272	Soil 4
1	167	167	167	146	
2	200	205	200	161	
3	224	222	220	180	
4	225	227	228	195	
5	244	232	236	205	
6	241	230	245	215	
7	227	245	255	228	

Table A - 6 Ultimate bearing capacity of square, circular, rectangular and strip footing with S/B=0 - 7

S/B	Qult (KN/m^2) at allowable settlement 25mm				sample
	squa.	Circ.	Rec.	Str.	
Isolated	420	405	435	405	Soil 1
1	264	267	261	231	
2	315	324	318	291	
3	363	357	354	336	
4	367.5	367.5	397.5	354	
5	387	387	405	390	
6	397.5	381	435	399	
7	408	399	423	408	
Isolated	246	237	262.5	276	Soil 2
1	168	186	252	159	
2	210	216	228	201	
3	237	225	246	228	
4	228	228	246	270	
5	219	237	267	255	
6	235.5	234	282	258	
7	240	234	258	270	
Isolated	507	483	534	510	Soil 3
1	354	348	337.5	306	
2	414	402	408	336	
3	453	454.5	456	387	
4	477	474	501	411	
5	507	477	507	435	
6	516	471	516	447	
7	507	480	534	474	
Isolated	753	741	822	816	Soil 4
1	501	501	501	438	
2	600	615	600	483	
3	672	666	660	540	
4	675	681	684	585	
5	732	696	708	615	
6	723	690	735	645	
7	681	735	765	684	

Table A - 7 BRC of square, circular, rectangular and strip footing with S/B=0-7

S/B	BCR correspond to Qult				sample
	Squa.	Circ.	Rec.	Str.	
1	0.63	0.67	0.57	0.56	Soil 1
2	0.74	0.81	0.74	0.67	
3	0.85	0.88	0.81	0.81	
4	0.88	0.92	0.92	0.87	
5	0.93	0.97	0.93	0.96	
6	0.94	0.97	1.00	0.99	
7	0.97	1.00	0.97	1.00	
1	0.70	0.78	0.62	0.60	soil 2
2	0.86	0.94	0.89	0.79	
3	0.98	0.99	0.97	0.90	
4	0.93	1.01	1.05	0.90	
5	0.86	1.02	1.03	0.96	
6	0.95	1.00	1.09	0.96	
7	0.96	1.00	0.98	1.01	
1	0.70	0.72	0.64	0.60	Soil 3
2	0.83	0.85	0.78	0.68	
3	0.90	0.94	0.87	0.75	
4	0.96	0.98	0.95	0.82	
5	1.02	0.99	0.96	0.86	
6	1.04	0.98	0.98	0.89	
7	1.02	0.99	1.00	0.93	
1	0.67	0.68	0.61	0.54	Soil 4
2	0.80	0.83	0.73	0.59	
3	0.89	0.90	0.80	0.66	
4	0.90	0.92	0.83	0.72	
5	0.97	0.94	0.86	0.75	
6	0.96	0.93	0.89	0.79	
7	0.90	0.99	0.93	0.84	

Table A - 8 Elastic settlement and rigid settlement of isolated square footing considering depth of influence H =2B and 5B

H	F1	F2	μ	q_o	α	B'	Es	I_S	I_f	Se	Se (rigid)
2B	0.437	0.031	0.35	140	4	1	6436	0.45	0.67	0.023	0.021
5B	0.498	0.016	0.35	140	4	1	6436	0.51	0.67	0.026	0.024
2B	0.437	0.031	0.35	82	4	1	3000	0.45	0.67	0.029	0.027
5B	0.498	0.016	0.35	82	4	1	3622	0.51	0.67	0.027	0.025
2B	0.437	0.031	0.35	169	4	1	7657	0.45	0.67	0.023	0.022
5B	0.498	0.016	0.35	169	4	1	8800	0.51	0.67	0.023	0.021
2B	0.437	0.031	0.35	251	4	1	16932	0.45	0.67	0.016	0.015
5B	0.498	0.016	0.35	251	4	1	13263	0.51	0.67	0.022	0.021

Table A - 9 Elastic settlement and rigid settlement of isolated circular footing considering depth of influence H =2B and 5B

H	F1	F2	μ	q_o	α	B'	Es	IS	If	Se	Se (rigid)
2B	0.437	0.031	0.35	135	4	1.13	6436	0.45	0.7	0.026	0.024
5B	0.498	0.016	0.35	135	4	1.13	6436	0.51	0.7	0.029	0.027
2B	0.437	0.031	0.35	79	4	1.13	3000	0.45	0.7	0.033	0.031
5B	0.498	0.016	0.35	79	4	1.13	3622	0.51	0.7	0.031	0.028
2B	0.437	0.031	0.35	161	4	1.13	7657	0.45	0.7	0.026	0.025
5B	0.498	0.016	0.35	161	4	1.13	8800	0.51	0.7	0.026	0.024
2B	0.437	0.031	0.35	247	4	1.13	16932	0.45	0.7	0.018	0.017
5B	0.498	0.016	0.35	247	4	1.13	13263	0.51	0.7	0.026	0.024

Table A - 10 Elastic settlement and rigid settlement of isolated rectangular footing considering depth of influence H =2B and 5B

H	F1	F2	μ	q_o	α	B'	Es	IS	If	Se	Se (rigid)
2B	0.588	0.032	0.35	145	4	0.8	6436	0.60	0.71	0.027	0.025
5B	0.584	0.024	0.35	145	4	0.8	6436	0.60	0.71	0.027	0.025
2B	0.588	0.032	0.35	87.5	4	0.8	3000	0.60	0.71	0.035	0.033
5B	0.584	0.024	0.35	87.5	4	0.8	3622	0.60	0.71	0.029	0.027
2B	0.588	0.032	0.35	178	4	0.8	7657	0.60	0.71	0.028	0.026
5B	0.584	0.024	0.35	178	4	0.8	8800	0.60	0.71	0.024	0.022
2B	0.588	0.032	0.35	274	4	0.8	16932	0.60	0.71	0.019	0.018
5B	0.584	0.024	0.35	274	4	0.8	13263	0.60	0.71	0.025	0.023

Table A - 11 Elastic settlement and rigid settlement of isolated strip footing considering depth of influence H =2B and 5B

h	F1	F2	μ	qo	α	B'	Es	IS	If	Se	Se (rigid)
2B	0.753	0.135	0.35	135	4	0.5	6436	0.82	0.8	0.024	0.022
5B	0.98	0.106	0.35	135	4	0.5	6436	1.03	0.8	0.030	0.028
2B	0.753	0.135	0.35	92	4	0.5	3000	0.82	0.8	0.036	0.034
5B	0.98	0.106	0.35	92	4	0.5	3622	1.03	0.8	0.035	0.032
2B	0.753	0.135	0.35	170	4	0.5	7657	0.82	0.8	0.025	0.024
5B	0.98	0.106	0.35	170	4	0.5	8800	1.03	0.8	0.028	0.026
2B	0.753	0.135	0.35	272	4	0.5	16932	0.82	0.8	0.018	0.017
5B	0.98	0.106	0.35	272	4	0.5	13263	1.03	0.8	0.030	0.028

Table A-12 Summary of effect of adjecent square, circular, rectangular and strip footings on ultimate bearing capacity

S/B	Ultimate bearing capacity increase from left to right	
0	Circular → strip → square → rectangular	Soil 1 figure 4.7 to 4.10 and Figure 4.11, a-h
1	Strip → *square → rectangular* → circular	
2	Strip → square → rectangular → circular	
3	Strip →*rectangular* → *circular* → square	
4	Strip → circular → square → rectangular	
5,6 &7	Circular → square → Strip → rectangular	
0	Circular → square → rectangular → strip	Soil 2 Appendix - B Figure B-2, a-l
1	Strip → rectangular → square → circular	
2	Strip → circular → square → rectangular	
3	circular → Strip → square →rectangular	
4	*square* → *circular* → Strip → rectangular	
5	square → Circular → Strip → rectangular	
6	Circular → square → Strip → rectangular	
7	Circular → square → rectangular → Strip	
0	Circular → square → strip → rectangular	Soil 3 Appendix - B Figure B-3, a-l
1	Strip → *rectangular* → *square* → circular	
2	Strip → circular → rectangular→ square	
3	Strip → square → *circular →rectangular*	
4	Strip → circular → square → rectangular	
5	Strip → Circular → *square* → *rectangular*	
6	Strip → Circular → *square* → *rectangular*	
7	Circular → Strip → square → rectangular	
0	Strip → circular → square → rectangular	Soil 4 Appendix - B Figure B-4, a-l
1	Strip → *circular* → *square* → rectangular	
2	Strip → rectangular → square → circular	
3	Strip → *circular* → *rectangular* → square	
4	Strip → square → rectangular → circular	
5	Strip → circular → rectangular → square	
6	Strip → circular → rectangular → square	
7	Strip→ square → circular → rectangular	

Appendix – B Borehole log sheets

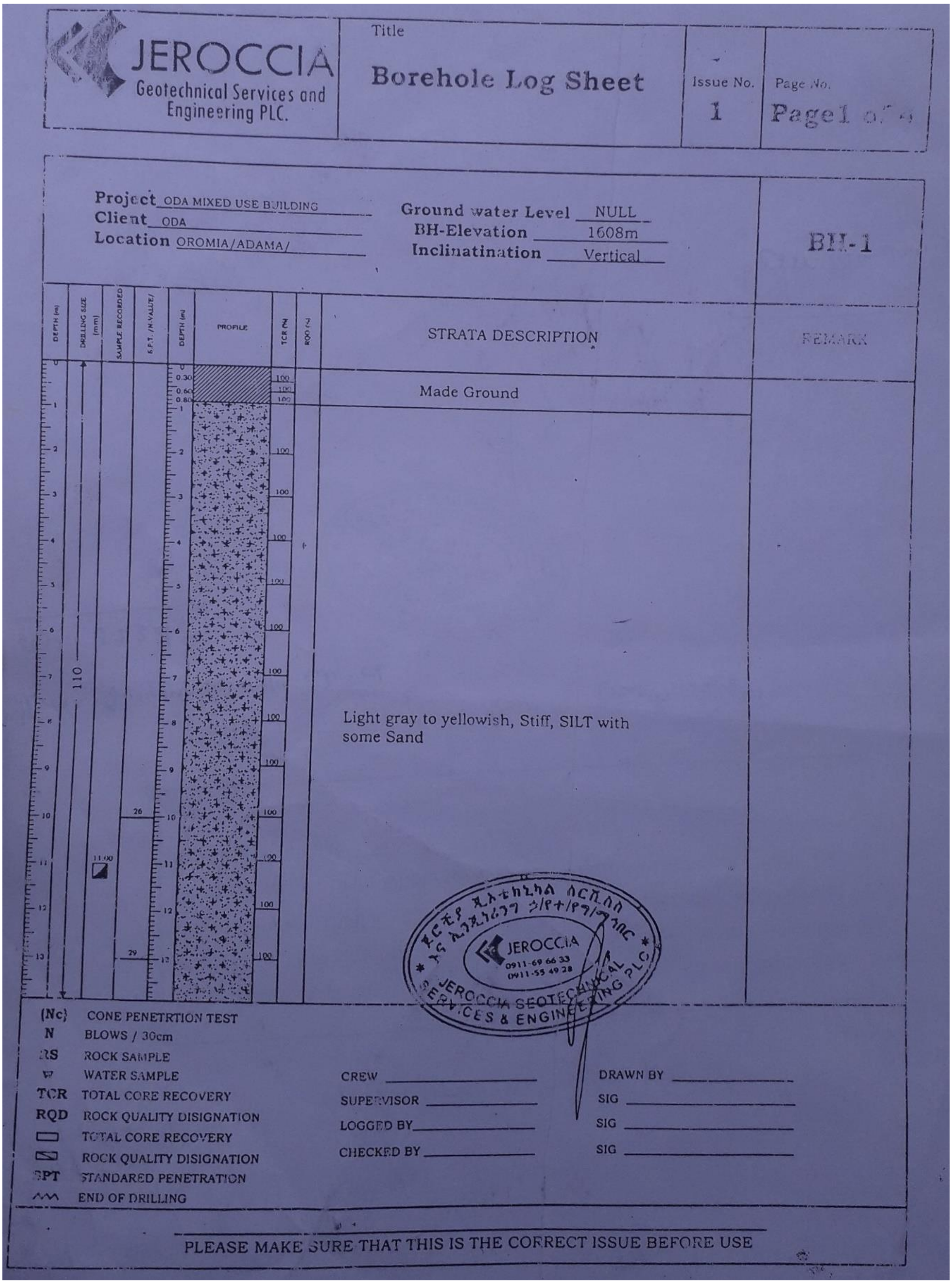
JEROCCIA Geotechnical Services and Engineering PLC.

Title	Issue No.	Page No.
Borehole Log Sheet	1	Page1 of 4

Project ODA MIXED USE BUILDING
Client ODA
Location OROMIA/ADAMA/

Ground water Level NULL
BH-Elevation 1608m
Inclinatination Vertical

BH-1

DEPTH (m)	DRILLING SIZE (mm)	SAMPLE RECORDED	S.P.T. / N-VALUE	DEPTH (m)	PROFILE	TCR (%)	RQD (%)	STRATA DESCRIPTION	REMARK
0 – 0.80	110			0.30, 0.60, 0.80		100, 100, 100		Made Ground	
0.80 – 13	110	11.00	26, 29			100, 100, 100, 100, 100, 100, 100, 100, 100, 100, 100, 100, 100		Light gray to yellowish, Stiff, SILT with some Sand	

(Nc) CONE PENETRTION TEST
N BLOWS / 30cm
RS ROCK SAMPLE
WATER SAMPLE
TCR TOTAL CORE RECOVERY
RQD ROCK QUALITY DISIGNATION
TOTAL CORE RECOVERY
ROCK QUALITY DISIGNATION
SPT STANDARED PENETRATION
END OF DRILLING

CREW
SUPERVISOR
LOGGED BY
CHECKED BY

DRAWN BY
SIG
SIG
SIG

PLEASE MAKE SURE THAT THIS IS THE CORRECT ISSUE BEFORE USE

Figure B-1 a bore hole data for ODA mixed used building

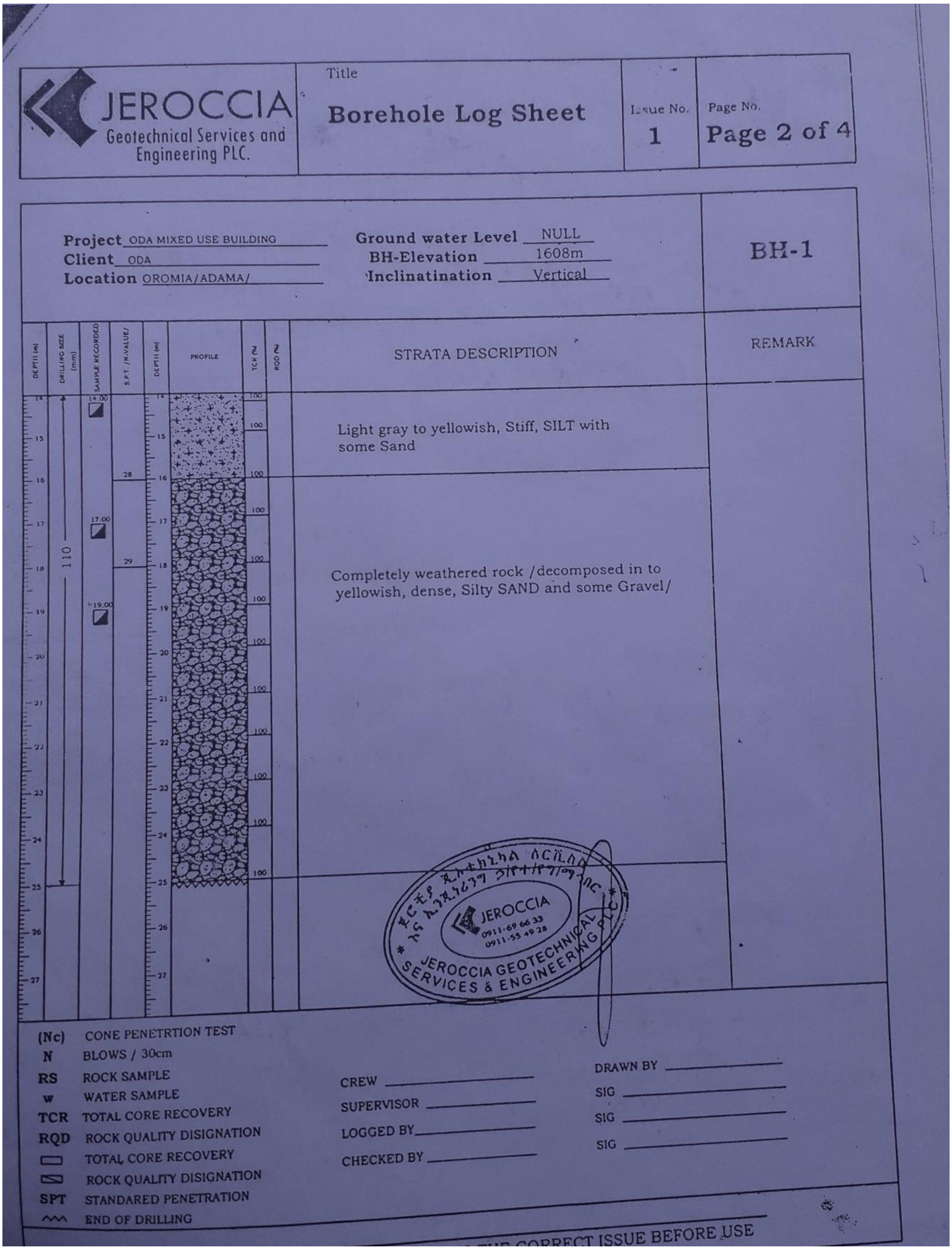

Title

Borehole Log Sheet

JEROCCIA Geotechnical Services and Engineering PLC.

Issue No.	Page No.
1	Page 2 of 4

Project ODA MIXED USE BUILDING
Client ODA
Location OROMIA/ADAMA/

Ground water Level NULL
BH-Elevation 1608m
Inclinatination Vertical

BH-1

DEPTH (m)	DRILLING SIZE (mm)	SAMPLE RECORDED	S.P.T. /N-VALUE/	DEPTH (m)	PROFILE	TCR (%)	RQD (%)	STRATA DESCRIPTION	REMARK
14–16	110	14.00	28	14–16		100, 100, 100		Light gray to yellowish, Stiff, SILT with some Sand	
16–25	110	17.00, 19.00	29	16–25		100, 100, 100, 100, 100, 100, 100, 100, 100, 100		Completely weathered rock /decomposed in to yellowish, dense, Silty SAND and some Gravel/	
25–27				25–27					

JEROCCIA GEOTECHNICAL SERVICES & ENGINEERING PLC
0911-69 66 33
0911-55 49 28

(Nc) CONE PENETRTION TEST
N BLOWS / 30cm
RS ROCK SAMPLE
w WATER SAMPLE
TCR TOTAL CORE RECOVERY
RQD ROCK QUALITY DISIGNATION
▭ TOTAL CORE RECOVERY
▨ ROCK QUALITY DISIGNATION
SPT STANDARED PENETRATION
^^^ END OF DRILLING

CREW ______
SUPERVISOR ______
LOGGED BY ______
CHECKED BY ______

DRAWN BY ______
SIG ______
SIG ______
SIG ______

... CORRECT ISSUE BEFORE USE

Figure B-1 b bore hole data for ODA mixed used building

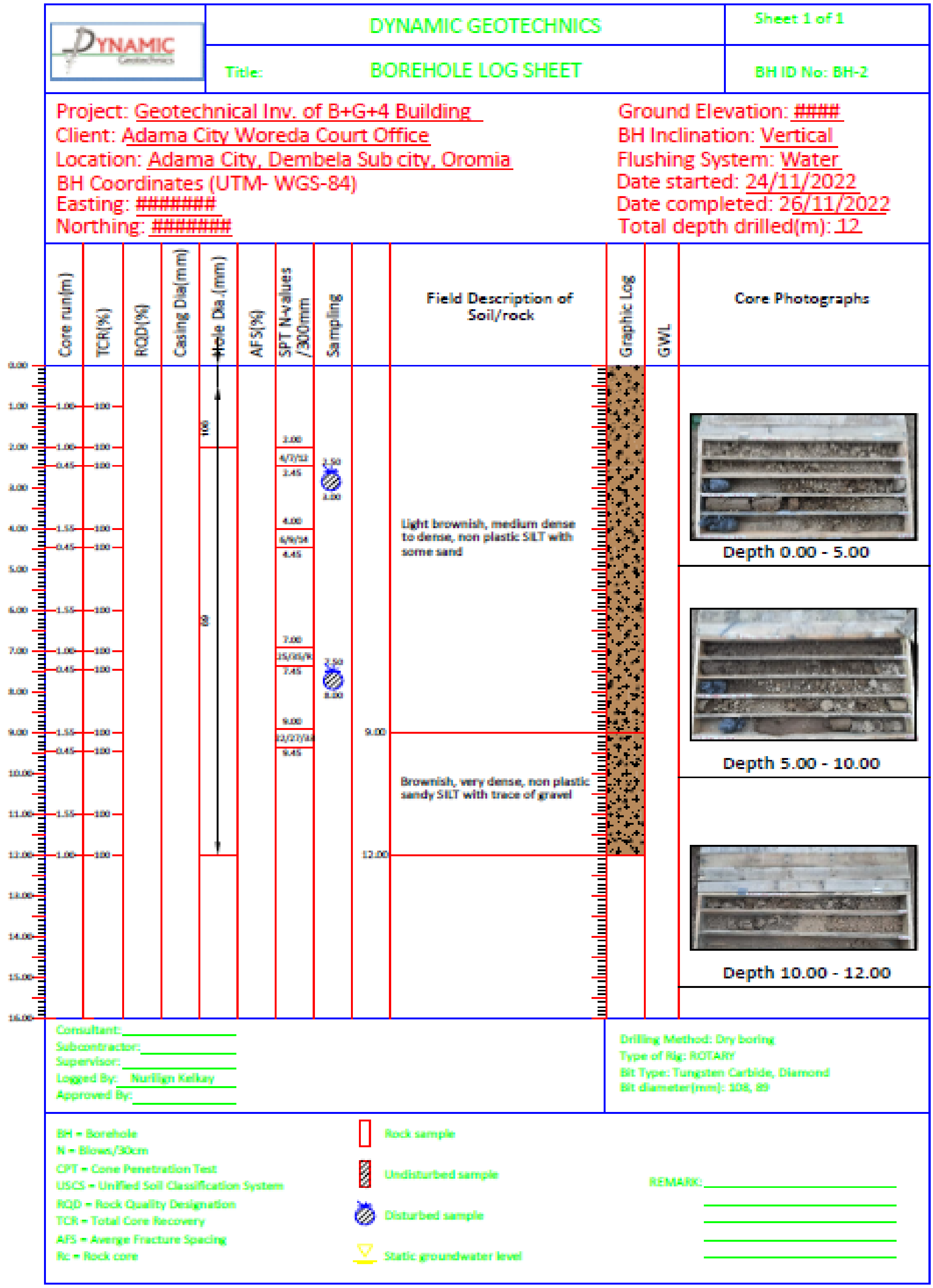

Figure B-2 bore hole data for Adama City Woreda Court Office building

ZTY ENGINEERING PLC

Sheet 1 of 2

Title : BOREHOLE LOG SHEET

BH ID No: BH-2-1

Project: Geotech. Inv. of B+G+10 Hotel Building
Client: Ato Teshale Kore
Location: Adama Town, Oromia Regional State

BH Inclination: Vertical
Flushing System: Water
Date started: 26/04/2022
Date completed: 28/04/2022
Total depth drilled(m): 20.00

Depth (m)	Core run(m)	TCR(%)	RQD(%)	Casing Dia(mm)	Hole Dia.(mm)	AFS(%)	SPT N-values /300mm	Sampling		Field Description of Soil/rock	Graphic Log	GWL	Core Photographs
0.00	0.60	100			110				0.40	Back fill material with concret cover			
1.00	0.40	100							1.60	Dark brown, stiff, medium to high plastic, clayey SILT with trace of sand and gravel			
	0.60	100											
2.00	0.40	100					2.00 / R / 2.45						
	0.35	100											
3.00	0.65	100											
4.00	1.00	100					4.00 / R / 4.45	4.00–4.50					
	0.45	100											
5.00	0.55	100											Depth: 00.00 - 5.00m
	0.50	100											
6.00	0.50	100					6.00 / R / 6.45						
	0.45	100											
7.00	0.55	100											
	0.50	100			89								
8.00	0.50	100					8.00 / 7/10/13 / 8.45	8.00–8.50		Light gray to yellowish, dense/stiff, none to low plastic, silty SAND/clayey sandy SILT with trace of gravel			
	0.45	100											
9.00	0.55	100											
	0.50	100											
10.00	0.50	100					10.00 / 13/15/17 / 10.45						Depth: 5.00 – 10.00m
	0.60	100											
11.00	0.40	100											
12.00	0.90	100					12.00 / 12/16/29 / 12.45	12.00–12.50					
	0.60	100											
13.00	0.50	100											
	0.50	100											
14.00	0.50	100					14.00 / R / 14.45						
	0.50	100											
15.00	0.50	100											Depth: 10.00 – 15.00m
	0.50	100											
16.00													

Depth: 00.00 - 5.00m

Depth: 5.00 – 10.00m

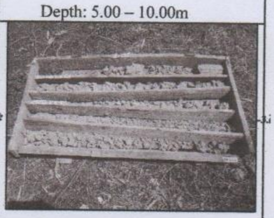

Depth: 10.00 – 15.00m

Consultant:
Subcontractor:
Supervisor:
Logged By: Yonas A. & Zelalem E.
Approved By:

Drilling Method: Dry boring
Type of Rig : ROTARY
Bit Type: Tungsten Carbide, Diamond
Bit diameter(mm): 108, 89

BH=Borehole
N=Blows/30cm
CPT=Cone Penetration Test
USCS=Unified Soil Classification System
RQD=Rock Quality Designation
TCR=Total Core Recovery
AFS=Averge Fracture Spacing
Rc=Rock core

Rock sample
Undisturbed sample
Disturbed sample
Static groundwater level

REMARK:

ZTY Engineering PLC 0910740614 0910821547

PLEASE MAKE SURE THIS IS THE CORRECT ISSUE BEFORE USE

Figure B-3 a bore hole data for ODA mixed used building

ZTY ENGINEERING PLC

Sheet 2 of 2

Title : BOREHOLE LOG SHEET

BH ID No: BH-2-2

Project: Geotech. Inv. of B+G+10 Hotel Building
Client: Ato Teshale Kore
Location: Adama Town, Oromia Regional State

BH Inclination: Vertical
Flushing System: Water
Date started: 03/02/2021
Date completed: 04/02/2021
Total depth drilled(m): 20.00

Depth (m)	Core run(m)	TCR(%)	RQD(%)	Casing Dia(mm)	Hole Dia.(mm)	AFS(%)	SPT N-values /300mm	Sampling		Field Description of Soil/rock	Graphic Log	GWL
16.00	0.30	100			89		16.00 R	16.00–16.50		Cont'd Light gray to yellowish, dense/stiff, none to low plastic, silty SAND/clayey sandy SILT with trace of gravel		
	0.45	100										
17.00	0.50	100										
	0.50	100										
18.00	0.50	100					18.00 R					
	0.50	100										
19.00	0.50	100										
	0.50	100										
20.00	0.50	100							20.00			
21.00												
22.00												
23.00												
24.00												
25.00												
26.00												
27.00												
28.00												
29.00												
30.00												
31.00												
32.00												

Core Photographs

Depth: 15.00 - 20.00m

Consultant:
Subcontractor:
Supervisor:
Logged By: Yonas A. & Zelalem E.
Approved By:

Drilling Method: Dry boring
Type of Rig : ROTARY
Bit Type: Tungsten Carbide, Diamond
Bit diameter(mm): 108, 89

BH=Borehole
N=Blows/30cm
CPT=Cone Penetration Test
USCS=Unified Soil Classification System
RQD=Rock Quality Designation
TCR=Total Core Recovery
AFS=Averge Fracture Spacing
Rc=Rock core

Rock sample
Undisturbed sample
Disturbed sample
Static groundwater level

REMARK

ZTY Engineering PLC
0910740614
0910821547

PLEASE MAKE SURE THIS IS THE CORRECT ISSUE BEFORE USE

Figure B-3 b bore hole data for ODA mixed used building

Appendix- C Load settlement curves and tables of footing on different soil

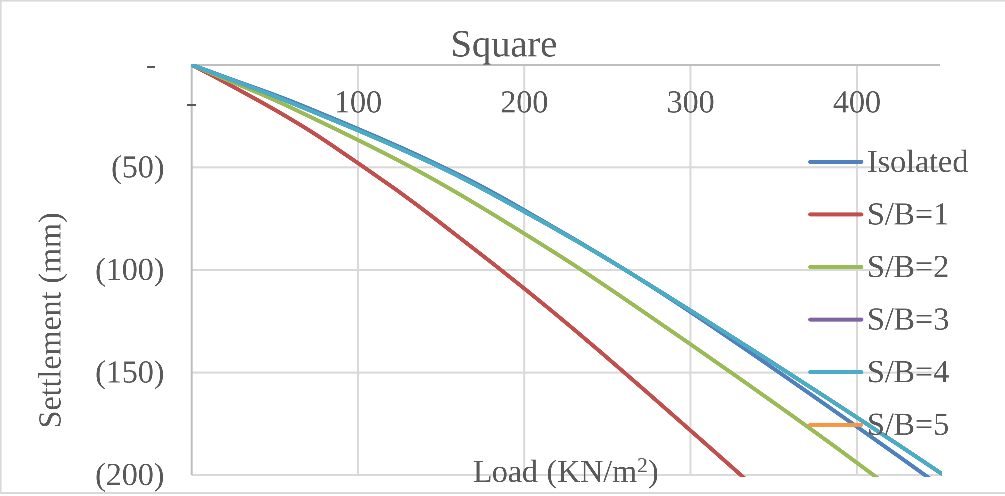

a

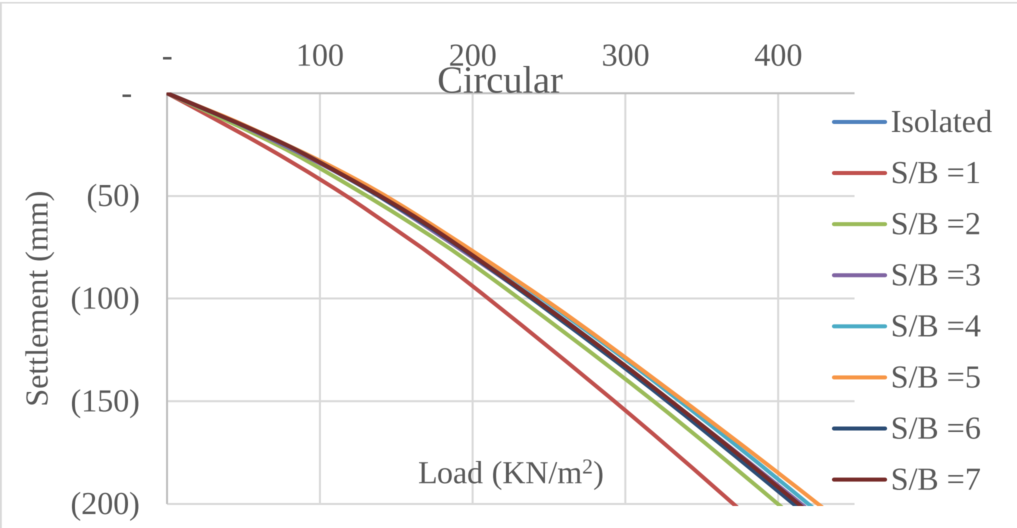

b

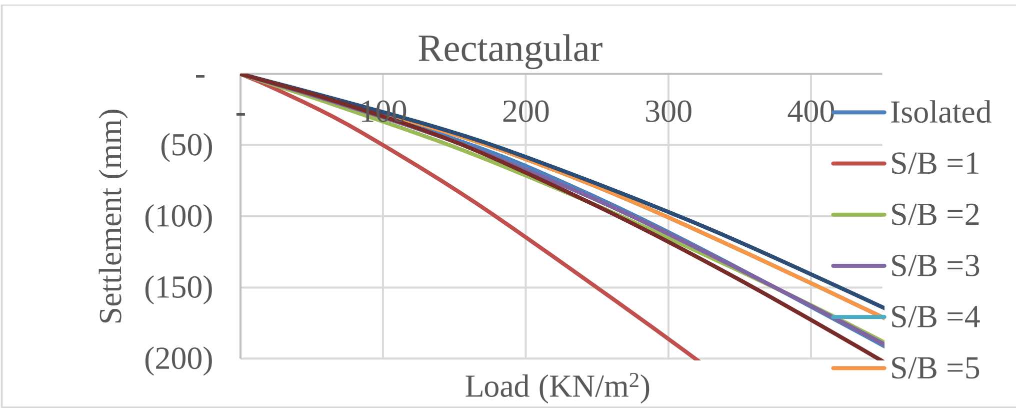

c

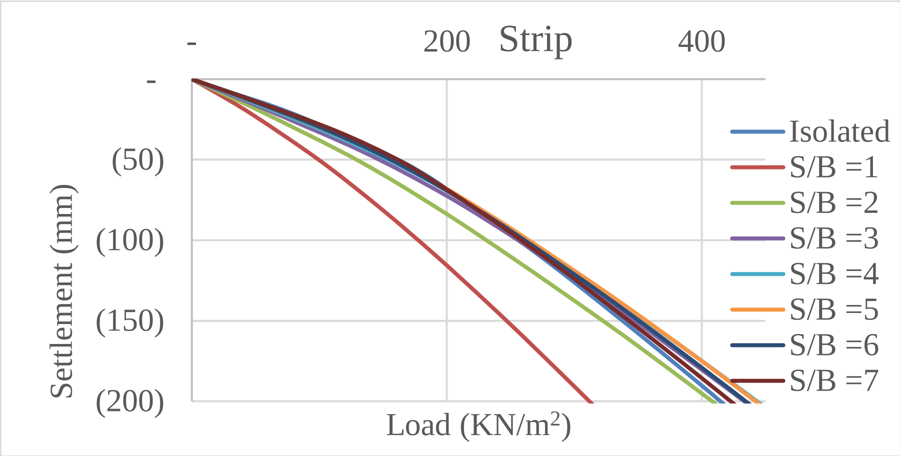
Strip
-
200
400
-
(50)
(100)
(150)
(200)
Settlement (mm)
Load (KN/m2)
Isolated
S/B =1
S/B =2
S/B =3
S/B =4
S/B =5
S/B =6
S/B =7

d

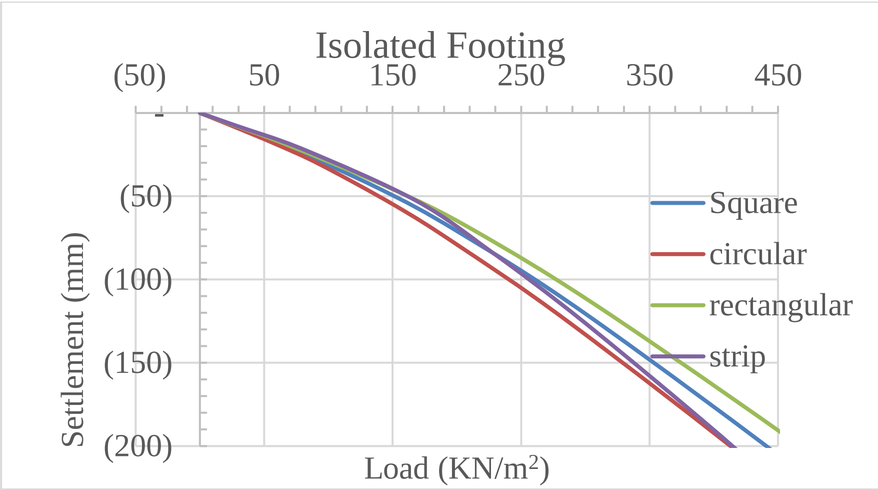
Isolated Footing
(50)
50
150
250
350
450
-
(50)
(100)
(150)
(200)
Settlement (mm)
Load (KN/m2)
Square
circular
rectangular
strip

e

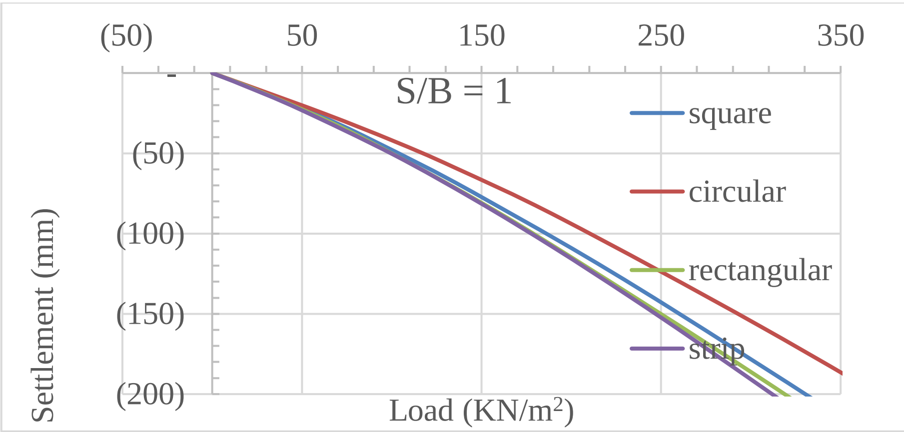
S/B = 1
(50)
50
150
250
350
-
(50)
(100)
(150)
(200)
Settlement (mm)
Load (KN/m2)
square
circular
rectangular
strip

f

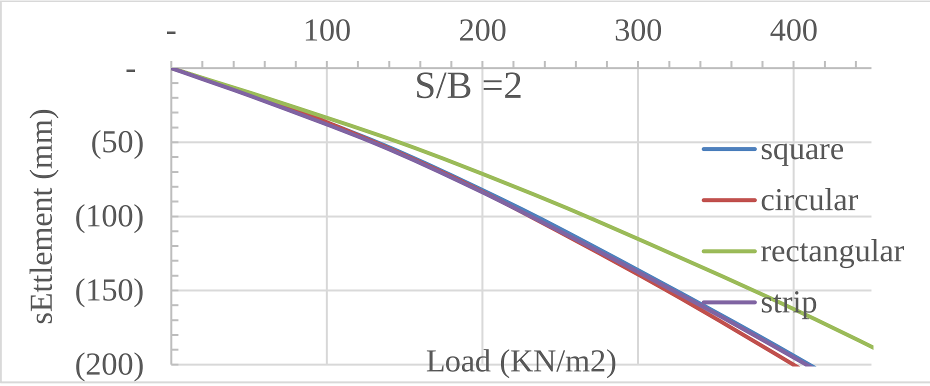
S/B =2
-
100
200
300
400
-
(50)
(100)
(150)
(200)
sEttlement (mm)
Load (KN/m2)
square
circular
rectangular
strip

g

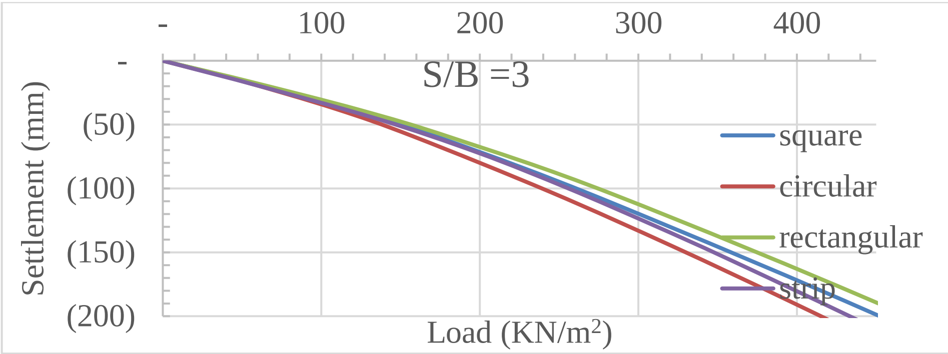
S/B =3
-
100
200
300
400
-
(50)
(100)
(150)
(200)
Settlement (mm)
Load (KN/m²)
square
circular
rectangular
strip

h

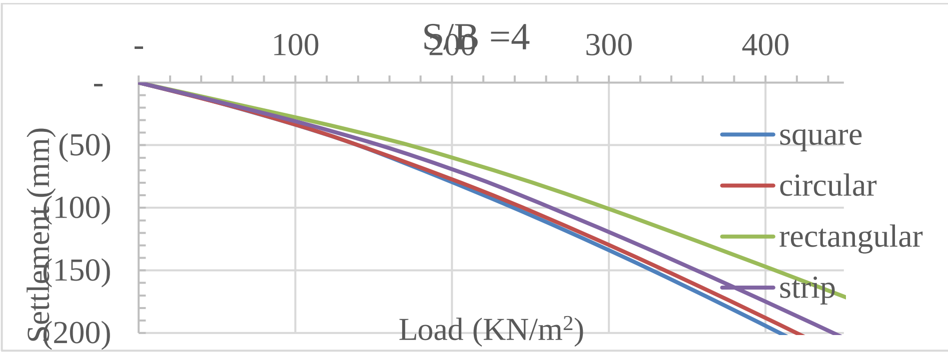
S/B =4
-
100
200
300
400
-
(50)
(100)
(150)
(200)
Settlement (mm)
Load (KN/m²)
square
circular
rectangular
strip

i

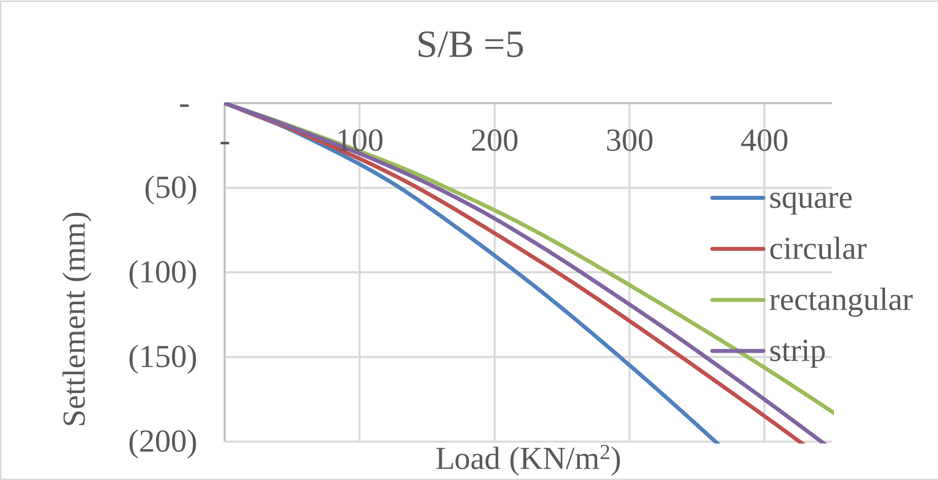

j

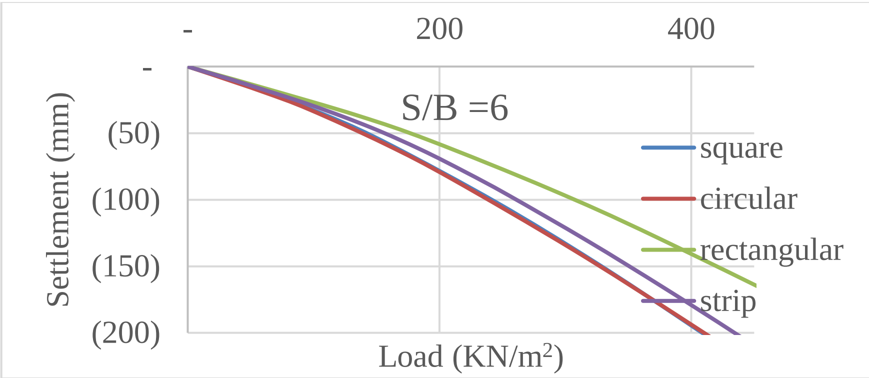

k

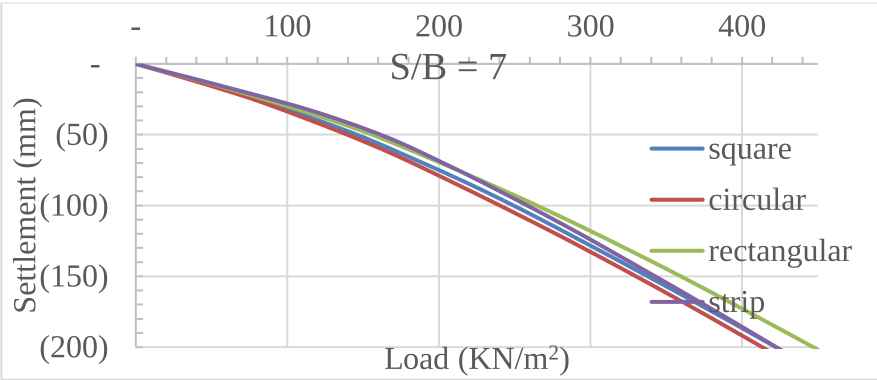

l

Figure C-1 a-1 settlement curve of footing with variying S/B ratio on soil 2

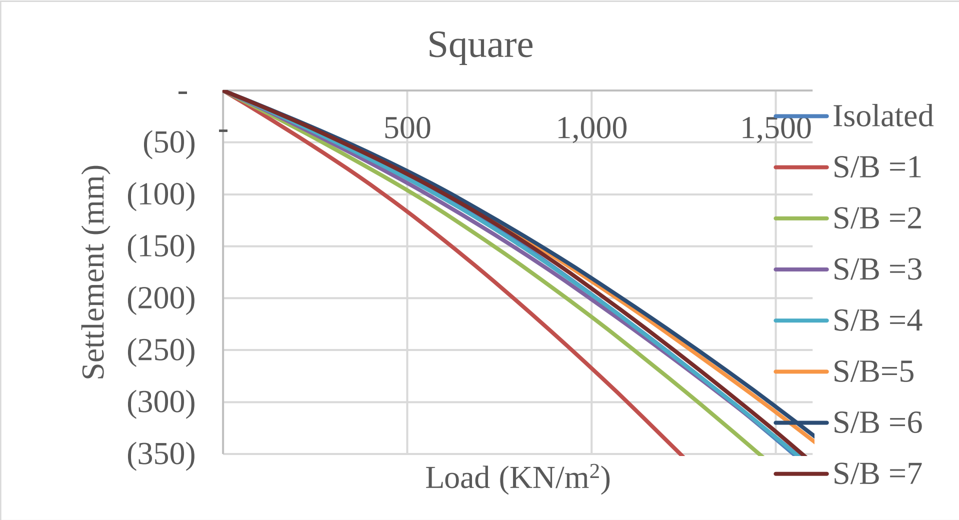
Square
-
(50)
(100)
(150)
(200)
(250)
(300)
(350)
Settlement (mm)
500
1,000
1,500
Load (KN/m2)
Isolated
S/B =1
S/B =2
S/B =3
S/B =4
S/B=5
S/B =6
S/B =7

a

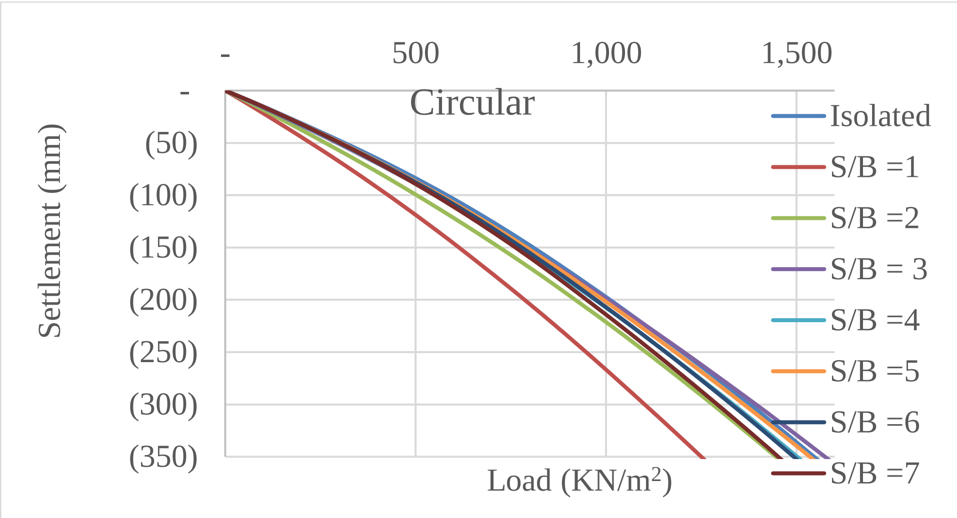
Circular
500
1,000
1,500
(50)
(100)
(150)
(200)
(250)
(300)
(350)
Settlement (mm)
Load (KN/m2)
Isolated
S/B =1
S/B =2
S/B = 3
S/B =4
S/B =5
S/B =6
S/B =7

b

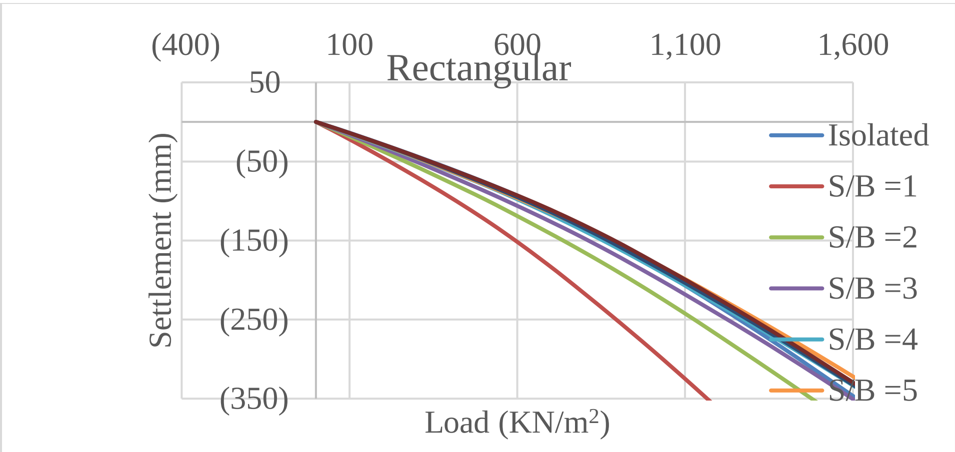
Rectangular
(400)
100
600
1,100
1,600
50
(50)
(150)
(250)
(350)
Settlement (mm)
Load (KN/m2)
Isolated
S/B =1
S/B =2
S/B =3
S/B =4
S/B =5

c

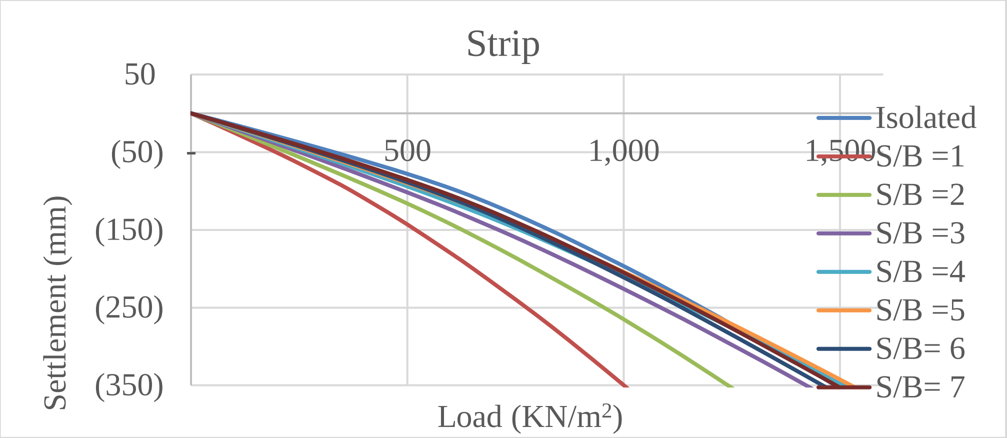
Strip
50
(50)
(150)
(250)
(350)
500
1,000
1,500
Settlement (mm)
Load (KN/m2)
Isolated
S/B =1
S/B =2
S/B =3
S/B =4
S/B =5
S/B= 6
S/B= 7

d

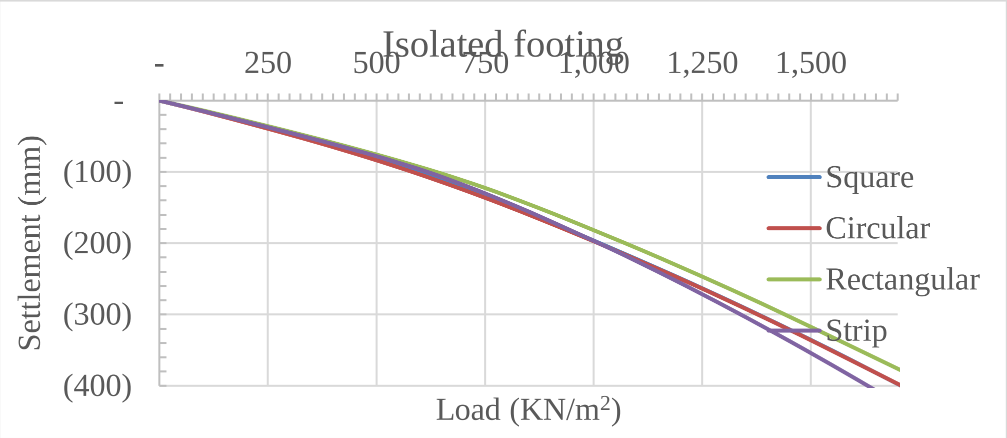
Isolated footing
-
250
500
750
1,000
1,250
1,500
(100)
(200)
(300)
(400)
Settlement (mm)
Load (KN/m2)
Square
Circular
Rectangular
Strip

e

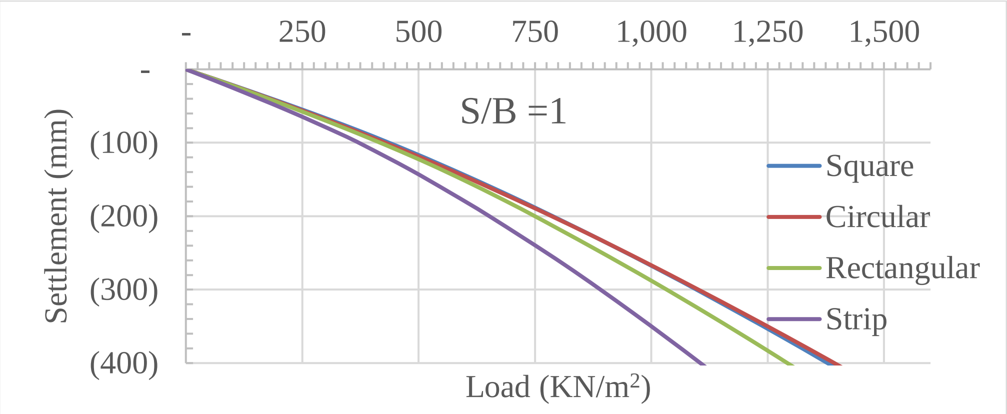
S/B =1
-
250
500
750
1,000
1,250
1,500
(100)
(200)
(300)
(400)
Settlement (mm)
Load (KN/m2)
Square
Circular
Rectangular
Strip

f

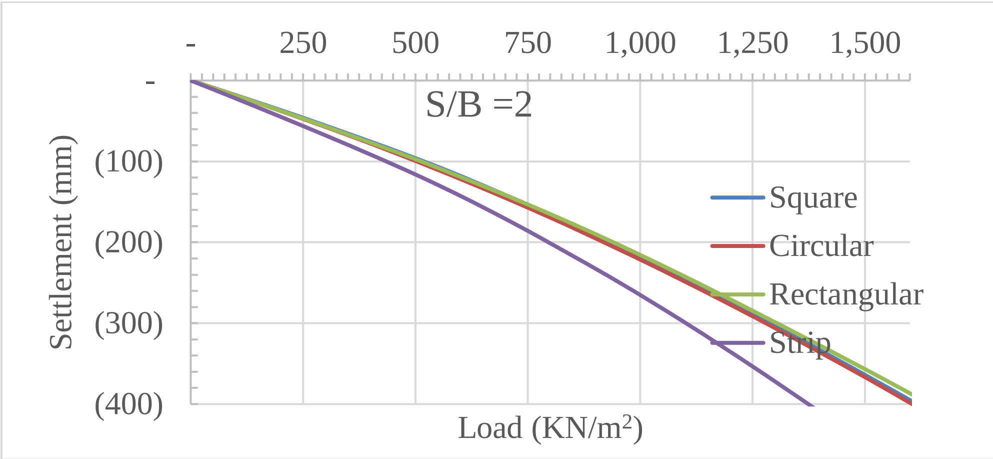
S/B =2
-
250
500
750
1,000
1,250
1,500
-
(100)
(200)
(300)
(400)
Settlement (mm)
Load (KN/m²)
Square
Circular
Rectangular
Strip

g

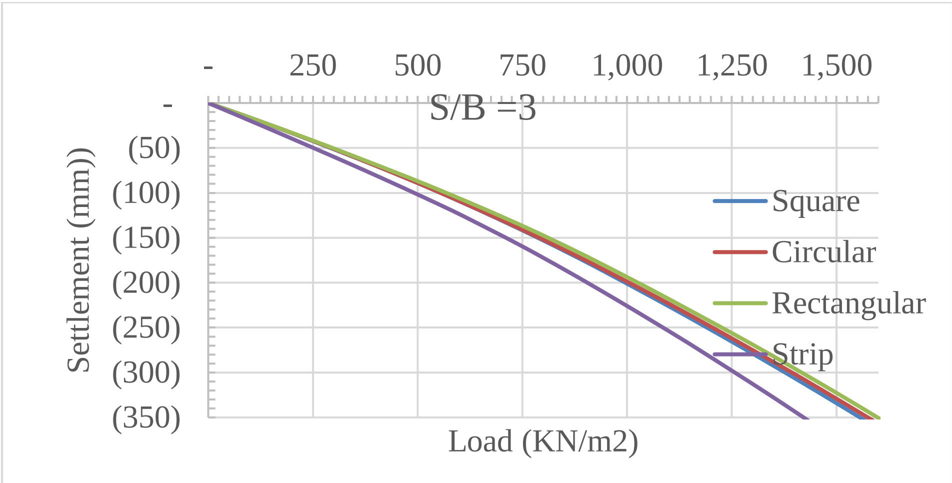
S/B =3
-
250
500
750
1,000
1,250
1,500
-
(50)
(100)
(150)
(200)
(250)
(300)
(350)
Settlement (mm)
Load (KN/m2)
Square
Circular
Rectangular
Strip

h

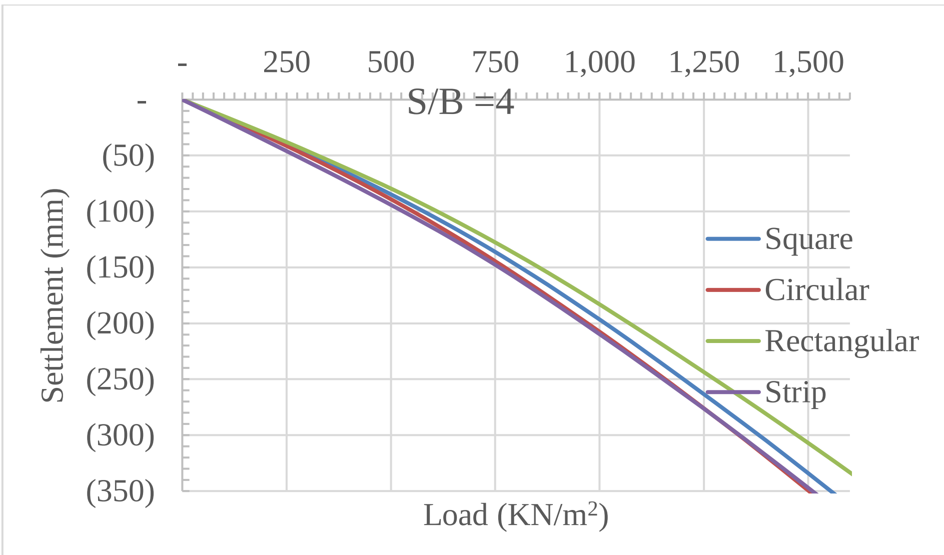
S/B =4
-
250
500
750
1,000
1,250
1,500
-
(50)
(100)
(150)
(200)
(250)
(300)
(350)
Settlement (mm)
Load (KN/m²)
Square
Circular
Rectangular
Strip

i

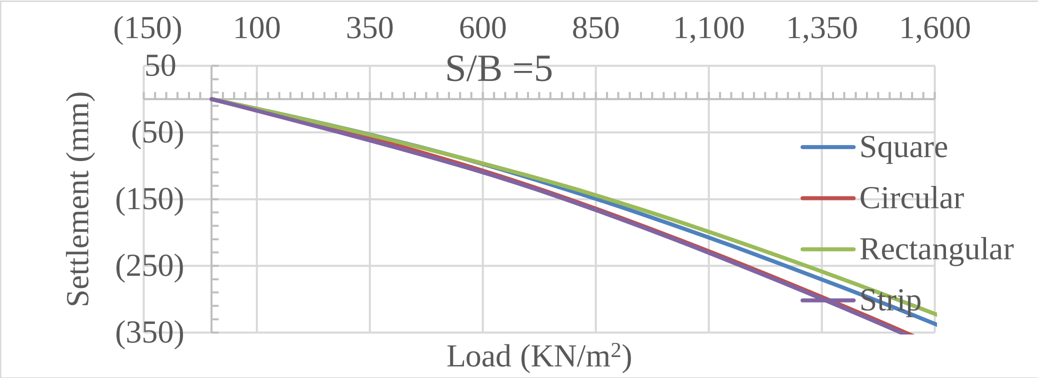

j

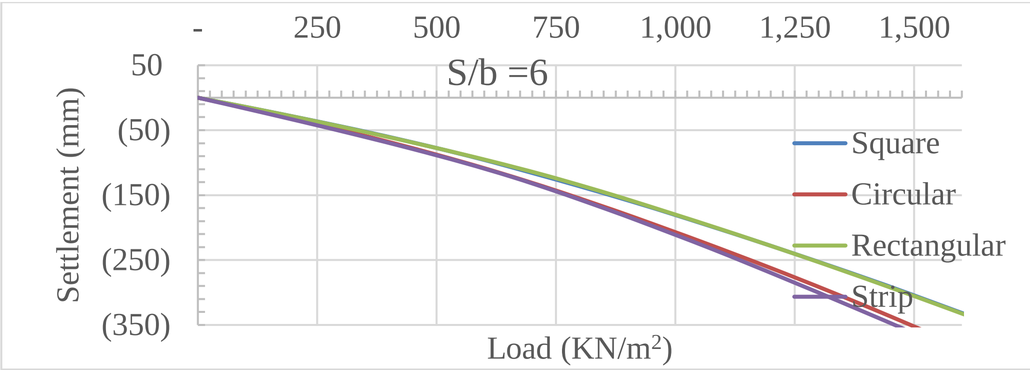

k

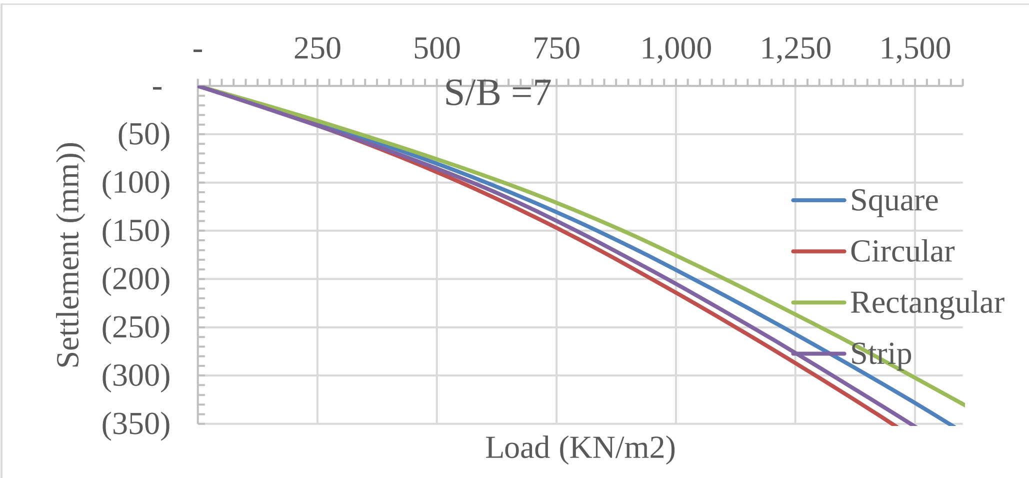

l

Figure C-2 a-n settlement curve of footing with variying S/B ratio on soil 3

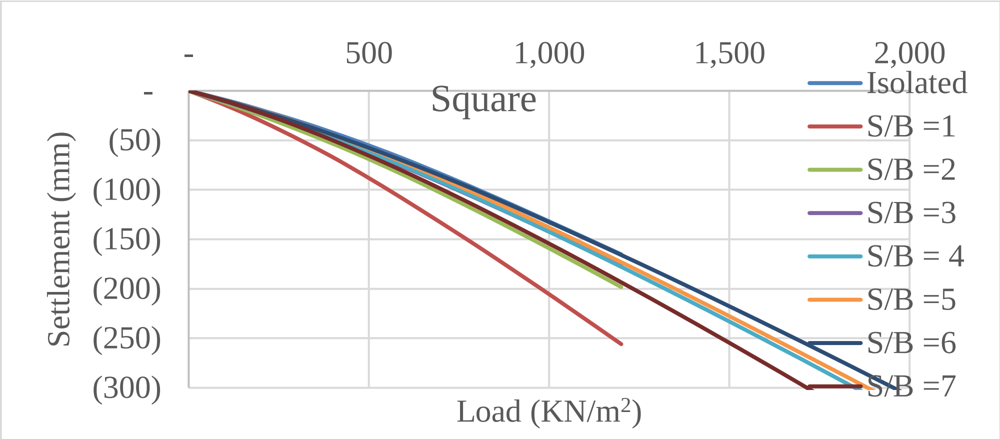
Square
Settlement (mm)
Load (KN/m²)
-
500
1,000
1,500
2,000
-
(50)
(100)
(150)
(200)
(250)
(300)
Isolated
S/B =1
S/B =2
S/B =3
S/B = 4
S/B =5
S/B =6
S/B =7

a

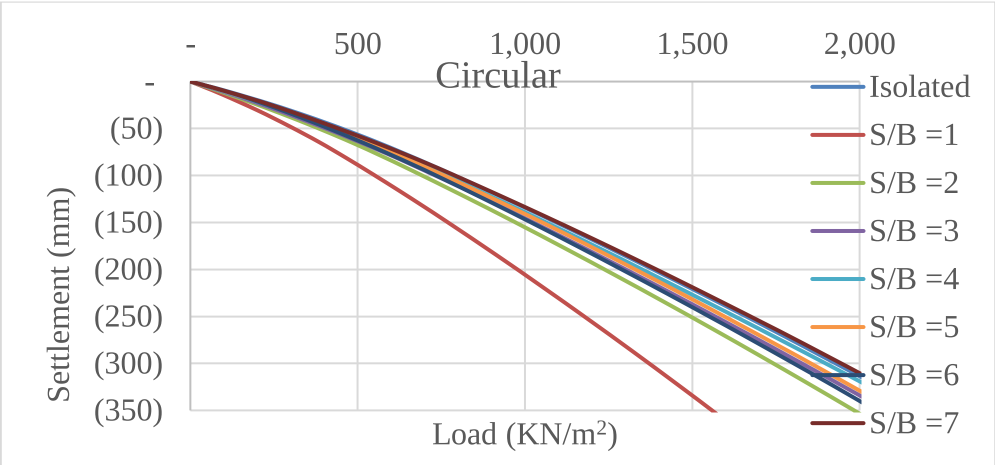
Circular
Settlement (mm)
Load (KN/m²)
-
500
1,000
1,500
2,000
-
(50)
(100)
(150)
(200)
(250)
(300)
(350)
Isolated
S/B =1
S/B =2
S/B =3
S/B =4
S/B =5
S/B =6
S/B =7

b

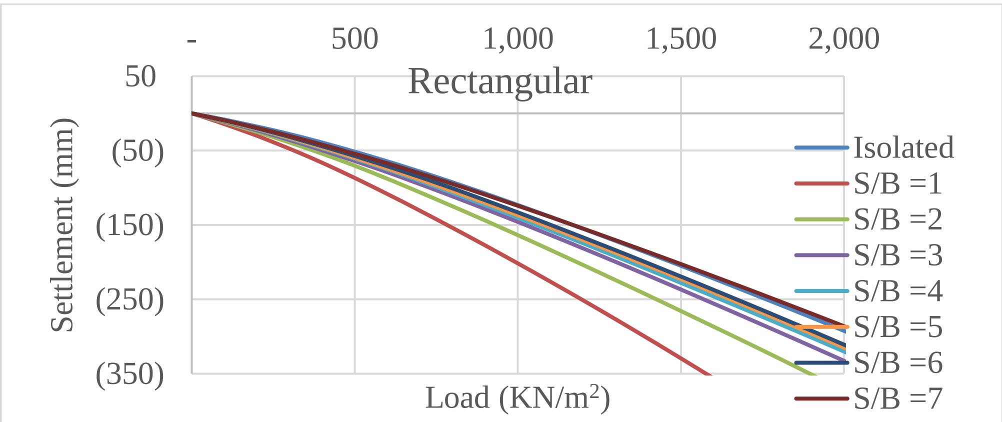
Rectangular
Settlement (mm)
Load (KN/m²)
-
500
1,000
1,500
2,000
50
(50)
(150)
(250)
(350)
Isolated
S/B =1
S/B =2
S/B =3
S/B =4
S/B =5
S/B =6
S/B =7

c

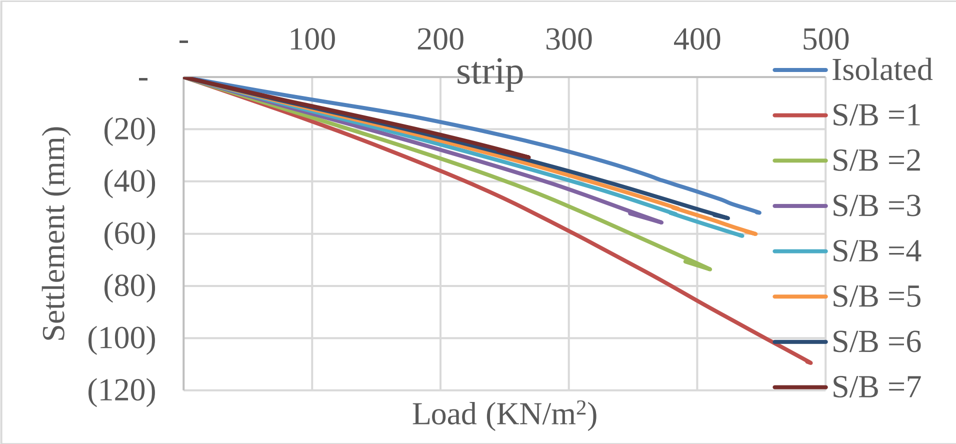

strip
Settlement (mm)
Load (KN/m2)
- 100 200 300 400 500
- (20) (40) (60) (80) (100) (120)
Isolated
S/B =1
S/B =2
S/B =3
S/B =4
S/B =5
S/B =6
S/B =7

d

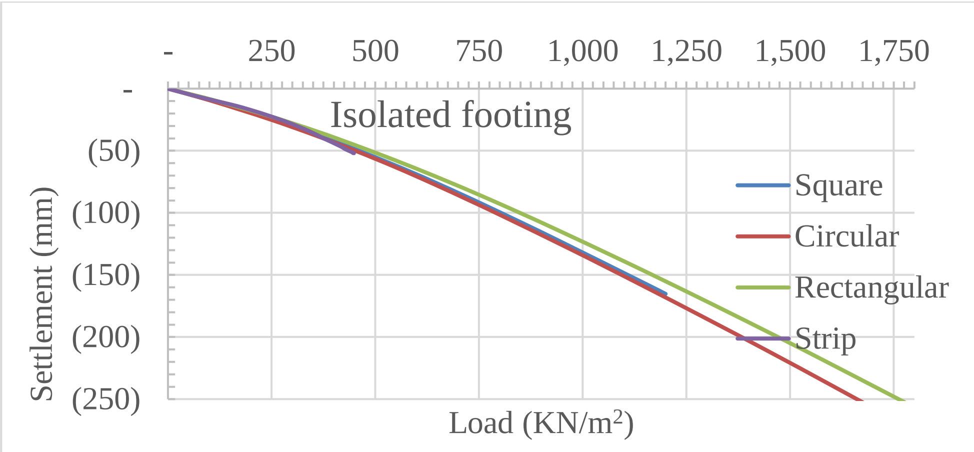

Isolated footing
Settlement (mm)
Load (KN/m2)
- 250 500 750 1,000 1,250 1,500 1,750
- (50) (100) (150) (200) (250)
Square
Circular
Rectangular
Strip

e

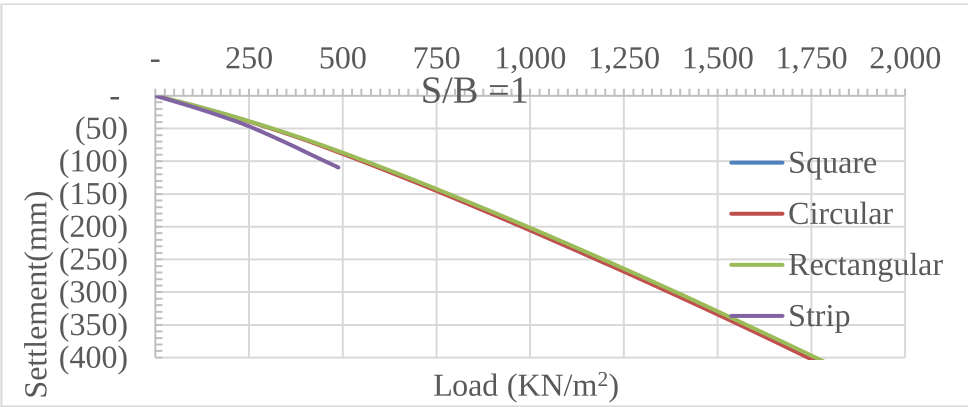

S/B =1
Settlement(mm)
Load (KN/m2)
- 250 500 750 1,000 1,250 1,500 1,750 2,000
- (50) (100) (150) (200) (250) (300) (350) (400)
Square
Circular
Rectangular
Strip

f

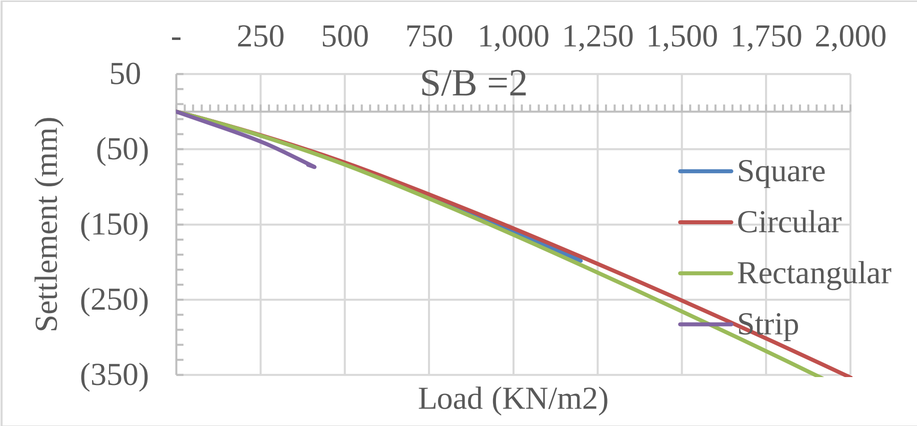

S/B =2
- 250 500 750 1,000 1,250 1,500 1,750 2,000
50
(50)
(150)
(250)
(350)
Settlement (mm)
Load (KN/m2)
Square
Circular
Rectangular
Strip

g

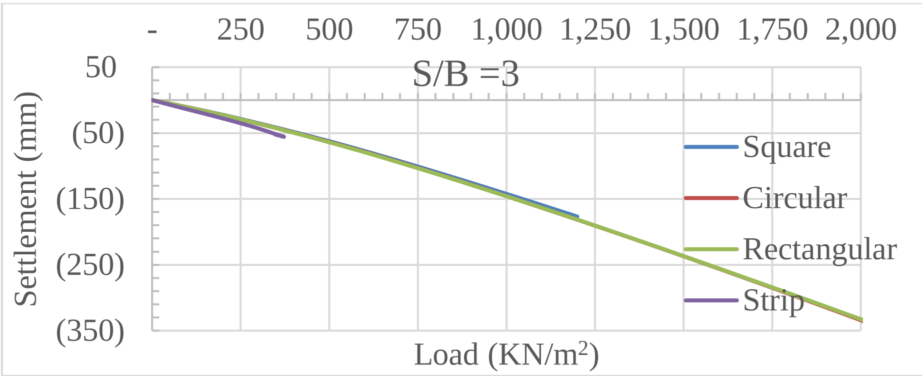

S/B =3
- 250 500 750 1,000 1,250 1,500 1,750 2,000
50
(50)
(150)
(250)
(350)
Settlement (mm)
Load (KN/m²)
Square
Circular
Rectangular
Strip

h

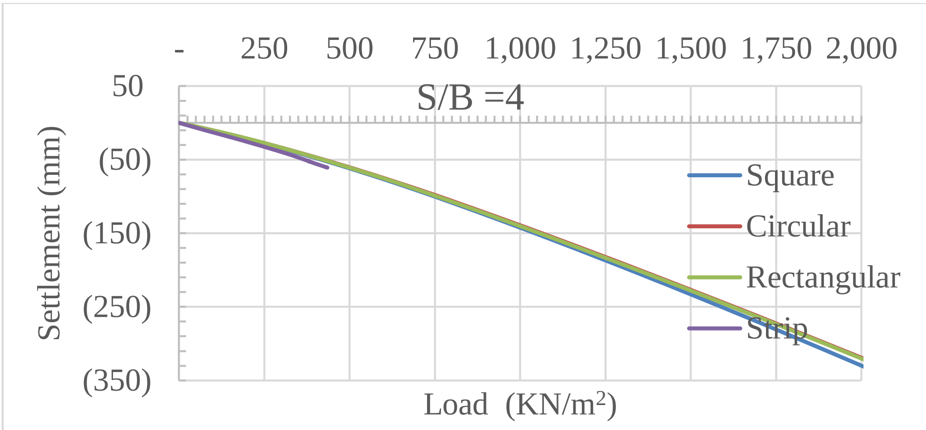

S/B =4
- 250 500 750 1,000 1,250 1,500 1,750 2,000
50
(50)
(150)
(250)
(350)
Settlement (mm)
Load (KN/m²)
Square
Circular
Rectangular
Strip

i

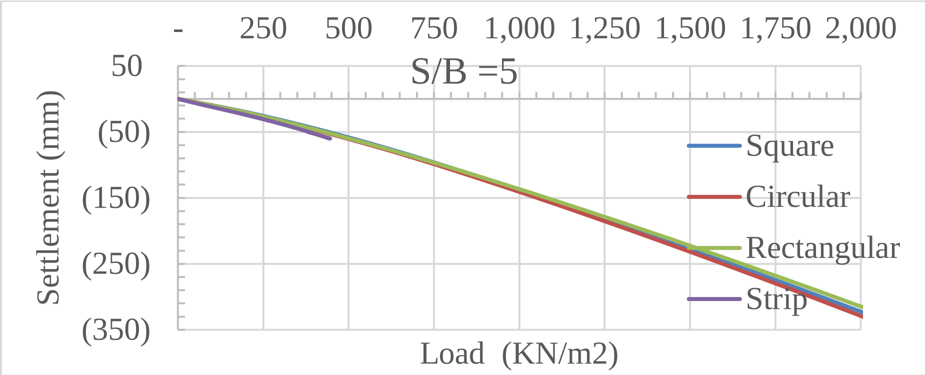

j

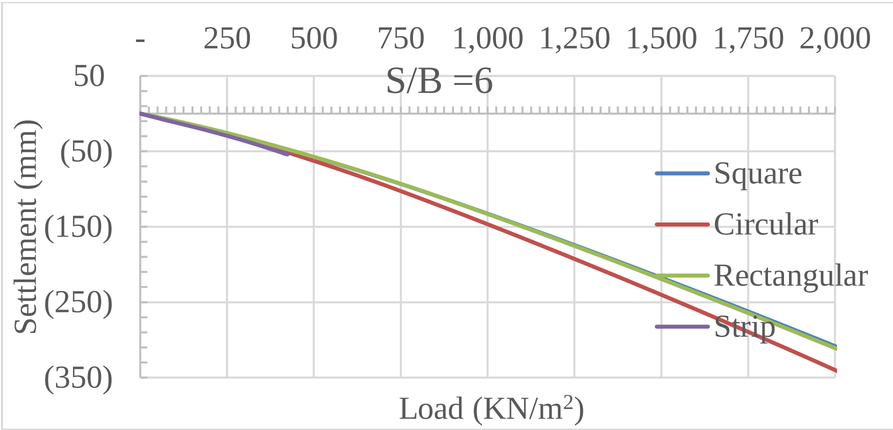

k

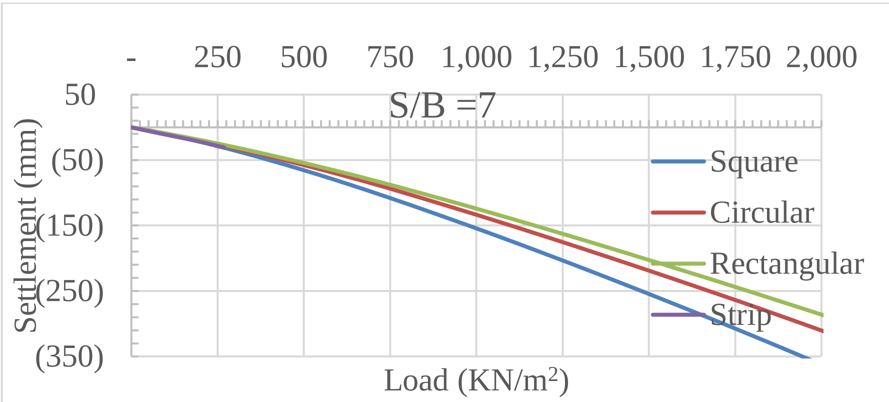

l

Figure C-3 a-l settlement curve of footing with variying S/B ratio on soil 4

Appendix – D some informative table from reference

Table D.1 Correction factor for SPT N values

e	Equipment variable	Hammer release mechanism	Correction	
			(BNBC 2015 Table 6.D.4) Efficiency	(Skempton, 1986) $C_E = {ER}/{60}$
Energy ratio for different Hammer type C_E	Donut hammer	Hand dropped	0.5	0.5-1
		Cathead + 2 turn	0.6	
	Safety hammer	Cathead + 2 turn	0.55-0.6	0.7-1.2
	Automatic hammer	Trip	0.7	0.8-1.5
	Drop /pin	Hand droped	0.45	
Borehole diameter C_B	65-115 mm 150 mm 200mm		1 1.05 1.15	
Sampling method C_S	Standard sampler Non-standard sampler		1 1.1-1.3	
Road length C_R	3 to 4 m 4 to 6 m 6 to 10 m 10 to 30m		0.75 0.85 0.95 1	

Table D.2 cohesion and friction angles of various soil type

Description	USCS	Cohesion			
		Min	Max	Specific value	ϕ
Silty sands normally consolidated	SM			22	32-35
Silty clays, sand, silt mix - Compacted	SM			20	34
Sand silt clay with slightly plastic fines - compacted	SM	45	56	50	34±1
Sand silt clay with slightly plastic fines - compacted	SM - SC	27	70	50	33±4
Clayey sands - Compacted	SC	58	86	72	31±4
Inorganic clays, silty clays, sandy clays of low plasticity Compacted	CL	72	96	86	31±4
Inorganic silts, silty or clayey fine sands, with slight plasticity	ML			7	27-41
Inorganic silts and clayey silts - compacted	ML	57	77	67	32±2
Mixture if inorganic silt and clay - compacted	ML CL	45	79	65	32±3
In organic silt of high plasticity saturate Compacted	MH	67	134	100	25±3
In organic silt of high plasticity compacted	MH			10	

(Transportation, 2017)

Table D.3 Poisons ratio of soil and concrete

Soil type	Poisson's ratio (μ)
Most clay soil	0.4- 0.5
Saturated clay soil	0.45-0.5
Cohesionless medium and dense	0.3-0.4
Cohesionless loose to medium	0.2 - 0.35
Clay unsaturated	0.1-0.3
Sandy clay	0.2-0.3
Silt	0.3-0.35
Sand, gravelly sand Commonly used	-0.1-1.0 0.3-0.4
Concrete	0.15
Steel	0.33

Table D -4 Penetration resistance and properties of soil on the basis of SPT N value

Various soil cohesion and SPT N values for intermediate soils

For granular soil				For cohesive soil	
N value	Relative density	Friction angle φ' (^{0})		N Value	Consistency
< 4	Very loose	<30		0 - 1	Very soft
4- 10	Loose	30 - 35		2 - 4	Soft
10 -30	Medium dense	35 -40		5 - 8	Medium stiff
30 - 50	Dense	40 - 45		9 -15	Stiff
>50	Very dense	>45		16 -30	Very stiff
				31 - 60	Hard
				>60	Very hard

(Transportation, 2017)

Table D – 5 Correlation between cohesion and SPT-V values (Karol, 1960)

Soil conditions	Dense	Medium	Loose
Cohesion in (kPa) SPT N Values	48 >30	5-48 10-30	5 <10

Table D – 5 Values of range of static stress-strain modulus Es for selected soil(Bowles, 1976).

Soil	Es, MPa
Clay	
Soft	2-15
Very soft	5-25
Medium	15-50
Hard	50-100
Sand	
Silty	5-20
Loose	10-25
Dense	50-81
Sand and gravel	
Loose	50-150
Dense	100-200
silt	2-20

Table D – 6 Presumptive values of bearing capacity for light loaded structures

Soil type	Soil description	Safe bearing capacity (kPa)
1	Soft rock and shale	400
2	Gravel, sandy gravel, slightly sandy gravel; very dense and offer high resistance to penetration during excavation (GW, GP, GM, GC)	440**
3	Sand (other than fine sand), gravely sand, silty sand; dry soil shall include the groups (SW, SP, SM, SC)	200
4	Fine sand; loose & dry (soil shall include the groups SW, SP)	100
5	Silt, clayey silt, clayey sand; dry lumps which can be easily crushed by finger (ML, SC, MH)	**150**
6	Clay, sandy clay; can be intended with strong thumb pressure (CL, CH)	150
7	Soft clay, can be intended with modest thumb pressure (CL, CH)	100

(Development, 2013; Eurocode, 2006; Transportation, 2017).

Table D – 7 Unit weight of different soil

Corrected SPT-N Sands	Description	γ_{moist} (kN/m^3)	Corrected SPT-N Clay	Description	γ_{moist} (kN/m^3)
0	Very loose	11-15.7	0	Very Soft	15.7-18.8
4	Loose	14.1-18.1	2	Soft	
10	Medium	17.3-20.4	4	Medium	17.3-20.4
30	Dense	18.8-22	8	Stiff	
50	Very dense	20.4-23.6	16	Very stiff	18.8- 22
			32	Hard	